Deutsches Geodätisches Forschungsinstitut (DGFI)

ANNUAL REPORT 2002/2003

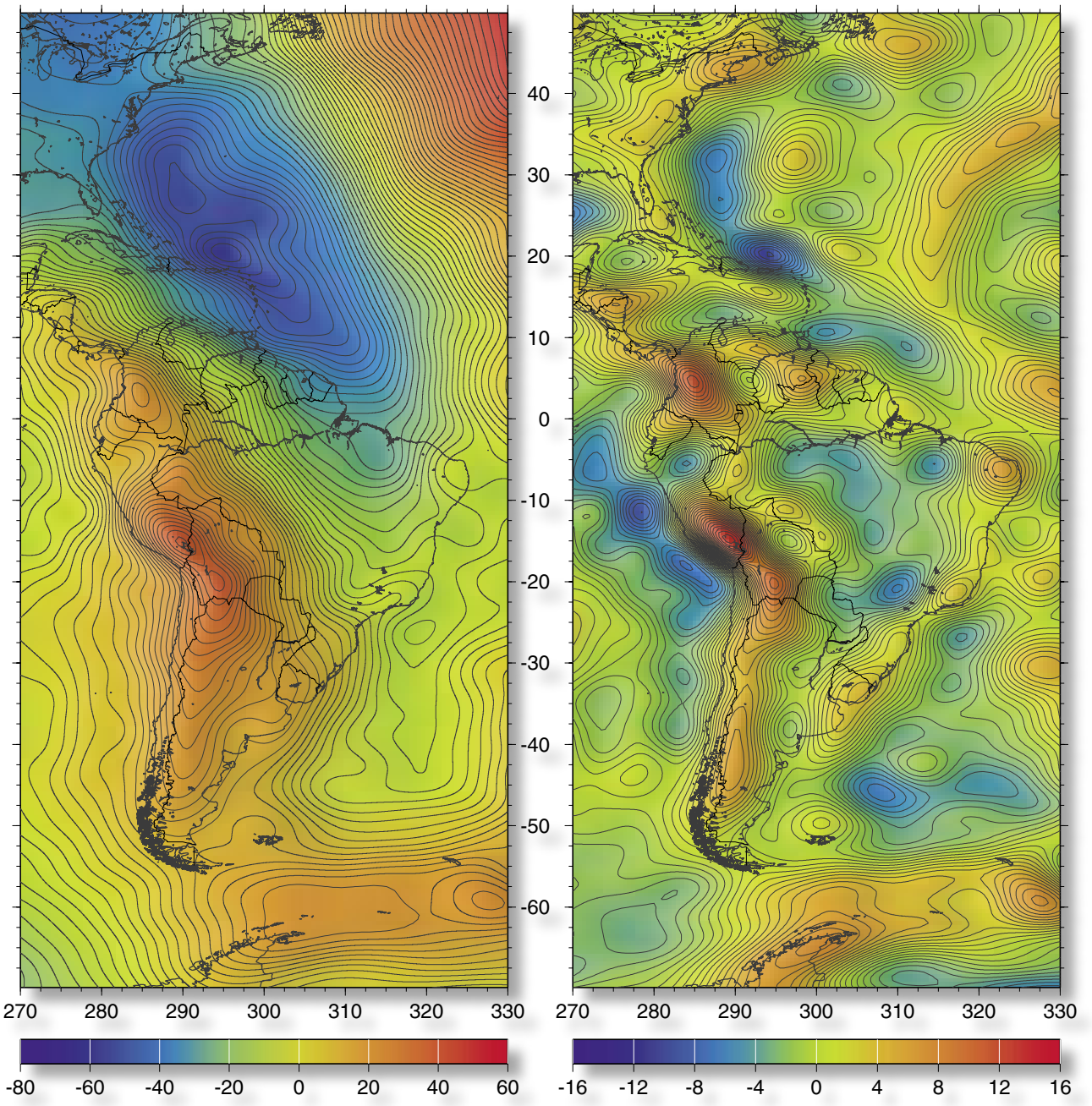

Regional multi-resolution decomposition of the GRACE gravity model GGM01 into frequency-dependent detail signals. The figure shows on the right hand side the detail signal of resolution level five. The sum of all detail signals up to level five yields the multi-resolution representation of the geoid undulations [m], shown on the left hand side (see project B2). For a three-dimensional view use chromatic 3-D glasses attachted on inside backcover.

Deutsches Geodätisches Forschungsinstitut (DGFI)
Marstallplatz 8, D-80539 München
Tel.: 089 23031-107 Fax: 089 23031-240
E-mail: mailer@dgfi.badw.de Internet: http://www.dgfi.badw.de

ANNUAL REPORT 2002/2003

Table of Contents

3nd Edition

The Institute

The German Geodetic Research Institute (Deutsches Geodätisches Forschungsinstitut, DGFI) is an autonomous and independent research institution located in Munich. It is supervised by the German Geodetic Commission (Deutsche Geodätische Kommission, DGK) at the Bavarian Academy of Sciences. The research covers all fields of geodesy and includes the participation in national and international research projects as well as functions in international bodies.

The Programme

The long-term research programme of DGFI is based on the general theme „Fundamentals of Geodetic Reference Systems“. The definition of geodetic reference systems is studied and methods for their realisation with modern space geodetic techniques are developed. Geodetic observations are analysed, approaches for the data processing are set up, tested and exemplarily applied.

Reference Systems

Reference systems are the necessary basis for the representation of geometrical or physical quantities, e.g., coordinates of points at the Earth’s surface or parameters describing the Earth’s outer gravity field. They are needed to transform geodetic observations into these parameters used in all kinds of precise positioning on Earth for geodesy, cadastre, engineering, geodynamics etc. But also geo-information systems, land management, navigation on land, in the sea and in air, and space research use the geodetic reference systems. Neighbouring disciplines like astronomy and geophysics apply geodetic reference systems for the orientation of spatial parameters. In general, geodetic reference systems are fundamentals for the global spatial infrastructure.

Motivation

The reason for the increasing importance of geodetic reference systems is the extensive use of space observation techniques in all fields of geodesy and neighbouring disciplines. Classical reference systems were defined and realised locally, e.g., by fixing a fundamental point with its coordinates and a local orientation. This was sufficient because the observation techniques were also locally oriented. Nowadays we need global reference systems to use appropriately the global observations.

Modern Reference Systems

To use the modern space techniques, e.g., satellite observations and radio-astrometry, we need a geometric terrestrial reference system covering the whole globe. The Earth’s gravity field is represented by physical reference surfaces, e.g., the geoid as an equipotential surface or the sea level as a natural surface in a state of nearly equilibrium. To understand the geometrical and physical systems as well as their variations in space and time we have to study and model dynamic processes which influence the geodetic observations and parameters.

Practical Applications

The research programme of DGFI forms the basis for many practical applications in various fields of geodesy and surveying. The realisations of global reference systems as terrestrial reference frames, like the ITRF, allow the integration of continental and national systems, e.g., the German Satellite Positioning Service, SAPOS, as regional densifications. Theoretical studies on physi-

cal reference surfaces and monitoring of the time-dependent sea level are fundamentals for the definition and realisation of height systems. These vertical reference systems have got an increasing importance because heights are today more and more determined by space techniques (e.g. GPS) rather than by terrestrial methods (e.g. levelling).

International Cooperation

The international geodetic community has developed an excellent cooperation during the last decades. Generally needed fundamentals, e.g. global reference systems, are studied jointly and established and maintained by mutual efforts. The International Association of Geodesy (IAG) as the most important body has installed several scientific services dealing with this problem and providing most important products free of charge. DGFI recognizes the outstanding role of these services for geodetic practice and research and cooperates in various of these services as data, analysis and research centre. Members of the DGFI staff have taken leading positions in the IAG and other organisations.

Neighbouring Disciplines

Geodetic parameters, e.g. from the realisation of reference frames, may be used, analysed and interpreted in other disciplines like astronomy, geophysics, hydrology, meteorology, oceanography etc. DGFI seeks the contact to these disciplines and provides all the data and results to the neighbouring sciences. Several research projects are carried out in close cooperation with scientists and institutions from these disciplines.

Structure of the Research Programme

The present research programme for the years 2003/2004 was set up on the basis of the above described arguments. It was reviewed by the scientific council of the German Geodetic Commission (DGK) and approved by the DGK General Assembly in October 2002. It is divided into four long-term major topics consisting of 21 projects as well as the information systems and scientific transfer. The major topics are:

A Geometric reference systems
B Physical reference surfaces
C Dynamic processes
D International services and projects
E Information systems and scientific transfer

Research Group Satellite Geodesy

The projects related to satellite geodesy are carried out in the frame of the research programme of the Research Group Satellite Geodesy (Forschungsgruppe Satellitengeodäsie, FGS) which is a cooperation of the Institute of Astronomical and Physical Geodesy (IAPG), the Research Establishment Satellite Geodesy (FESG), both at the Technical University Munich, the Geodetic Institute of the University Bonn (GIUB), the Federal Agency for Cartography and Geodesy (BKG), and the German Geodetic Research Institute (DGFI).

A Geometric Reference Systems

Global reference frames provide the framework for measuring and mapping the Earth's surface and its variations in time. They are also basis for studies of the Earth system for many practical applications (e.g. regional and national networks, engineering, precise navigation, geo-information, geodynamics, sea level studies, and other geosciences). Today space geodetic observation techniques, such as the Global Navigation Satellite System (GNSS), Satellite Laser Ranging (SLR) and the Very Long Baseline Interferometry (VLBI) allow accurate positioning for materialised points (station monuments) at the Earth's surface. The global terrestrial reference system is realised by positions of these global tracking sites and their variations in time. Each of the different observation techniques has its strengths and weaknesses concerning the determination of various parameters, and the accuracy achieved today is mainly limited by systematic errors of the individual techniques. DGFI studies mathematical and physical models for the different space geodetic observations to understand the origin of still existing systematic differences and to achieve further improvements. A major goal is to develop optimal integration and combination methods to provide highly accurate and consistent results and to realise a unified global reference system. One important step towards a rigorous combination of the different data types is the adaption to common standards (e.g. IERS Conventions 2000, IAU Resolutions 2000), models and parametrisations. Another major issue is a consistent realisation of the geodetic datum for the various space techniques and for the combined solution. For the definition of the kinematic datum we propose to use plate kinematic models based on present-day geodetic data (e.g. APKIM) instead of geophysical models (e.g. NNR NUVEL-1A) to ensure that the no-net-rotation condition can more accurately be fulfilled.

A1 Modelling for GNSS

This project aims at improving the height determination performance of Global Navigation Satellite Systems. According to the actual two year research programme studies related to the weighting of GPS phase data, to loading effects due to atmospheric pressure and to ocean tides, and to refined tropospheric mapping functions are planned. During the past period of one year the first three of these four topics have been addressed. The performed analyses apply to stations of the EUREF permanent GPS network because it includes many sites exposed to large loading displacements.

Weight Function for GPS Phase Data

The motivation for this study was that presently no extensive comparison of weighting alternatives using real data is available. Applying $\cos^2 z$ as recommended in EUREF accounts for the fact that some measurements and modelling errors increase with zenith distance. On the other hand, there are also errors such as vertical loading effects which decrease with zenith distance. In addition, exploiting the low elevation data by not down-weighting would improve the decorrelation of height and troposphere parameters. Therefore, a European network of 32 stations displayed in figure A1.1 was processed during three periods of 10 or 11 days according to the following strategies:

- Varying the elevation mask from 8° to 20° in steps of 2°,
- applying weight functions $P = 1$, $P = \cos^2 z$ and $P = \cos^2 z + a \cdot \sin^2 z$, setting a to 0.3 or 0.5, respectively.

Accepting daily repeatabilities as the performance measure, the results can be summarised as follows (see figure A1.2):

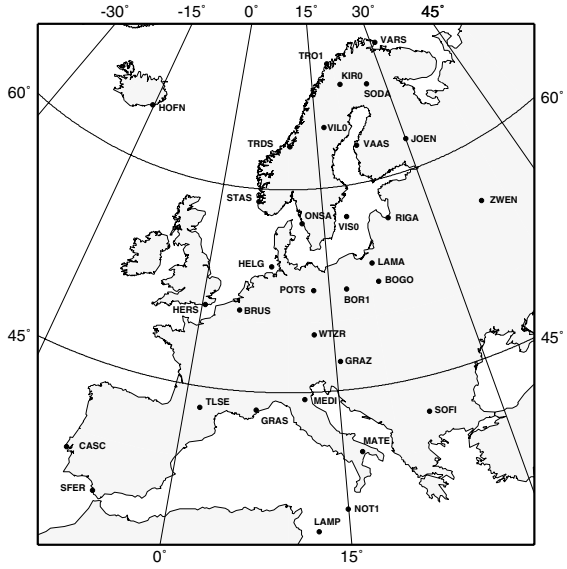

Fig. A1.1 Analysed network

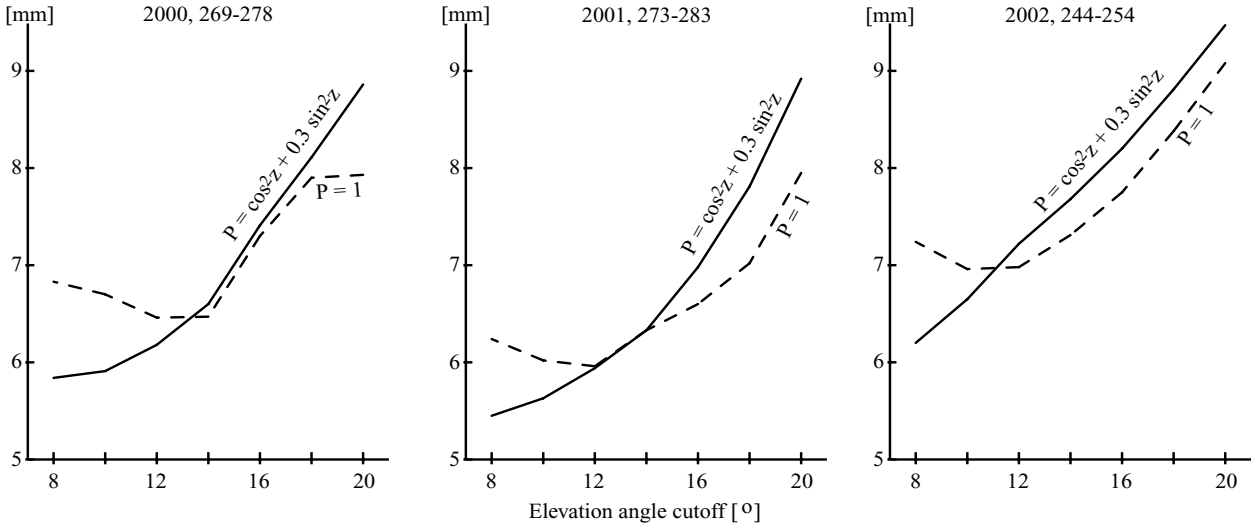

Fig. A1.2 Height repeatabilities as function of elevation mask and weight function for the three analysed periods

– If the elevation mask is set to 14° or less, equal weighting performs worse than the other functions in all three position components.

– If the elevation mask is raised above 14° or no observations below this mask are available, equal weighting should be applied.

– The results for the weight functions involving the $\cos^2 z$ term differ only slightly.

Atmospheric Pressure Loading

The investigations related to the determination of site dependent vertical pressure loading coefficients from GPS observations required most of the available resources. The analysed network is identical with the one shown in figure A1.1. The processed 11 data periods of in total 126 days are distributed between March 1999 and February 2003 in order to allow the estimation of vertical site velocities. Another selection criterion was the occurrence of high pressure anomalies mainly in the northern part of the network. Daily free network adjustments were performed generat-

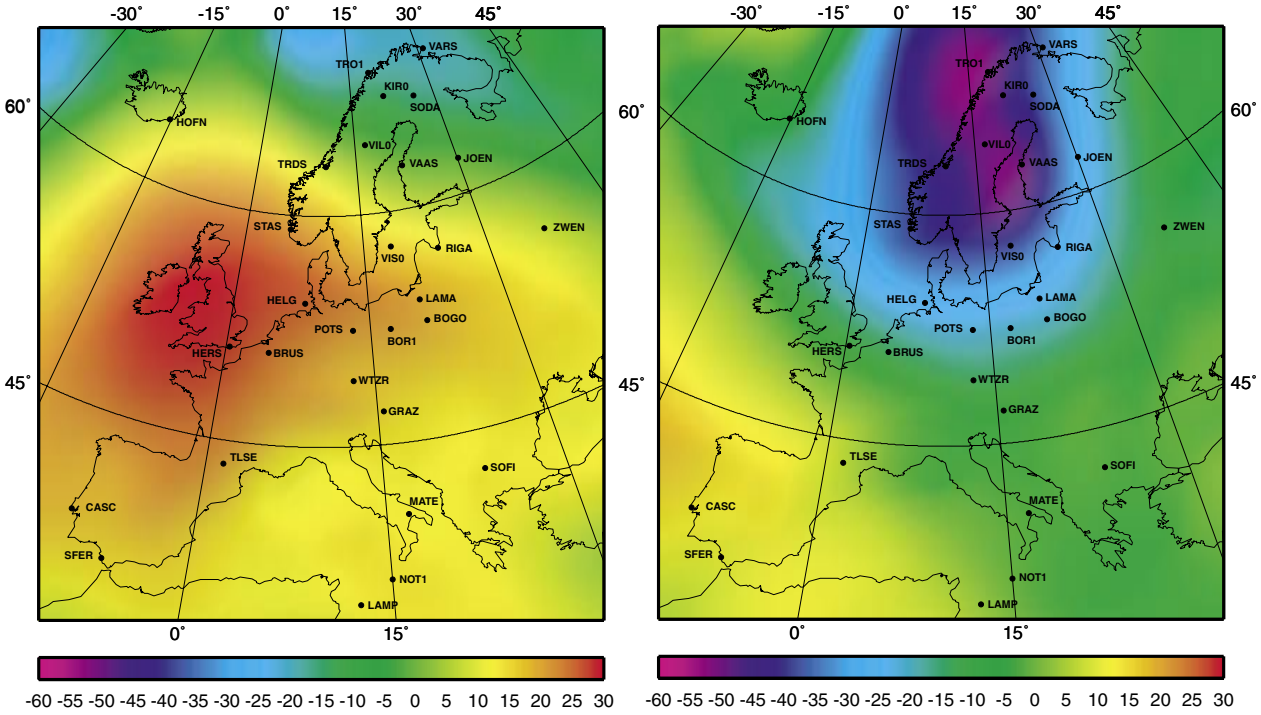

Fig. A1.3 Pressure anomalies in the network area on Feb. 17, 2001, and Feb. 23, 2002 [hPa]

ing a coordinate solution, a covariance matrix and normal equations. The analysis followed two different strategies:

– Ellipsoidal height differences with their full covariance matrix were derived from the daily solutions and introduced as correlated observations into a common adjustment of all days. Pressure anomalies were derived from daily mean pressure values available from the U.S. National Center for Atmospheric Research for a 2.5 × 2.5° grid. Figure A1.3 shows examples of the pressure anomalies in the network area during two days included in the analysis.

– The second strategy is based on the daily normal equations. Site dependent vertical loading coefficients were implemented as a new parameter type in the Bernese GPS software and were then included in the normal equations, which were accumulated to a common solution. In this case, pressure data with 1° × 1° and 6 hrs resolution originating from the U.S. National Center for Environmental Prediction could be used.

Both strategies solve for the same parameter set: Site dependent vertical pressure loading coefficients, mean ellipsoidal heights referring to a reference epoch and a reference pressure, vertical site velocities, and height discontinuities due to antenna configuration changes if necessary.

Table A1.1 gives examples of the resulting vertical loading parameters. It can be stated that the accuracy of the estimated parameters increases with the range of the pressure anomalies and thus with the latitude. Several islands or coastal sites experience

Table A1.1 Examples of estimated vertical pressure loading coefficients ΔH_P [mm/hPa]

Station	ΔH_P	Station	ΔH_P
KIRØ	- 0.54	HELG	- 0.14
VILØ	- 0.62	BOGO	- 0.44
HOFN	- 0.11	HERS	- 0.13
JOEN	- 0.55	WTZR	- 0.40
RIGA	- 0.54	LAMP	- 0.18

only very small or even no displacements supporting the inverted barometer hypothesis.

Ocean Tides Loading

Investigations on the feasibility of determining the vertical site displacements due to loading caused by oceanic tides from GPS observations were initiated. As these displacements are considerably large at the European Atlantic coast, the network displayed in figure A1.4 was selected as a demonstration candidate. The work performed so far includes:

– Implementation of the capability to estimate the local phases and amplitudes of the vertical displacements caused by the main partial tidal waves M_2, S_2, N_2, K_2 and K_1 directly in the GPS data processing with the Bernese software.

– Processing of the selected network with the modified software on every fifth day during the period Jan. 2001 – April 2002, thus on 97 days in total; unlike the processing of 97 consecutive days, this spacing enables the decorrelation of diurnal and semi-diurnal tidal constituents with very similar periods.

As a very preliminary result, table A1.2 gives the estimated M_2-amplitudes for some sites at the Atlantic coast in comparison to predictions based on three different ocean tide models. The investigations will be continued.

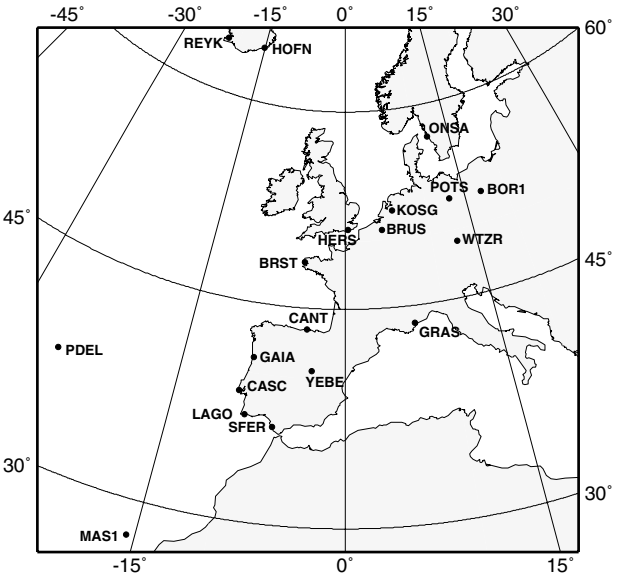

Fig. A1.4 Network selected for ocean loading analysis

Table A1.2 M_2-amplitudes estimated from GPS and derived from three different ocean tide models [mm]

Site	CSR 4.0	FES 99	GOT00_2	GPS
ACOR	36.0	38.3	35.1	37.5
BRST	40.8	43.7	40.2	41.3
CANT	32.9	32.0	31.7	31.9
CASC	33.5	33.7	32.4	31.4
LAGO	32.7	32.0	31.0	32.3
SFER	22.5	23.7	21.3	24.4

A2 Modelling for SLR

Laser ranging observations to satellites are processed with the programme DOGS-OC (**D**GFI **O**rbit and **G**eodetic Parameter Estimation **S**oftware - **O**rbit **C**omputation). The program uses an iterative differential correction process to fit a precise satellite orbit to data from various geodetic satellite methods. The solve-for variables comprise the orbital elements of the satellite, the positions of the terrestrial observing stations and their orientation in inertial space, and parameters of physical models. The latter include the following:

- Models of forces acting on the satellite (e.g. gravitational potentials, atmospheric drag, radiation pressure, ...),
- geodynamical models for the periodic movements of stations (e.g. tides, loading deformation, ...),
- and observation models (e.g. tropospheric refraction, clock errors, ...).

Continuous maintenance of the programs is needed to keep the models close to the progressing scientific knowledge. For ITRF (see D1) the IERS Conventions 2000 had to be fulfilled, whereas for pilot projects and benchmarking within the ILRS (see D4) the models from the IERS Conventions 1996 were requested.

Ocean Loading

Ocean loading results in 3-D site displacements. These displacements are modelled as a harmonic function of time whose coefficients are compiled by H. G. Scherneck for each individual site and ocean model. Formerly, these coefficients had to be introduced into the program code by means of data blocks. This year, Scherneck began to supply ocean loading coefficients in the HARPOS format, too. It is designed for describing site displacements which can be represented by a finite sum of harmonic components and is well suited to serve as DOGS-OC input card. Each record of the harmonic definition, the site definition, and the displacement definition is identified by a one-letter code, which is supplemented in the front to become a six-letter DOGS-OC keyword. Such ocean loading records were collated for all SLR sites and for two different ocean tide models. Thus, ocean loading modelling in DOGS-OC is entirely contolled by the input.

Modelling Earth Orientation

The satellite techniques require the interpolation and derivation of Earth orientation parameters (EOP) as a link between satellite and ground stations. Let f be one of three EOP-functions x_{pol}, y_{pol} or ΔUT1, given by a sequence of points (t_i, f_i), i=1,...,n, with $f_i \approx f(t_i)$. Then, an interpolating function I$f(t)$ together with dIf / dt and ∂I$f / \partial f_i$ is needed.

Besides a second model for the diurnal and semi-diurnal ocean tidal variation of the EOP-functions – the model coming from the IERS Conventions 2000 –, three alternative models of piece wise polynomial interpolation were implemented:

1. Continuous piece wise linear interpolation: In the interval $[t_i, t_{i+1}]$, the interpolant depends on the points (t_i, f_i) and (t_{i+1}, f_{i+1}), and these are the only points which can be corrected from any observation within that interval. That is to say the method is local. The approximation order is $O(h^2)$, where h is the grid width, and for uniform grids $O(n^{-2})$ with n being the number of interpolation points (t_i, f_i). But there is no way to get a reliable estimation of the time derivative $dI f/dt$, what is required for the ILRS pilot projects.

2. Continuously differentiable piece wise cubic Bessel interpolation: In the interval $[t_i, t_{i+1}]$ the interpolant If is constructed from $f_{i-1}, f_i, f_{i+1}, f_{i+2}$. The method is local, too. For equally spaced grids of width h, Bessel interpolation provides an $O(h^4)$ approximation to the function f, but only $O(h^2)$ to the derivative df/dt.

3. Continuously differentiable piece wise cubic Hermite interpolation: In the interval $[t_i, t_{i+1}]$ the interpolant is constructed from $f_i, f_i', f_{i+1}, f_{i+1}$, thereby making the method local. It provides an $O(h^4)$-approximation to the function and $O(h^3)$ to the derivative.

4. The interpolating cubic spline was eliminated because of its non-locality. This means that any observation produces partial derivatives with respect to all f_i, and hence robustness is reduced.

The norm wise approximation orders given here hold only if the function to be interpolated has four continuous derivatives. This is not the case with the official IERS series EOPC04.

The developed formulas are described in the "DOGS-Manual IV, Parameterschätzung in DOGS-OC", chapter 5.

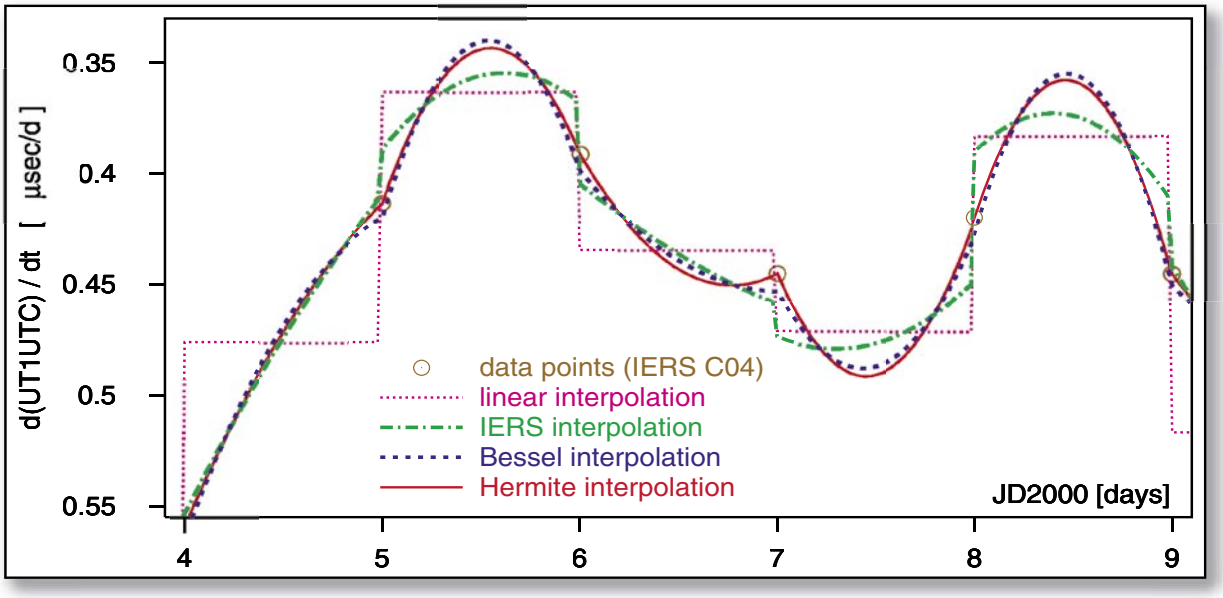

Fig. A2.1 The effect of the derivative d/dt(ΔUT1) = -LOD for different methods of interpolating ΔUT1

A3 Modelling for VLBI

Two main branches of work are carried out within this project. On the one hand there are intense studies on VLBI modelling. On the other hand the VLBI software OCCAM is developed together with groups at Geoscience Australia (Canberra, Australia), the Vienna University of Technology (Vienna, Austria), the St. Petersburg University, and the Institute of Applied Astronomy (both St. Petersburg, Russia). The models implemented in OCCAM are state-of-the-art.

Refinement of the Stochastic Model of VLBI Observations

Up to now, improvements of modelling the observations of "Very Long Baseline Interferometry (VLBI)" are mainly achieved by refining the functional representation of the geometric-physical properties of the observations. Further progress in this field mostly needs big efforts and is not possible with any precision. In contrast, the stochastic properties of the observations (which comprise functionally not representable influences) have not been handled thoroughly.

The refinement of the stochastic VLBI model considered here is based on two principal ideas: (1) Discrepancies between the functional model and the observations can be understood at least approximately as variances of the observations. (2) Deficits of the functional model which affect several observations more or less systematically might be interpreted as covariances (correlations) between observations. For this reason, the deficits of the stochastic model of VLBI observations were studied in order to set up a more adequate structure of the variance-covariance matrix of the observations. The associated unknown variance and covariance components were estimated according to the MINQUE principle.

As illustrated in figure A3.1, the most significant improvements of the conventional stochastic VLBI model were found to be related to the individual observing stations (site-specific effects) and the elevation angles (tropospheric effects).

Although standard VLBI solutions can be improved by the refined stochastic model for the observations, the potential of the refinement is not yet exhausted, and further investigations are needed.

Parameter Constraints in VLBI Data Analysis

It is common practice in VLBI parameter estimation to model two types of parameters. On the one hand there are classical target parameters such as station coordinates and Earth orientation parameters. On the other hand there are additional parameters like, e.g., the coefficients of the piece wise linear functions for the troposphere and the clocks as well as the offsets of the horizontal tropospheric gradients per station. In order to stabilize the estimation, prior information on the additional parameters is added by means of pseudo-observations (soft constraints).

For assessing the impact of these constraints on the VLBI results, several aspects were studied such as the bias of the parameters, the respective contribution of the constraints to the estimation,

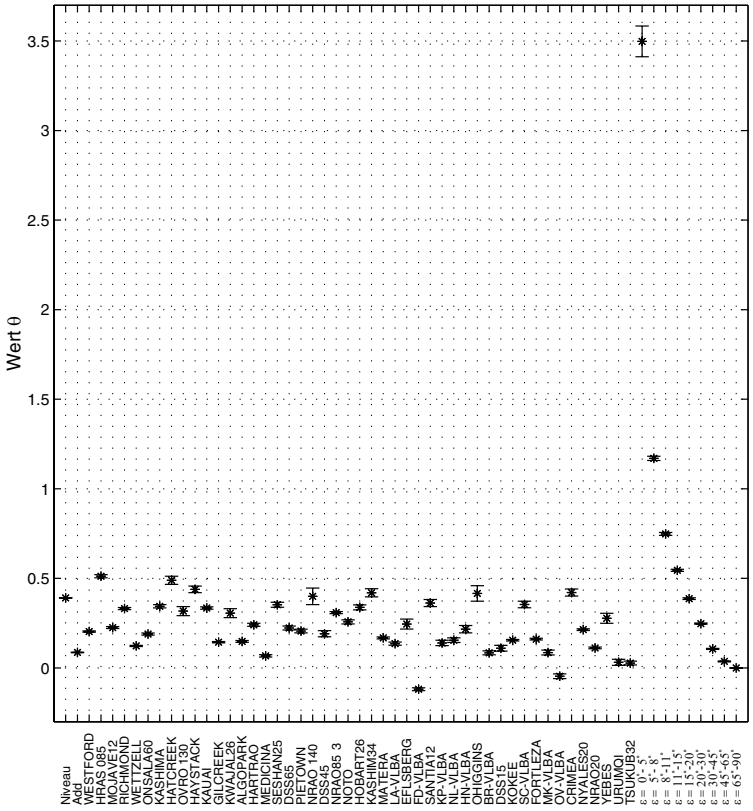

Figure A3.1 MINQUE-determined variance components which describe a refinement of the conventional stochastic model of VLBI observations. The components quantify mainly station and elevation dependent stochastic properties of the observations. They do not directly represent variances. For this reason single componentscan have negative values.

and the consistency of observed data and prior information. Numerical results were derived from the NEOS-A sessions of 2000 and 2001 using the VLBI software OCCAM 5.0 (Least Squares Method).

Figure A3.2 shows the impact of the increase and the decrease, respectively, of the weights of the constraints by a factor of 100 with respect to the weighting which is typically applied at DGFI in VLBI data processing. As the standard deviation of daily ΔUT1 is less than 5 ms the actual variation of the parameters is just below significance. The contribution of the constraints to the estimated parameters (in terms of partial redundancies calculated for the constraints) is rather moderate in the standard case but becomes dominant in case of increased weights, in particular for the gradient offsets. This is underlined by results for the statistical consistency of the constraints and the observed data which are not shown here. Note that particular care must taken in case of weakly configured networks, which can be due to temporary losses of observations on single VLBI sites.

CONT02 VLBI Normal Equations for a Rigorous Combination with GPS

From 16th to 31st of October 2003, the CONT02 VLBI observation campaign, which was initiated by the IVS, was carried out. This campaign is especially suitable for the combination of VLBI observation equations or normal equations with those of other space-geodetic techniques.

In order to provide the optimum conditions for combining VLBI and GPS as rigorously as possible, much care was taken to set up VLBI normal equations with models and estimated parameters which are adapted to those of the used GPS normal equations. The

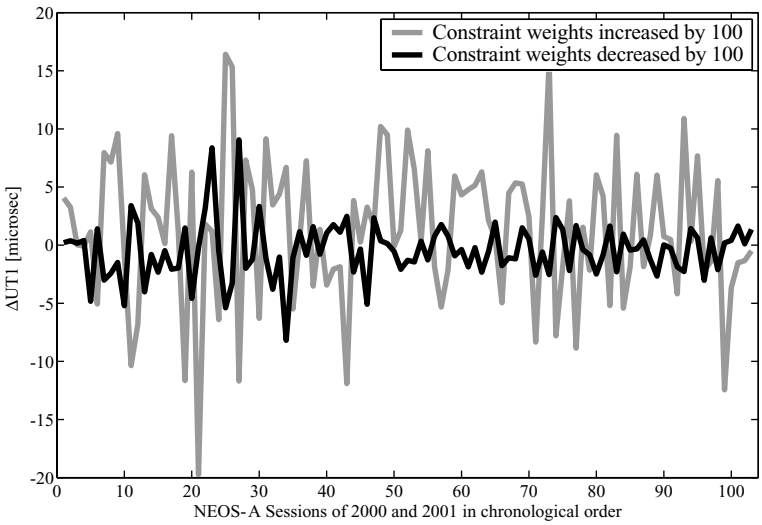

Figure A3.2 Possible bias of the ΔUT1 values with respect to OCCAM standard weighting due to different weights of the constraints.

following models or parameter representations had to be verified or modified, respectively, in the VLBI software OCCAM: solid Earth tides, pole tide, ocean loading, tropospheric delay, subdaily EOP variations, daily a-priori EOP values and their interpolation as well as the nutation model. The VLBI observation data were additionally reformatted from 24h blocks, beginning at 18 h UTC to blocks beginning at 0 h in order to avoid a potential error source. The normal equations were supplied in the SINEX 1.0 format. First CONT02 combination results of VLBI and GPS data are presented in project D1.

The research activities within this project contributed to the work of the IVS Special Analysis Centre at DGFI (see project D6). Further cooperation exists with the projects A4 and D1. The work within A3 is partially funded by the ‘Deutsche Forschungsgemeinschaft‘ under the grant DR 143/11-1.

A4 Combination of Geodetic Space Techniques (GPS, SLR, VLBI, DORIS)

An optimal combination of geodetic space techniques for the creation of a highly accurate and reliable terrestrial reference frame requires intensive investigations on the specific features of the heterogeneous space techniques such as GPS, SLR, VLBI and DORIS. Individual technique solutions differ from each other in the geodetic datum, in stochastic and systematic error behaviour and in the mathematical modelling of the physics. These differences must be analysed before combining and be homogenised in a consistent way during combining. Further on, the combination procedure is to be developed towards automated processing. In the following, the last years progress of these investigations is presented.

Datum Realisation

If a reference frame is realised by combining solutions, it is essential to investigate how well the parameters which can be used for the datum realisation (e.g. the centre of mass) are determined by different space geodetic observations. This is needed to decide whether differences between solutions are systematic or the parameters are just weakly determined.

To investigate this aspect the covariance matrix of a network is computed using loose constraints. It is then transformed by an S-Transformation to a covariance matrix where the uncertainties in the underlying coordinate system are removed. This means that the covariance matrix of the transformation parameters only depends on the first datum realisation. Two examples of a covariance matrix for datum parameters are shown for a session of a VLBI network and a weekly SLR solution (see figure A4.1.).

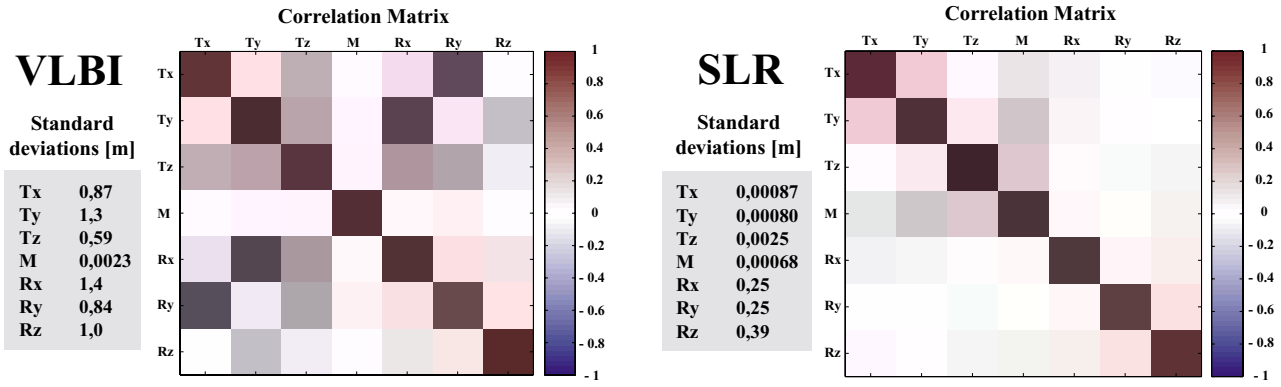

Fig. A4.1 Covariance matrix of the datum parameters of a session VLBI network and a weekly SLR solution (both computed with 1 m loose constraints). The covariance matrix was divided into standard deviations (in meter on the Earth's surface) and a correlation matrix

The standard deviations prove that the VLBI scale and the SLR scale and translations are well-determined. The SLR *z*-translation has a higher standard deviation than the translations in *x* and *y*. This result is consistent with theoretical considerations, as the *z*-component is determined by the disturbed satellite motion due to the influence of the Earth's gravity field only, whereas the *x*- and *y*- components are additionally determined by the earth rota-

tion. The correlation of the *x* and *y* translation might be explained by the earth rotation.

Towards Rigorous Combination

In cooperation with FESG (Forschungseinrichtung Satellitengeodäsie TU München), DGFI has performed the first steps towards a rigorous combination for VLBI CONT02 and GPS data (see D1). Much care was taken to adapt identical models and parametrisations for the analysis of GPS (with Bernese at FESG) and VLBI data (with OCCAM at DGFI, see A3). In this combination, all parameters will be considered which are common to GPS and VLBI (e.g., station positions, 2-hourly EOPs, tropospheric and nutation parameters). First results of CONT02 are presented in D1. Further studies are necessary to develop optimal methods for a rigorous combination.

Another important issue is the parametrisation for the TRF combination of multi-year solutions (see ITRS Combination Centre, D1). The current parametrisation (station positions and constant velocities) is in conflict with observed non-linear effects in station positions and datum parameters. Hence, a better monitoring of the TRF may require non-linear components (e.g. time series of weekly estimated station positions). For that purpose, station position and datum parameter time series of the different techniques (GPS, VLBI, SLR and DORIS) were studied, considering especially their periodic (e.g. seasonal) and long term behaviour. Another important aspect in this context is the interrelation of the TRF with other parameters. The influence of a daily or monthly VLBI datum realisation on EOP and scale estimations was analysed in the SINEX combination campaign (see D1)

Automated Intra-Technique Combination

The ILRS project “Positioning & Earth Orientation” requires the combination of SLR solutions. The automated processing flow on highest level is presented in figure A4.2 and is realised by the software package DOGS-AS.

The main part of the processing flow is realized by the script for quality control and combination. A flow chart is presented in figure A4.3.

After having deconstrained the normal matrices by use of the estimated and a-priori covariance matrices the standardized eigenvalues of the normals are analysed. By theory the four smallest eigenvalues should obtain zero values. For the input solutions given so far this is fulfilled within numerical limits.

The next method computes internal solutions by adding to the normal equation the minimal constraints term which is defined for the coordinates over core stations. Hence, all internal solutions are based on the same minimal constraints set and are comparable for further analysis. The covariance matrices are rescaled so that the precision level for positions of core stations are comparable.

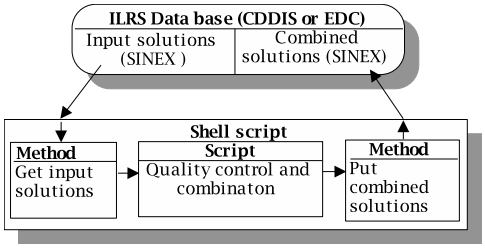

Fig. A4.2 Automated processing flow

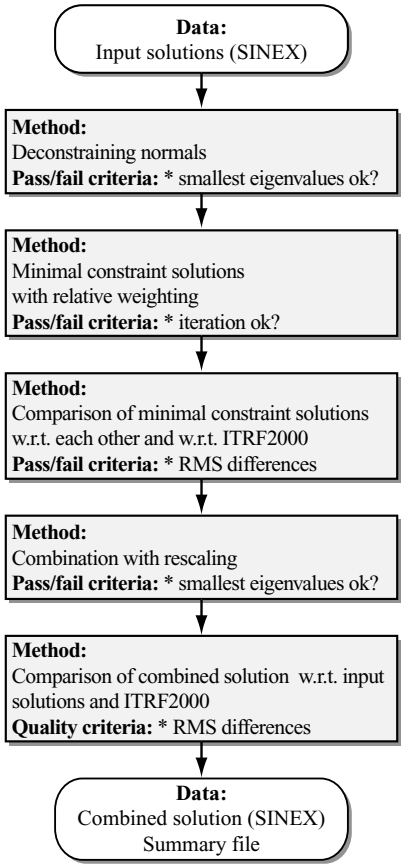

Fig. A4.3 Quality control and combination

The internal solutions are directly compared to each other by analysing the r.m.s. differences of the parameters. Additionally, Helmert transformations between the solution parameters and the ITRF2000 values are performed and analysed.

The deconstrained normal equation systems of those solutions which passed the pass/fail criteria so far are combined and solved by applying the same set of minimal constraints as before. Up to now, the four smallest eigenvalues of the combined solution were zero within numerical limits. A rescaling of the combined covariance matrix follows in order to obtain a precision level which is comparable to the input solutions.

Finally, a quality control is performed by directly comparing the combined solution with each input solution and with ITRF2000 after a Helmert transformation.

The activities concentrate on a refinement of the combination methodology of the ITRS Combination Centre (see D1), enhancement of the combination software, and improvements of tools and software for quality control and validation of the combination results. Methods for the detection of outliers in the intra-technique combination, the choice of local ties and the weighting of different solutions have been improved. The combination procedure, the processing flow and the relevant software packages are shown in figure A4.4.

TRF Combination Procedure and Software Enhancement

In order to validate the various software components and tools, and to verify the combination procedure we have computed a combined TRF solution based on multi-year solutions with station coordinates and velocities of different space techniques (see D1).

DOGS-CS Updating

New features of parameter handling as well as position and velocity transformations were implemented in the software package DOGS-CS, e.g.:

- The parameter vector may be scaled in order to change the units or to equilibrate the normal equation systems.
- The handling of Helmert transformation and Helmert parameter estimation was updated to be more flexible.
- Coordinate epochs may be transformed to arbitrary reference epochs by using given position velocities .

These features are part of a general transformation model and are realised in the programs "`cs-trafo`" and "`cs-inpar`". They can be applied on the observation equation, normal equation or solution level.

Extended Combination Model

After linearisation, the combination model is commonly defined as a Gauss-Markov-Model (GMM) – see step 1 in figure A4.5 – and is solved in a single step. The main feature of the extended model is the fact that it is an iterative model by definition, because it is extended by variance component estimation (VCE) – see step 2 of figure A4.5 - and by robust estimation (RE) – see

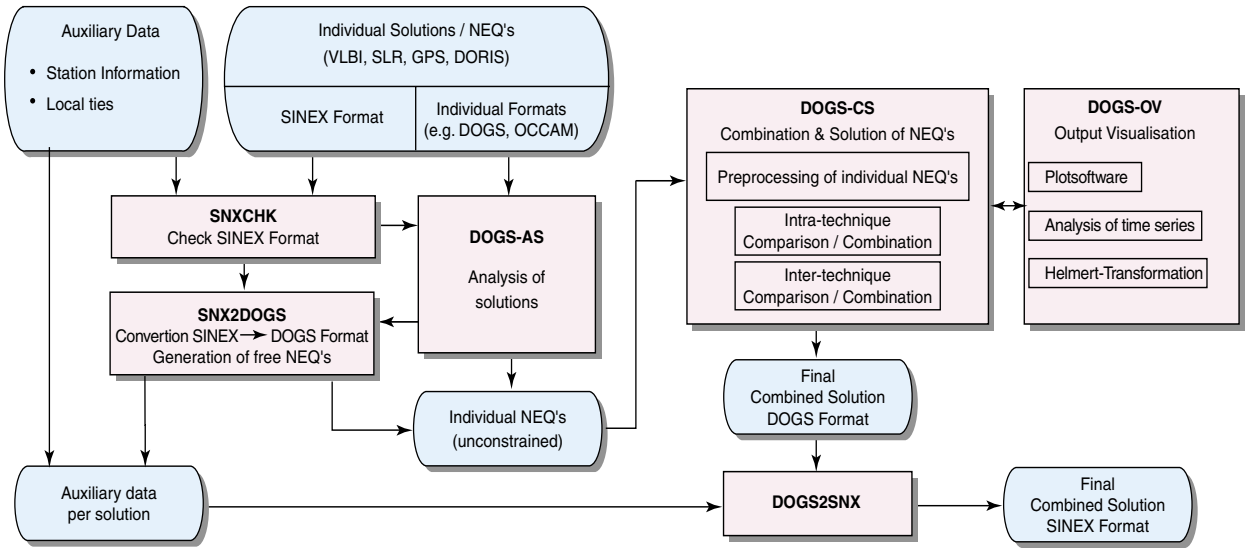

Fig. A4.4 Data flow and TRF combination procedure

step 3 of figure A4.5. Both estimation methods require iteration by theory. The extended combination model is in development.

The iteration process starts with initial values for the combined parameter vector **p** and for the variance factor s_i^2 of the *i*-th input solution. For each iteration run it holds:

In step 1 it is presumed that the covariance matrix $\mathbf{C}_{ii}$ of the *i*-th input solution is stochastically independent from the others so that **C** is a block diagonal matrix. The iteration process is stopped either by VCE in the case that in the last row of step 2 the estimated variance factor s_i^2 $(\mathbf{S}^{-1}\mathbf{q})_i$ is converging to s_i^2, which is the variance factor of the iteration step before. Or the process is stopped by RE when in the last row of step 3 the standardized residual w_i is obtaining a value between -*c* and *c*, whereby *c* is an empirical criterion value depending on the type of robust estimation model.

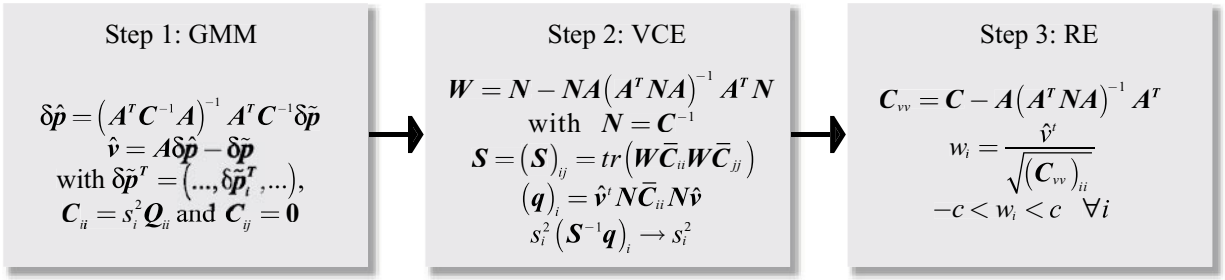

Fig. A4.5 Computation steps within the iteration process. A "~" indicates stochastic input values, a "^" estimated values.

A5 Modelling the Celestial Intermediate System

Investigations for an Optimal Parametrization of Precession

The first step of the transformation from a space-fixed reference system to an earth-fixed one, which is due to precession and nutation, leads to a celestial intermediate system. In the past, the space-fixed system was the mean equator system of epoch (FK5 system), and the celestial intermediate system was the true equator system of date. Its third axis was directed towards the Celestial Ephemeris Pole (CEP), and its first axis was directed towards the true vernal equinox. The precession matrix, which transforms from the mean equator system of epoch to the mean equator system of date, is parametrised by three Euler angles ζ, θ, z. Although the orientations of the mean and true equatorial systems of date are close to each other, the transformation between these two systems requires the detour via the ecliptic system of date because the nutation parameters $\Delta\psi$, $\Delta\varepsilon$ describe the deviation of the CEP from the mean pole with respect to the ecliptic of date (Nevertheless, the resulting nutation matrix **N** expresses a small rotation and can at a lower accuracy level be treated as a differential rotation matrix). The total transformation from the space-fixed system to the true equator system of date contains thus six elementary rotations with four precession parameters ζ, θ, z, ε and the two nutation parameters $\Delta\psi$, $\Delta\varepsilon$ (black part of the diagram in fig. A5.1).

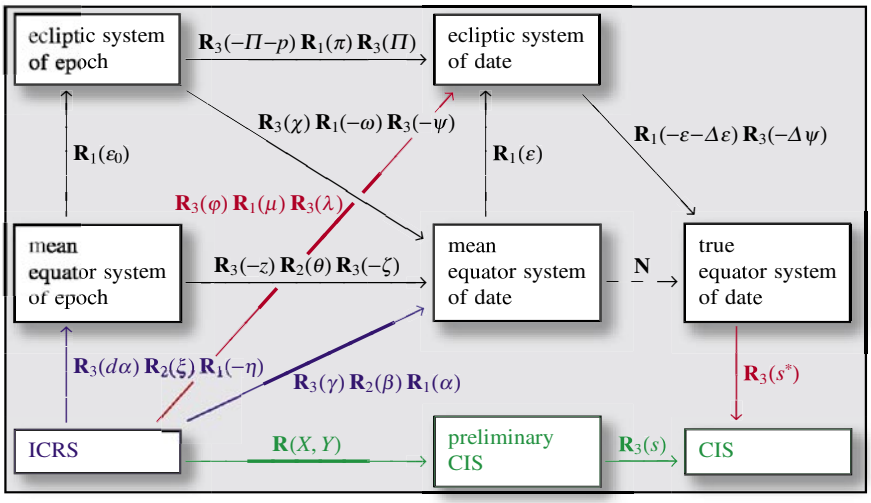

Fig. A5.1 Diagram of celestial reference systems and transformations between them.

The New Regulations of the IAU

According to the new IAU regulations, the space-fixed system is now the International Celestial Reference System (ICRS), which is realised by extragalactic radio sources. The orientation of the mean equator system of epoch with respect to the ICRS is given by the three constant Cardan angles $-\eta$, ξ, $d\alpha$ describing the offsets of the mean pole and of the mean equinox of epoch (blue extension of the diagram in fig. A5.1). The new Celestial Intermediate System (CIS) has its third axis toward the Celestial Intermediate Pole (CIP), which practically coincides with the previous CEP and whose variable direction is described by the new precession and nutation model IAU2000. Its first axis is directed to the Celestial Ephemeris Origin, which has no component of motion along the true equator. The transformation from the space-fixed system leads at first to a preliminary CIS, whose third axis is the CIP and which has then to be rotated around its third axis by an angle s being the integral of the third coordinate of the rotation vector of the preliminary CIS relative to a space-fixed system.

The IERS Conventions (2000) give an approach which is based on the Cartesian coordinates X, Y of the CIP unit vector with respect to the ICRS (green extension of the diagram in fig. A5.1).

These coordinates are calculated from the direction parameters ψ, ω of the mean pole with respect to the ecliptic system of epoch, which are given by the precession model, and from the nutation parameters and are then transformed into the ICRS by means of the obliquity ε_0 of epoch and the offset angles η, ξ, $d\alpha$. An essential disadvantage of this approach is that the nutation parameters $\Delta\psi$, $\Delta\varepsilon$, which are given by the nutation model with respect to the ecliptic system of date, have to be transformed into the ecliptic system of epoch in order to be added to the precession parameters ψ, ω.

An Alternative Way of Transformation

An alternative approach uses the true equator system of date, which already served as the old celestial intermediate system, as the preliminary CIS. Then the previous structure of the transformation from the space-fixed system to this system can essentially be maintained. However, two changes have to be taken into account.

Firstly, the old precession and nutation model has to be replaced by the new one. The treatment of nutation remains unchanged because the nutation parameters $\Delta\psi$, $\Delta\varepsilon$ of the new model play the same role as those of the old model. But whereas the old precession model described the rotations of the ecliptic and the mean equator systems by all the precession parameters given in the black part of the diagram, the new precession model merely describes the motion of the mean pole by corrections to the parameters ψ, ω referring to the ecliptic system of epoch. As a part of the transformation to the true equator system of date, however, the precession model must also provide information on the orientation of the ecliptic and hence on the direction of the mean equinox. This is indispensable, although the new CIS is no longer oriented to the equinox, because the nutation parameters still refer the ecliptic of date. As the new IAU precession model does not do that, it is a good choice to extend it in such a way that the motion of the ecliptic remains the same as in the old IAU precession model.

Such a full precession model is necessary both for the transformation from the mean equator system of epoch to the mean equator system of date and for a correct connection with nutation. A new precession model which was recently presented by Fukushima fulfils this requirement, but it is based on his own numerical computation of the motion of the pole and is therefore not in full accordance with the IAU precession.

Secondly, the ICRS has to be substituted for the mean equator system of epoch as the basic space-fixed reference system. Since the transformation between these two systems includes a small rotation component around the first axis, the resulting transformation from the ICRS to the mean equator system of date can no longer be expressed by three relatively small Euler angles about the second and third axes, but three small Cardan angles, which are denoted by α, β, γ in the diagram of figure A5.1, have to be used instead. Then the transformation from the space-fixed sys-

tem to the true equator system of date consists as before of six elementary rotations with four precession parameters α, β, γ, ε and the two nutation parameters $\Delta\psi$, $\Delta\varepsilon$.

An Optimal Parametrisation of Precession

According to this procedure, which is only a minor modification of the traditional one, the precession matrix leads to the mean equator system of date and hence rather close to the true equator system of date. This has no practical advantage because nutation involves the detour via the ecliptic system of date (unless the accuracy requirements enable the nutation matrix to be used in a differential form). Therefore another precession matrix which directly leads to the ecliptic system of date may be more favourable. As the black part of the diagram in figure A5.1 shows, there are several paths from the mean equator system of epoch to the true equator system of date using different precession parameters respectively. For example, the path via the ecliptic system of epoch contains only five elementary rotations with the four precession parameters $\prod$, π, p, ε and thus requires less computations than the traditional path via the mean equator system of date. This advantage, however, is lost when the starting system is the ICRS because that would increase the number of elementary rotations by two (but with constant angles).

A better way was recently proposed by Fukushima. As a modification of a transformation by Williams, which started from the mean equator system of epoch, he suggested to go from the ICRS straight to the ecliptic system of date by means of three Euler rotation angles λ, μ, φ (red connection in the diagram of fig. A5.1). λ and μ describe the direction of the ecliptic normal vector with respect to the ICRS. As the last of these three elementary rotations by the angle φ is around the third axis, it can be combined with the following elementary rotation by the nutation angle $\Delta\psi$ to a single elementary rotation. The total transformation from the ICRS to the true equator system of date contains thus only four elementary rotations with four precession parameters λ, μ, φ, ε and the two nutation parameters $\Delta\psi$, $\Delta\varepsilon$.

As a resume, there are two alternative paths from the ICRS to the true equator system of date to be taken into consideration: the modified traditional path with the resulting rotation matrix

$$\mathbf{R}_1(-\varepsilon-\Delta\varepsilon)\,\mathbf{R}_3(-\Delta\psi)\,\mathbf{R}_1(\varepsilon)\,\mathbf{R}_3(\gamma)\,\mathbf{R}_2(\beta)\,\mathbf{R}_1(\alpha)$$

and the optimised path

$$\mathbf{R}_1(-\varepsilon-\Delta\varepsilon)\,\mathbf{R}_3(\varphi-\Delta\psi)\,\mathbf{R}_1(\mu)\,\mathbf{R}_3(\lambda)$$

For the precession parameters α, β, γ, ε and λ, μ, φ, ε, respectively, power series have to be computed on the basis of the new IAU model. An additional series expansion is needed for the rotation angle s^* transforming from the true equator system of date to the CIS. This series expansion will have a similar structure as that of the angle s, which is given in the IERS Conventions (2000).

A6 Actual Plate Kinematic Models (APKIM)

DGFI has computed Actual Plate Kinematics and crustal deformation Models (APKIM) from always the latest space geodetic observations in approximately annual rhythm since 1988. The model APKIM2002 is based on 392 station velocities from 11 individual global solutions:

Data

- 199 GPS station velocities of the combined IGS solution IGS03P01;
- 65 SLR station velocities combined from the solutions of Communications Research Laboratory (CRL), Japan, Centre for Space Research (CSR), USA, Joint Centre for Earth System Technology (JCET), USA, and Deutsches Geodätisches Forschungsinstitut (DGFI);
- 75 VLBI station velocities combined from the solutions of Geodetic Institute University Bonn, (GIUB), Germany, Goddard Space Flight Center (GSFC), USA, Shanghai Astronomical Observatory, China, and Deutsches Geodätisches Forschungsinstitut (DGFI);
- 53 DORIS station velocities combined from the solutions of Groupe de Recherche de Géodésie Spatiale (GRGS) and Institut Géographique National (IGN), France.

Processing

Each of the 392 stations (occupations) was attributed to a rigid plate or a block in a deformation zone, respectively, according to the DGFI plate model. The total set was then processed in an adjustment of plate rotation vectors. A total of twelve rigid plates and six blocks in deformation zones is covered by the input data. These include ten rigid plates of the NUVEL-1A model (Cocos and India plates are missing due to lack of data) and, in addition, an Asia plate (East Asia) and a Somalia plate which are considered different from the Eurasian and African plates, respectively, where they are assigned to in the NUVEL model. The blocks in deformation zones include the Mediterranean (Adria, Aegea, Anatolia blocks), Japan, California, and the central Andes.

In addition to the plate and block rotations, relative datum rotation vectors for the solutions of the individual techniques were estimated in the adjustment procedure. For this purpose, the initial datum of the GPS solution (IGS03P01) served as the a-priori datum, and one datum rotation vector was estimated for each of SLR, VLBI, and DORIS combined solutions with respect to the IGS03P01 velocities. By this means the combined solution of rotation vectors refers to the IGS03P01 kinematic datum. Relative weights of the techniques (i.e., SLR, VLBI, DORIS w.r.t. GPS) were determined by an iterative a-posteriori variance estimation after Helmert.

NNR Datum

In order to fulfil the “no-net-rotation” (NNR) condition, a 1°×1° geographical grid was computed by appointing each grid point to a certain plate or block. A common rotation vector of this grid was then estimated and reduced from the previously determined plate and block rotation vectors. The result is given numerically in table A6.1 and graphically in figure A6.1 in comparison with the NNR NUVEL−1A geophysical model. Regarding the r.m.s.

errors of the estimated rotation vectors, we find many significant differences. The figure shows in particular the discrepancies in the plate boundary zones (California, Andes, Mediterranean, Japan).

Table A6.1 Rotation poles and velocities of the geodetic and geologic-geophysical plate models

	APKIM 2002			NNR NUVEL-1A		
Plate	Latitude [°]	Longitude [°]	Velocity [°/Ma]	Latitude [°]	Longit. [°]	Velocity [°/Ma]
AFRC	51.61 ± 0.52	276.60 ± 1.22	0.2906 ± 0.0025	50.57	286.04	0.2909
ANTA	62.73 ± 1.23	237.54 ± 2.04	0.2390 ± 0.0100	62.99	244.24	0.2383
ARAB	29.38 ± 56.7	277.58 ± 61.1	0.4146 ± 0.1997	45.23	355.54	0.5455
AUST	33.69 ± 0.25	36.90 ± 0.43	0.6300 ± 0.0023	33.85	33.17	0.6461
CARB	45.21 ± 2.08	246.56 ± 10.5	0.2008 ± 0.0211	25.01	266.99	0.2143
EURA	56.53 ± 0.50	261.52 ± 0.71	0.2726 ± 0.0018	50.62	247.73	0.2337
NAZC	46.21 ± 1.67	260.97 ± 0.60	0.6526 ± 0.0123	47.80	259.87	0.7432
NOAM	-1.55 ± 0.77	277.41 ± 0.35	0.1957 ± 0.0021	-2.43	274.10	0.2069
PCFC	-64.30 ± 0.18	105.52 ± 1.15	0.6588 ± 0.0029	-63.05	107.33	0.6409
SOAM	-10.74 ± 1.59	239.63 ± 4.34	0.1094 ± 0.0028	-25.35	235.58	0.1164
ASIA	59.61 ± 2.30	253.51 ± 3.81	0.3257 ± 0.0040	50.62	247.73	0.2337
SOML	53.65 ± 3.91	270.34 ± 7.25	0.3273 ± 0.0204	50.57	286.04	0.2909
Block						
ADRI	59.15 ± 4.60	282.66 ± 16.8	0.3350 ± 0.0340	50.62	247.73	0.2337
AGEA	49.62 ± 11.0	47.53 ± 39.4	0.3874 ± 0.4798	50.62	247.73	0.2337
ANAT	39.76 ± 0.18	28.80 ± 0.30	2.2508 ± 0.1323	50.62	247.73	0.2337
ANDE	4.15 ± 2.21	268.57 ± 2.09	0.3551 ± 0.0311	-25.35	235.58	0.1164
CALI	-32.19 ± 14.6	263.92 ± 5.43	0.1881 ± 0.0104	-2.43	274.10	0.2069
JAPN	-36.28 ± 0.26	312.40 ± 0.66	0.8502 ± 0.0761	50.62	247.73	0.2337
Technique						
SLR	64.08 ± 5.59	275.43 ± 9.84	0.0082 ± 0.0018			
VLBI	63.58 ± 24.3	330.10 ± 21.4	0.0211 ± 0.0014			
DORI	16.33 ± 19.9	285.33 ± 15.3	0.0277 ± 0.0053			

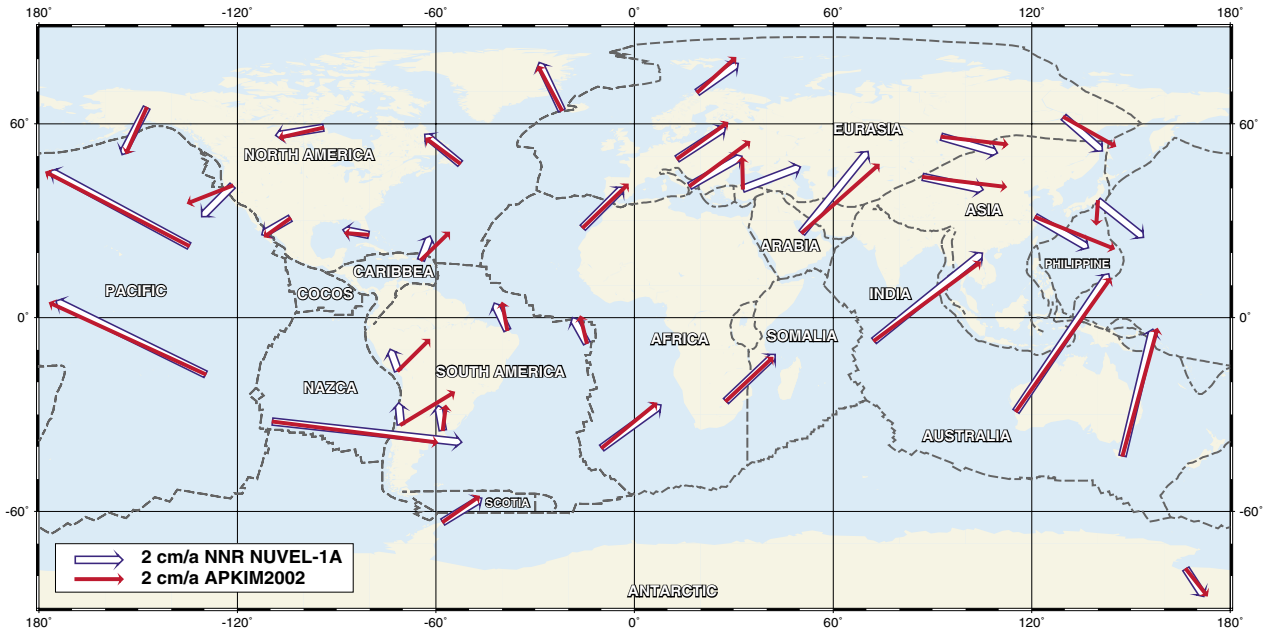

Fig. A6.1 Comparison of selected NNR NUVEL-1A and APKIM2002 station velocities

B Physical Reference Surfaces

The most important physical reference surfaces are determined by the Earth gravity field. They reflect the irregular distribution of masses on and inside the Earth. The Earth gravity field also affects satellite orbits and is important for the surveying of the Earth. Heights, for example, should refer to a unique global height reference surface. Only a precise knowledge of the gravity field allows to determine point positions and heights with the utmost accuracy. DGFI investigates high resolutions and improved representations of the Earth gravity field and contributes to the evaluation of new and upcoming gravity field missions (CHAMP, GRACE and GOCE). The sea level adjusts itself to the gravity field. It is, however, also affected by temperature, air pressure and ocean circulations. Surveying the sea level and analysing temporal sea level changes gives information on general processes within the system Earth. By satellite altimetry sea surface heights can be obtained with centimetre precision. DGFI also determines temporal sea level changes, compares them with tide gauge records and investigates their influence on the gravity field and the rotation of the Earth.

B1 Analysis of Global Gravity Field Variations

The new dedicated gravity field missions CHAMP and GRACE will not only improve dramatically the knowledge of the long and medium wavelengths of the Earth gravity field. In particular GRACE promises to observe also temporal gravity variation. Unfortunately, up to now no time series for the gravity field has been published. Table B1.1 compiles the basic characteristics of the most recent gravity field models generated with data of CHAMP and GRACE. Figure B1.1 indicates the increased significance of the GRACE gravity field coefficients. While CHAMP solutions have less than one significant digit for nearly all coefficients above degree 40 the GRACE model exhibits the same significance up to degree 90-100.

Because time series of gravity field models are not yet available, the investigations focused on strategies for combining satellite-only gravity field models with high resolution surface data.

High resolution gravity from satellite altimetry

The improved resolution of the gravity field by the new missions CHAMP, GRACE, and GOCE is achieved through dedicated space technologies (satellite-to-satellite tracking and gradiometry) and low orbiting satellites. In spite of these improvements, the downward continuation remains a fundamental problem: the observations are taken at satellite height, the gravity field, however, has to be developed down to the Earth surface. It is well known that downward continuation is an improp-

Tab. B1.1 Characteristics of new gravity field models computed with data from CHAMP and GRACE. For some orders the GFZ models have some additional coefficients above the maximum degree and order (indicated by ++) in order to account for resonant orders. Note, GFZ and CSR use different scaling coefficient A and different tide systems.

	using CHAMP data			using GRACE data		
	EIGEN-1S	EIGEN-2S	TEG4	EIGEN-GR01S	GGM01S	GGM01C
issued by	GFZ	GFZ	CSR	GFZ	CSR	CSR
year	2001	2002	2001	2003	2003	2003
type	CHAMP-only	CHAMP-only	combined	GRACE-only	GRACE-only	combined
max degree/order	119 ++)	120 ++)	200	120 ++)	120	200
GM [$10^9 m^3/s^2$]	398600,4415	398600,4415	398600,4415	398600,4415	398600,4415	398600,4415
A[m]	6378136.46	6378136.46	6378136.3	6378136.46	6378136.3	6378136.3
tide system	tide-free	tide-free	zero-tide	tide-free	zero-tide	zero-tide

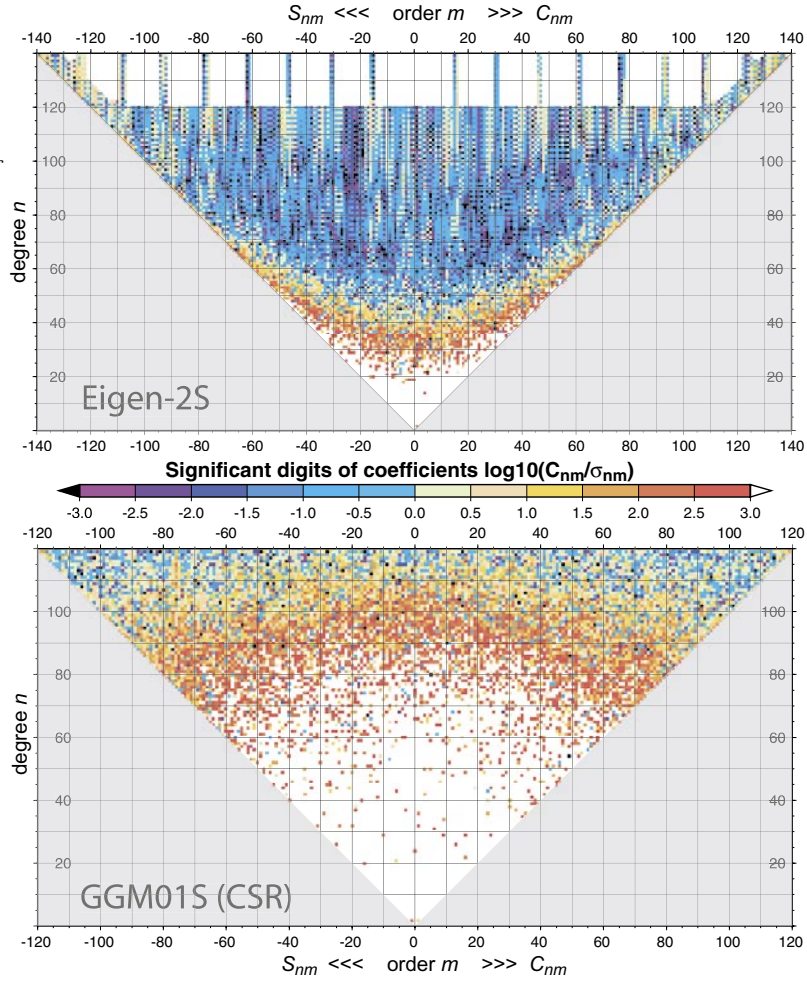

Fig. B1.1
The accuracy of CHAMP-only (here EIGEN-2S, upper panel) and GRACE-only gravity fields (GGM01S, lower panel), compared by means of the significant digits of individual coefficients expressed by log10($|C_{nm}| / \sigma_{Cnm}$). Coefficients with orange or red color, for example, have at least two significant digits. White coloured coefficients have three or even more significant digits. There are significantly more orange, red, and white areas for the GRACE-only gravity field.

erly posed problem. Satellite altimetry may stabilize this process because it directly observes the ocean surface which is closely related to the geoid. Moreover, with a grid resolution of 2'x2' altimetric models of the mean sea surface provide a much higher spatial resolution than any satellite based gravity field model. Thus, the high frequency information of the marine gravity field will be further based on satellite altimetry.

Altimetry Derived Gravity Anomalies

Up to now, altimetry and satellite-derived gravity field models were combined on the basis of gravity anomalies. The recovery of marine gravity anomalies is founded on famous geometry – gravity relationships, expressed by the Stokes and Vening-Meinesz formulas. The inversion of these formulas allows deriving gravity anomalies Δg either from the geoid or from the slopes of the geoid, like the deflections of the vertical. The inversion can be realised either by a Fast Fourier Transform (FFT) or by Least Squares Collocation (LSC) technique. For global applications both methods are one by one applied to a sequence of local areas in order to avoid – in case of LSC – the inversion of huge matrices or – in case of FFT – to ensure the validity of the planar approximation. To localize the inversion, a remove-restore technique is applied, generating in advance residual quantities by subtracting a state-of-the art gravity field like EGM96. After inversion, the gravity anomalies of this reference field are restored.

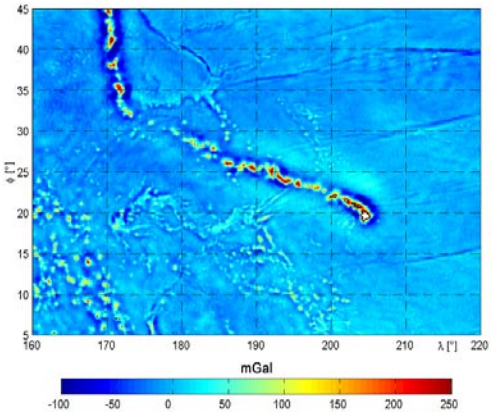

Fig. B1.2 Gravity anomalies in the central Pacific, computed from altimetry by the MatLab toolbox.

It is worthwhile to review this procedure because (i) marine gravity will be further needed for high resolution gravity field modelling even if improved gravity fields become available and (ii) the procedure implies many approximations which are to be justified. Consequently, investigations were conducted for following topics:

1. The derivative of gravity anomalies was realised by a MatLab toolbox in order to modify or tune the inversion procedure. Preliminary results (see figure B1.2) were computed with the data from the geodetic phase of ERS-1 for a test area in the central Pacific. Comparisons with the most recent data sets from Smith and Sandwell (version 9.2) and from Kort&Matrikelstyrelsen (KMS, version 2001) indicate that the toolbox gives correct results. The resolution of the anomalies may be improved by using also the geodetic mission data of GEOSAT

.

Long-Wavelength Errors of Marine Gravity

2. The new GRACE gravity field models should allow to investigate long wavelength errors in the marine gravity data. Such errors could be generated, for example, if the procedures described above *do not* account for the dynamic sea surface topography. Therefore, comparisons were initiated between the GRACE-only model GGM01S and the marine gravity data which was created by NIMA for the modelling of the EGM96 gravity field model. The NIMA data set consists of mean values for 30'×30'-equi-angular blocks. Because GGM01S is limited to degree and order 120 and (as shown above) has significant coefficients only up to degree 90 ($\approx 2°\times 2°$), the comparison must be performed with much lower resolution. It was decided to compare anomalies averaged over 3°×3° or even larger equi-angular blocks. The smoothing of GGM01S is also obligatory, because up to now all new satellite-only gravity fields exhibit a certain "trackiness" which becomes visible when slopes of the ge-

Fig. B1.3 Differences of 3°×3° mean gravity anomalies (mGal) between the GRACE-only model GGM01S and NIMA's gravity anomaly data set used for modelling of EGM96. Considerable discrepancies are found in polar areas, but also at the western boundary of the Pacific, north of New Zealand, in the Caribbean Sea, and in the east Atlantic, northwest of Africa.

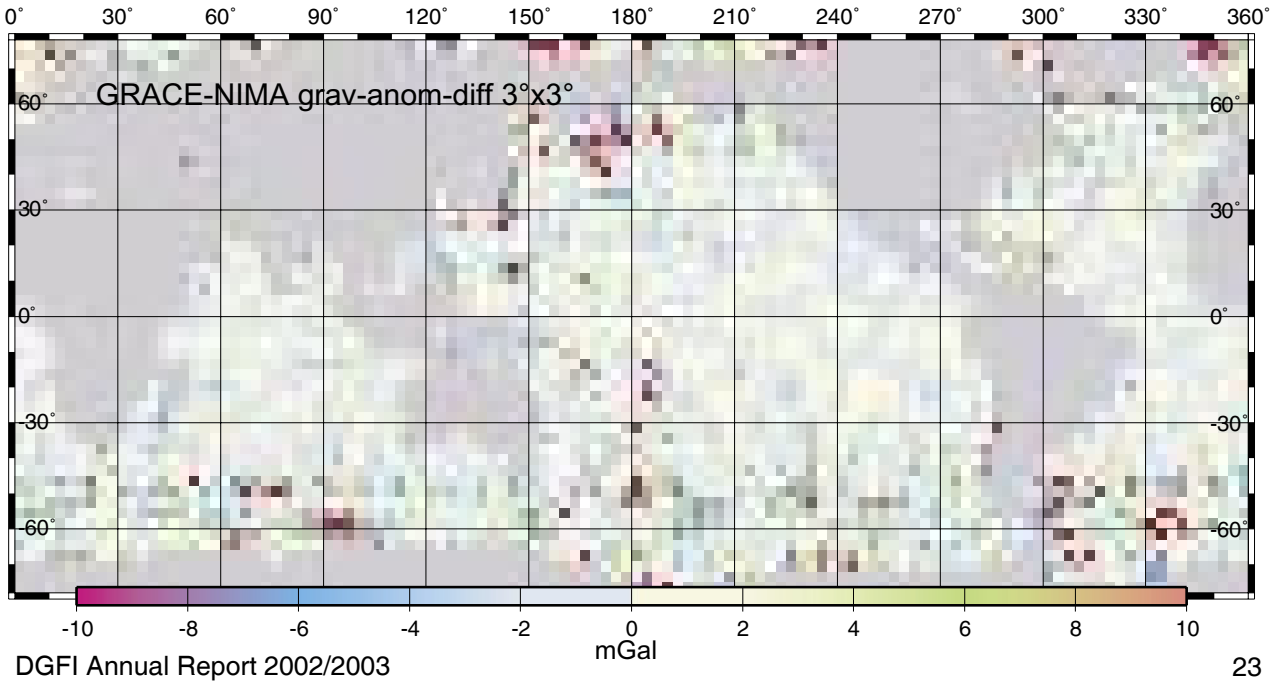

oid heights are computed and displayed. The strong track dependency is supposed to be caused by the decaying orbit. Figure B1.3 shows the anomaly differences GGM01S-NIMA for 3°×3° blocks.

3. Alternatives for estimating gravity anomalies from sea level slopes are investigated. As shown below, other gravity quantities may be used as well for the combination with satellite-derived gravity field models.

Gravity Gradients from the Mean Curvature

A much simpler gravity-geometry relationship may be used to combine altimetry and satellite-derived gravity field models. It is based on a combination of the Laplace differential equation and the Bruns formula:

$$-T_{zz} = T_{xx} + T_{yy} \quad \text{and} \quad N = \frac{T}{\gamma}$$

$$-T_{zz} = \gamma\,(N_{xx} + N_{yy}) + 2\gamma_y N_y + N\gamma_{yy}$$

where T is the disturbing potential, N the geoid undulation and γ the normal gravity. The second and third term of the right hand side of the last equation can be neglected such that the relationship reduces to

$$-T_{zz} = 2\gamma J \qquad \text{with} \qquad J := (N_{xx} + N_{yy})/2$$

Thus, the mean curvature J of the geoid is proportional to the gravity gradient of the disturbing potential.

It can be shown that the curvature – even more than the slope – is little or not at all affected by the long wavelength structure of the stationary dynamic topography. Consider a local approximation of the geoid by a second order surface

$$F(x,y) = a + pdx + qdy + rdx^2 + sdxdy + tdy^2$$

Note, a, p and q would vanish, if the surface is described in the tangential plane. The mean curvature J of the surface is

$$J = \frac{r(1+q^2) - 2pqs + t(1+p^2)}{2\sqrt{(1+p^2+q^2)^3}}$$

showing that

- J is not at all depending on the level of the geoid, and
- the slope parameter p and q are squared or multiplied with each other. Their influence is thus of second order. Moreover, typical slopes of the mean dynamic topography remain below 15 μrad.

Thus, the mean curvature of the mean sea level is a very accurate measure of the mean curvature of the geoid.

Numerical simulations were initiated in order to demonstrate that the curvature of the mean sea surface may be used to derive – in combination with satellite-only fields – high resolution gravity field structures. The computations are not yet completed and will be described in the next annual report.

B2 Multi-Scale Representation of the Gravity Field

In the last year's annual report we presented filter bank schemes to compute a multi-scale representation of the geopotential based on spherical wavelets. This year we outline how to apply parameter estimation techniques to calculate unknown model parameters. Although the modern gravity satellite missions like CHAMP or GRACE allow a precise determination of the series (Stokes) coefficients of a spherical harmonics representation of the Earth's geopotential up to a certain degree, e.g. 70 or 120, the calculation of a high-resolution gravity model requires the combination of satellite data with terrestrial and/or airborne gravity measurements. Whereas satellite data is almost globally distributed, unfortunately terrestrial and airborne observations are always restricted to certain regions or local areas. Nethertheless, the computation of any Stokes coefficient requires preferable homogeneously distributed global data sets.

Combined Approach with Spherical Harmonics and Wavelets

As an alternative to the classical spherical harmonics approach we prefer the so-called *combined approach*, i.e. the gravity field is split into an expansion in terms of spherical harmonics for the long-wavelength part and an expansion in terms of spherical wavelets for the medium- and the high-frequency parts. In this way we keep the physical meaning of the low-frequency Stokes coefficients (see also project C2). The general observation equation of the combined approach reads

$$y\ \mathbf{t} \quad e\ \mathbf{t} \quad \sum_{n\ 0}^{n} \sum_{m\ \ n}^{n} X_{n\,m}^{R} Y_{n\,m}^{R} \quad \theta_{I\ \ 1}^{R}\ \ x\ \ \mathbf{t} \quad s_{I\ \ 1}\ \mathbf{t} \qquad (1)$$

wherein $x\ \mathbf{t} \quad y\ \mathbf{t} \quad e\ \mathbf{t}$ is assumed to be a harmonic deterministic function like the disturbing potential; $y\ \mathbf{t}$ and $e\ \mathbf{t}$ denote the observation and the measurement error in an observation point $P \quad P\ \mathbf{t}$ with position vector $\mathbf{t}$ (on or outside a sphere Ω_R with radius R). $X_{n\,m}^{R}$ and $Y_{n\,m}^{R}\ \mathbf{t}$ are the Stokes coefficients and spherical harmonics of degree n and order m, respectively; the symbol " " means the spherical convolution. The scaling function $\theta_{I\ \ 1}^{R}\ \mathbf{t}\ \mathbf{t}_p$ of resolution level $I \quad 1$ is assumed to be radial symmetric. The approximation (truncation) error $s_{I\ \ 1}\ \mathbf{t}$, which is the difference between a complete spherical harmonics representation and the modelled part of the right hand side of Eq. (1), depends on the chosen scaling function. The observation equation (1) can be rewritten as *multi-scale representation* (multi-resolution representation = MRR) of the observed signal $y\ \mathbf{t}$, namely

$$y\ \mathbf{t} \quad e\ \mathbf{t} \quad x_{0\ \ n}\ \mathbf{t} \quad \sum_{i\ \ i}^{I} g_i\ \mathbf{t} \quad s_{I\ \ 1}\ \mathbf{t} \qquad (2)$$

wherein the first term on the right hand side denotes the spherical harmonics part. To be more specific, the detail signal $g_i\ \mathbf{t}$ of level i is computed by means of the spherical convolutions

$$g_i\ \mathbf{t} \quad \psi_i^R \quad \psi_i^R \quad x\ \ \mathbf{t} \qquad (3)$$

Since every wavelet function $\psi_i^R\ \mathbf{t}\ \mathbf{t}_p$ of level i, computed by means of the Legendre coefficients $\Psi_i\ n$, is related to a certain

frequency-band, the corresponding detail signal $g_i\ \mathbf{t}$ is a band-pass filtered version of the input signal.

Adjustment Model

For the numerical evaluation of the convolution in Eq. (1) we assume, that the function $x\ \mathbf{t}$ is band-limited, i.e. a spherical harmonics representation would provide $X^R_{n\,m}\quad 0$ for $n\quad n$ and $n\quad n$. Furthermore, we use the *smoothed Shannon scaling function*. Hence, if the condition $I\quad \log_2 n\quad 1$ holds for the chosen value of the highest resolution level I, the approximation error $s_{I\ 1}\ \mathbf{t}$ vanishes in Eqs. (1) and (2). Next, an appropriate admissible system of discrete computation points $P\ \mathbf{t}_{I\,k}$ with $k\quad 1\quad N_I$ and $\mathbf{t}_{I\,k}\quad \Omega_R$ is chosen, so that the band-limited function $x\ \mathbf{t}$ can be modelled exactly. In Figure B2.1 a level-3 *Reuter grid* is shown, which consists of altogether $N_3\quad 278$ points. On the other hand geodetic measurements $y\ \mathbf{t}$

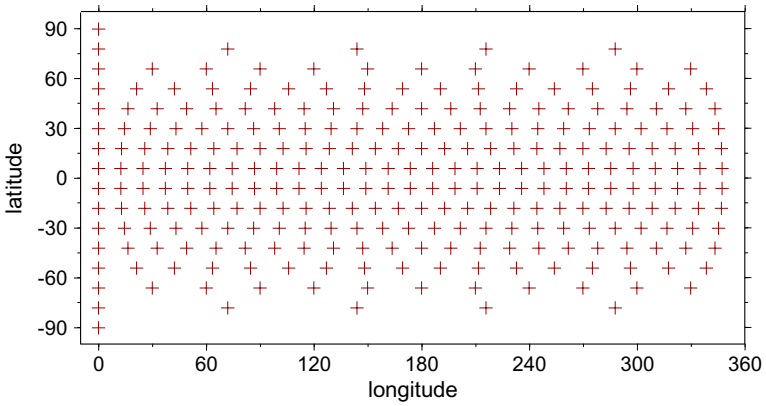

Fig. B2.1 Level-3 Reuter grid with N_3 = 278 points. Reuter grids are non-hierarchical but equidistributed point systems on the sphere.

are invariably attached to scattered observation points $P\ \mathbf{t}_p$ with $p\quad 1\quad N$. Under these assumptions the observation equation (1) yields the *linear model*

$$\mathbf{y}\quad \mathbf{e}\quad \mathbf{X}_1\boldsymbol{\beta}_1\quad \mathbf{X}_2\boldsymbol{\beta}_2\qquad \text{with}\qquad D\ \mathbf{y}\quad \sigma^2\boldsymbol{\Sigma}_y \tag{4}$$

wherein $\mathbf{y}$ and $\mathbf{e}$ denote the $N\quad 1$ vectors of observations and measurement errors, respectively. $\mathbf{X}_1$ and $\mathbf{X}_2$ are the known $N\quad u_1$ and $N\quad u_2$ coefficient matrices of the spherical harmonics part and the spherical wavelet part. The vector $\boldsymbol{\beta}_1$ contains the $n\quad 1^{\ 2}\ : u_1$ Stokes coefficients, the vector $\boldsymbol{\beta}_2\quad \mathbf{d}_I$ the $N_I\quad : u_2$ scaling coefficients. Furthermore, σ^2 and $\boldsymbol{\Sigma}_y$ are denoted as the variance of unit weight and the matrix of cofactors, respectively.

Parameter Estimation using Bayesian Inference

Since the smoothed Shannon scaling function is band-limited, the rank of the normal equation matrix of model (4) is equal to $2^{2I\ \ 2}$, i.e. a rank deficiency of $r\quad u_1\quad u_2\quad 2^{2I\ \ 2}$ exists. Note, that the regularisation problem due to the downward continuation of satellite data will be treated later. If the scaling function is chosen in an appropriate way, the spherical wavelet model part $\mathbf{X}_2\boldsymbol{\beta}_2$ is independent of the spherical harmonics part $\mathbf{X}_1\boldsymbol{\beta}_1$. Hence, the normal equation system degenerates into two parts and allows a separate determination of the estimators $\boldsymbol{\beta}_1$ and $\boldsymbol{\beta}_2$ of the unknown parameter vectors $\boldsymbol{\beta}_1$ and $\boldsymbol{\beta}_2$. To overcome the rank

deficiency problem mentioned before, the normal equation system might be solved by means of *Bayesian inference*, i.e. we assume that in the linear model (4) the unknown parameter vectors $\boldsymbol{\beta}_k$ with $k = 1\,2$ are random vectors, which might be normally distributed according to $\boldsymbol{\beta}_k \quad N\ \boldsymbol{\mu}_k\ \sigma^2 \boldsymbol{\Sigma}_k$ with the parameters $\boldsymbol{\mu}_k$ and $\sigma^2 \boldsymbol{\Sigma}_k$. If the observation vector $\mathbf{y}$ is normally distributed, too, the Bayes theorem leads to the solution

$$\boldsymbol{\beta}_k \quad \mathbf{N}_{k\,k} \quad \boldsymbol{\Sigma}_k^{\ 1} \quad {}^{1}\ \mathbf{X}_k^T \boldsymbol{\Sigma}_y^{\ 1} \mathbf{y} \quad \boldsymbol{\Sigma}_k^{\ 1} \boldsymbol{\mu}_k \tag{5}$$

for the estimator of $\boldsymbol{\beta}_k$ with the covariance matrix $D\ \boldsymbol{\beta}_k$ $\sigma^2\ \mathbf{N}_{k\,k} \quad \boldsymbol{\Sigma}_k^{\ 1} \quad {}^{1}$.

Estimated Multi-Resolution Representation

The calculation of the estimator $\boldsymbol{\beta}_2 \quad \mathbf{d}_I$ means the *initial step* of a decomposition algorithm. The following pyramid steps were explained in detail in the last year's annual report. We just want to repeat that the estimator $\mathbf{d}_i$ of the vector $\mathbf{d}_i$ in the $I \quad i^{\,th}$ *pyramid step* is obtained by successive substitution, namely

$$\mathbf{d}_i \quad \mathbf{H}_i\, \mathbf{H}_{i\ 1} \qquad \mathbf{H}_{I\ 1}\, \mathbf{d}_I \quad : \mathbf{A}_i\, \boldsymbol{\beta}_2 \tag{6}$$

In order to estimate the detail signal $g_i\ \mathbf{t}$, as defined in Eq. (3), we introduce the $N \quad N_i$ matrix $\mathbf{Q}_i \qquad \psi_i^R \quad \psi_i^R\ \mathbf{t}_p\ \mathbf{t}_{i\,k}$ and obtain the estimated detail signal vector

$$\mathbf{g}_i \quad \mathbf{Q}_i\, \mathbf{d}_i \quad \mathbf{Q}_i\, \mathbf{A}_i\, \boldsymbol{\beta}_2 \tag{7}$$

of level i. Applying the law of error propagation to this result yields the covariance matrix

$$C\ \mathbf{g}_i\ \mathbf{g}_j \qquad \sigma^2\, \mathbf{Q}_i \mathbf{A}_i\ \mathbf{N}_{k\,k} \quad \boldsymbol{\Sigma}_k^{\ 1} \quad {}^{1} \mathbf{A}_j^T\, \mathbf{Q}_j^T \tag{8}$$

between the estimated detail signal vectors $\mathbf{g}_i$ and $\mathbf{g}_j$ of levels i and j. Finally, according to Eq. (2) the *estimated MRR* of the $N \quad 1$ vector $\mathbf{x} \qquad x\ \mathbf{t}_p$ reads

$$\mathbf{x} \quad \mathbf{x}_0 \quad {}_n \quad \sum_{i\ i}^{I} \mathbf{g}_i \tag{9}$$

The first term on the right hand side means the estimation of the spherical harmonics part.

Example

Next, the combined approach is applied to *gravity anomalies of EGM 96*. In order to demonstrate the method we set $I \quad 5$ and $n \quad 7$ in the observation equation (1). Hence, we can resolve signal parts until degree $n \quad 63$, i.e. the corresponding spherical harmonics representation would contain $64^2 \quad 4096$ Stokes coefficients $X_{n\,m}^R$. Consequently, the number N_5 of points of the level-5 admissible system is restricted to $N_5 \quad 4096$. To be more specific, we choose a level-5 Reuter grid with altogether $N_5 \quad 4863$ points $P\ \mathbf{t}_{5\,k}$. With $u_1 \qquad n \quad 1\ ^2 \quad 64$ and $u_2 \quad N_5 \quad 4863$ the rank deficiency of the normal equation matrix amounts $r \quad 831$. Since Reuter grids are equidistributed point systems on the sphere, we set $\boldsymbol{\Sigma}_2 \quad c\ \mathbf{I}$ in Eq. (5), wherein c is a positive constant and $\mathbf{I}$

the unit matrix. The estimator (5) for k 2 is used to compute the detail vector $\mathbf{g}_5$ according to Eq. (7). Choosing i 3 in Eq. (2) the MRR (9) consists of the vectors $\mathbf{x}_{0\ 7}$, $\mathbf{g}_3$, $\mathbf{g}_4$ and $\mathbf{g}_5$. To compute the detail vectors $\mathbf{g}_3$ and $\mathbf{g}_4$, following Eq. (7), we use level-3 and level-4 Reuter grids with N_3 278 and N_4 1210 points, respectively; see Figure B2.1. As mentioned in the context of Eq. (1) we want to avoid the approximation error s_6 **t** . Hence, the maximum degree n of the input data is set to n 31 for I 5 (Figure B2.2a). The Figures B2.2b, c display the four estimated components $\mathbf{x}_{0\ 7}$, $\mathbf{g}_3$, $\mathbf{g}_4$ and $\mathbf{g}_5$ of the MRR. The deviations (not shown here) between the input signal and the MRR are in the range of the computational accuracy.

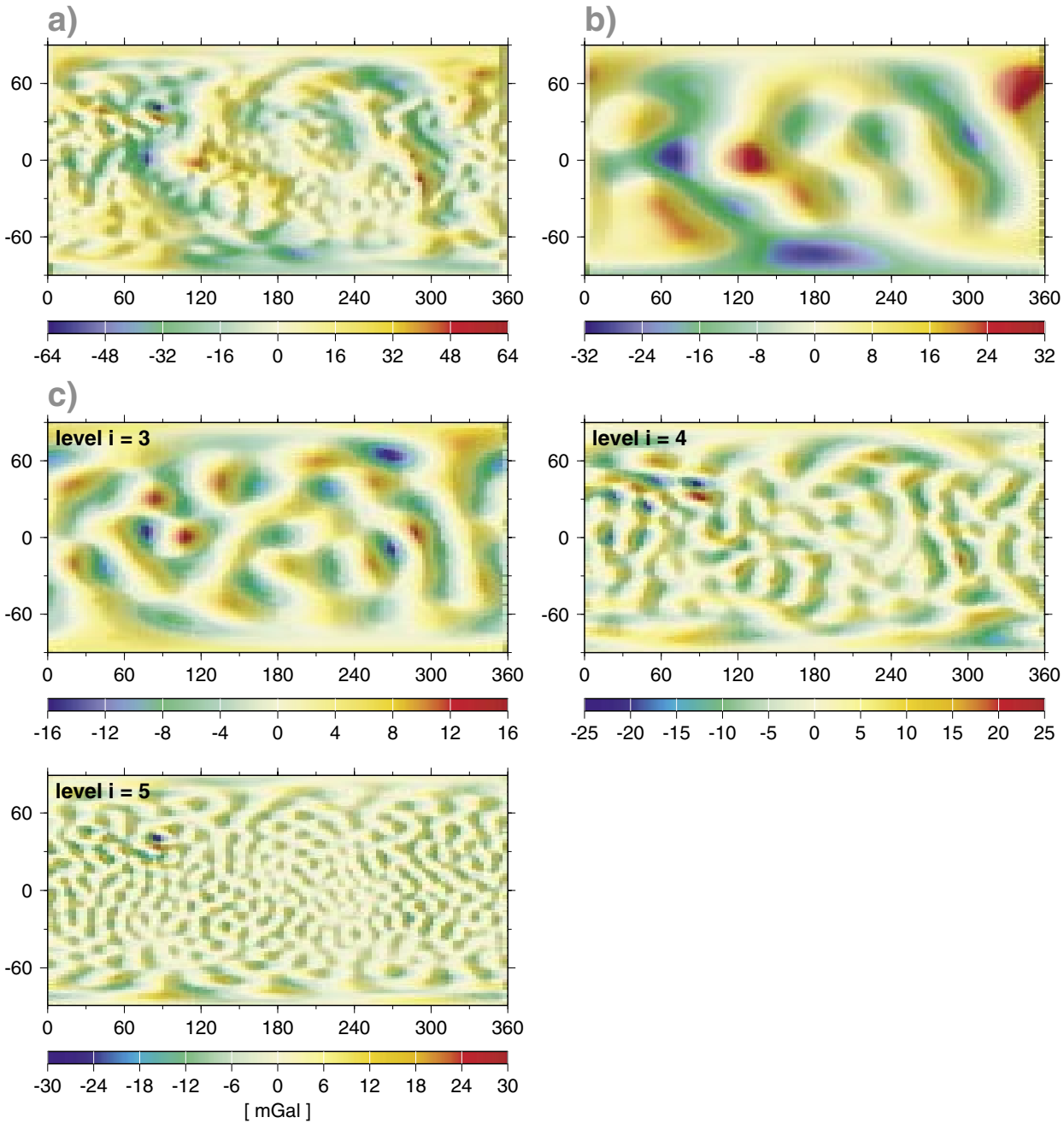

Fig. B2.2 Results of the combined estimation according to Eq. (9). a) input signal: gravity anomalies up to degree n=31; b) estimated spherical harmonic signal up to degree n=7; c) estimated detail signals for levels 3, 4, and 5.

Regularization with Wavelets

Solving Eq. (1) for the unknown function $x(\mathbf{t})$ means an *inverse problem*. As mentioned before the normal equation matrix of model (4) has possibly a rank deficiency if the applied scaling function is band-limited. Furthermore, model (4) might be ill-posed if for instance satellite observations $y(\mathbf{t})$ shall be used to estimate the disturbing potential $x(\mathbf{t}_p)$ on a sphere Ω_R close to the real Earth's surface. Consequently, another focal point of project B2 concerns the regularisation of this *downward continuation* problem. Besides Bayesian inference various other techniques are proposed, especially the Tykhonov regularisation is often used. In order to explain the functioning of regularisation in the spherical wavelet context we start with the equation $x_\rho(\mathbf{t}) = \lambda(\mathbf{t}, \mathbf{t}_p)\, x_R(\mathbf{t})$, wherein $x_R(\mathbf{t}_p)$ and $x_\rho(\mathbf{t})$ are e.g. disturbing potential values on the spheres Ω_R and Ω_ρ with $\rho > R$. The latter means the orbital sphere of the satellite, i.e. $\mathbf{t} \in \Omega_\rho$ and $\mathbf{t}_p \in \Omega_R$. The Abel-Poisson kernel $\lambda(\mathbf{t}, \mathbf{t}_p)$ with Legendre coefficients $\Lambda(n) = R(\rho^{n+1})$ provides the upward continuation. Since the *"inverse" Abel-Poisson kernel* with Legendre coefficients $\Lambda^{-1}(n) = \rho(R^{n+1})$ does not exist, the ill-posed problem $x_R(\mathbf{t}_p) = \lambda^{-1}(\mathbf{t}, \mathbf{t}_p)\, x_\rho(\mathbf{t})$ needs some kind of regularisation. We approximate it by the convolution

$$x_R(\mathbf{t}_p) = \theta^\rho_{I-1}(\mathbf{t}, \mathbf{t}_p) * x_\rho(\mathbf{t}_p) := x_R(\mathbf{t}_p) \tag{9}$$

of the function $x_\rho(\mathbf{t})$ given at satellite altitude with the scaling function $\theta^\rho_{I-1}(\mathbf{t}, \mathbf{t}_p)$, which contains the Legendre coefficients of the "inverse" Abel-Poisson kernel. The corresponding wavelet functions are computed in the usual way from the scaling function. In order to determine the resolution level $I - 1$ in Eqs. (1) or (9) we have to study the total regularisation error $\delta x(\mathbf{t}_p) := x_R(\mathbf{t}_p) - x_R(\mathbf{t}_p)$. Setting $x_\rho(\mathbf{t}) := y(\mathbf{t})$ and considering the measurement error $e(\mathbf{t})$ in Eq. (9), we obtain

$$\delta x(\mathbf{t}_p) = \theta^\rho_{I-1}(\mathbf{t}, \mathbf{t}_p) * \lambda^{-1}(\mathbf{t}, \mathbf{t}_p) * y(\mathbf{t}_p) - \theta^\rho_{I-1}(\mathbf{t}, \mathbf{t}_p) * e(\mathbf{t}_p) \tag{10}$$

Whereas the *regularisation error* (first term on the right hand side of Eq. (10)) decreases if the resolution level I increases, the *data error* (second term on the right hand side) is characterised by the opposed behaviour, because the scaling function acts as a low-pass filter. Obviously the high-frequency part of the stochastic measurement error $e(\mathbf{t})$ can be subpressed by using a band-limited scaling function.

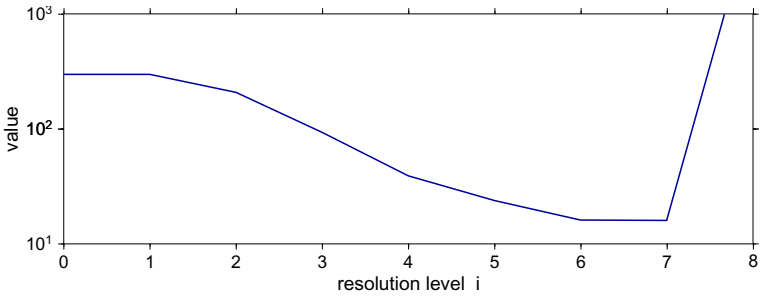

Fig. B2.3 Square root of the total quadratic error of the downward continuation of CHAMP disturbing potential data to a sphere with radius R = 6371 km. The optimal resolution level is I + 1 = 7 or I = 6.

In order to determine the *optimal resolution level I* we minimize the total quadratic error, i. e. the sum of the quadratic regularisation error and the quadratic data error, whereas the first term

is computable by means of the degree variances of the function $x_R(\mathbf{t}_p)$, e.g. from EGM 96, the latter can be calculated using the degree variances of the satellite measurement error $e(\mathbf{t})$. Figure B2.3 shows the square root of the total quadratic error in dependence on the resolution level i for the downward continuation of CHAMP disturbing potential values from satellite altitude to a sphere close to the Earth's surface.

Downward Continuation to almost Spherical Surfaces

Whereas Eq. (9) describes the downward continuation of a signal given on the orbital sphere Ω_ρ to the Earth-bounded sphere Ω_R, it is more desirable to calculate the potential e.g. for points on the reference ellipsoid or the real Earth's surface. In other words we are interested in the downward continuation to an almost spherical surface Σ. However, replacing in $\Lambda(n)$ the radius R by the radial distance $r(\mathbf{t})$ of a point $P(\mathbf{t})$ with $\mathbf{t} \in \Sigma$, we see that the resulting scaling function $\theta_{I\ 1}^{\rho}(\mathbf{t}, \mathbf{t}_p)$ is not radial symmetric anymore. Furthermore, we assume now that Ω_R is an approximating interior sphere of Σ with $R \leq \inf_{\mathbf{t} \in \Sigma} r(\mathbf{t})$ such that the *relative height* $\eta(\mathbf{t}) := r(\mathbf{t}) - R$ fulfills $0 \leq \eta(\mathbf{t}) < 1$. Next, we expand the Legendre coefficients $\rho(r(\mathbf{t}))^{n+1}$ $\rho(R)^{n+1}(1+\eta(\mathbf{t}))^{n+1}$ into the binomial series

$$\left(\frac{\rho}{r(\mathbf{t})}\right)^{n+1} \left(\frac{\rho}{R}\right)^{n+1} \sum_{k=0}^{\infty} \alpha_{n,k}\, \eta(\mathbf{t})^k \tag{11}$$

wherein $\alpha_{n,k} := (-1)^k \binom{n+1}{k}$ are the binomial coefficients. Since on the right hand side of Eq. (11) only the relative height depends on the position vector $\mathbf{t}$, the scaling function $\theta_{I\ 1}^{\rho}(\mathbf{t}, \mathbf{t}_p)$ reads with $\mathbf{t} \in \Omega_\rho$ and $\mathbf{t}_p \in \Sigma$

$$\theta_{I\ 1}^{\rho}(\mathbf{t}, \mathbf{t}_p) = \sum_{k=0}^{\infty} \eta(\mathbf{t}_p)^k\, \theta_{I\ 1}^{\rho,k}(\mathbf{t}, \mathbf{t}_p) \tag{12}$$

wherein the so-called *gradient regularisation scaling functions* $\theta_{I\ 1}^{\rho,k}(\mathbf{t}, \mathbf{t}_p)$ are again radial symmetric. The series expansion (12) implies, that according to Eq. (9) the potential value $x_\Sigma(\mathbf{t}_p)$ in a point $P(\mathbf{t}_p)$ with $\mathbf{t}_p \in \Sigma$ is calculable by means of the gradient potentials $\theta_{I\ 1}^{\rho,k}(x_\rho)(\mathbf{t}_p)$, namely

$$x_\Sigma(\mathbf{t}_p) = \sum_{k=0}^{\infty} \eta(\mathbf{t}_p)^k\, \theta_{I\ 1}^{\rho,k}(x_\rho)(\mathbf{t}_p) \tag{13}$$

On the other hand Eq. (13) also allows the *determination of equipotential surfaces*. By setting the left hand side to a constant potential value, i.e. $x_\Sigma(\mathbf{t}_p) = V_0$, the series reversal provides the relative height $\eta(\mathbf{t}_p)$ of points $P(\mathbf{t}_p)$ of the equipotential surface. We tested this procedure using CHAMP disturbing potential data. Although these first results (not shown here) are very promising, further investigations are needed, especially in order to combine satellite data with terrestrial and airborne gravity measurements. In this way we are able to compute a high-resolution gravity model based on spherical harmonics and spherical wavelets.

B3 Modelling the Sea Surface with Multi-Mission Altimetry

The mapping of the sea surface and its temporal variation is a basic product for many applications. In order to obtain long time series or a sufficient spatial resolution the data of different altimeter missions have to be combined. A consistent vertical reference with a controlled long-term stability requires a careful modelling and analysis of systematic errors. Two projects are considered in this context. The first is dedicated to the cross-calibration of ERS-2 and ENVISAT, proposed and accepted as AO416 in response to an announcement of opportunity, issued by ESA. The second project, called GeoZirk, shall provide altimeter data from all available missions for an improved numerical modelling of the antarctic circum polar current. GeoZirk is planned as a cooperation with the Alfred-Wegener-Insitut für Meeres- und Polarforschung and the Institut für Physikalische Geodäsie der Technische Universität München. GeoZirk is still in expert assessment review by the Deutsche Forschungsgemeinschaft, DFG.

AO416: Cross-Calibration between ERS-2 and ENVISAT

The cross-calibration between ERS-2 and ENVISAT is important: it enables to further extend the time series of high latitude altimeter observations, initiated by ERS-1 and continued by ERS-2. In general, altimeter missions with different orbit configurations can be linked by means of dual-satellite crossovers. However, satellites flying in tandem configuration (like ERS-2 & ENVISAT or TOPEX/Poseidon & JASON-1) are more precisely cross-calibrated by colinear analysis. This approach can give very precise estimates of the relative range bias, in particular if the temporal and spatial sampling of the two missions to be compared coincide approximately. By orbit manoeuvres the cross-track distance of repeated passes is maintained within ± 1 km. This is also true for the passes of ERS-2 and ENVISAT which follow each other over the same ground track about 30 minutes apart. There are no changes of the sea level within this short time difference. Therefore, it suggests itself to compare global sea surface heights measured by ERS-2 and ENVISAT with a mean sea surface height model.

In the final phase of the calibration period only data of two common cycles were made available: cycles 078 and 079 of ERS-2 and cycles 010 and 011 of ENVISAT. Unfortunately, the data was in a preliminary state. Media and geophysical corrections were incomplete or missing. Measurement quality of ENVISAT was not yet indicated. The satellite heights were related to different ellipsoids, the ocean tide corrections were based on different models, and the altimeter range was offset by 737 mm – an instrumental error detected later. The harmonisation of the data sets was not always possible. The overall situation allowed only a very preliminary comparison. Nevertheless, averaging the large number of observations promised to reduce the noise level.

The data of both missions was decoded and transformed to the same ellipsoid. Corrections for the inverse barometer effect and the electromagnetic bias (yet uncalibrated for ENVISAT) were not at all applied. For every one second averaged observation sea

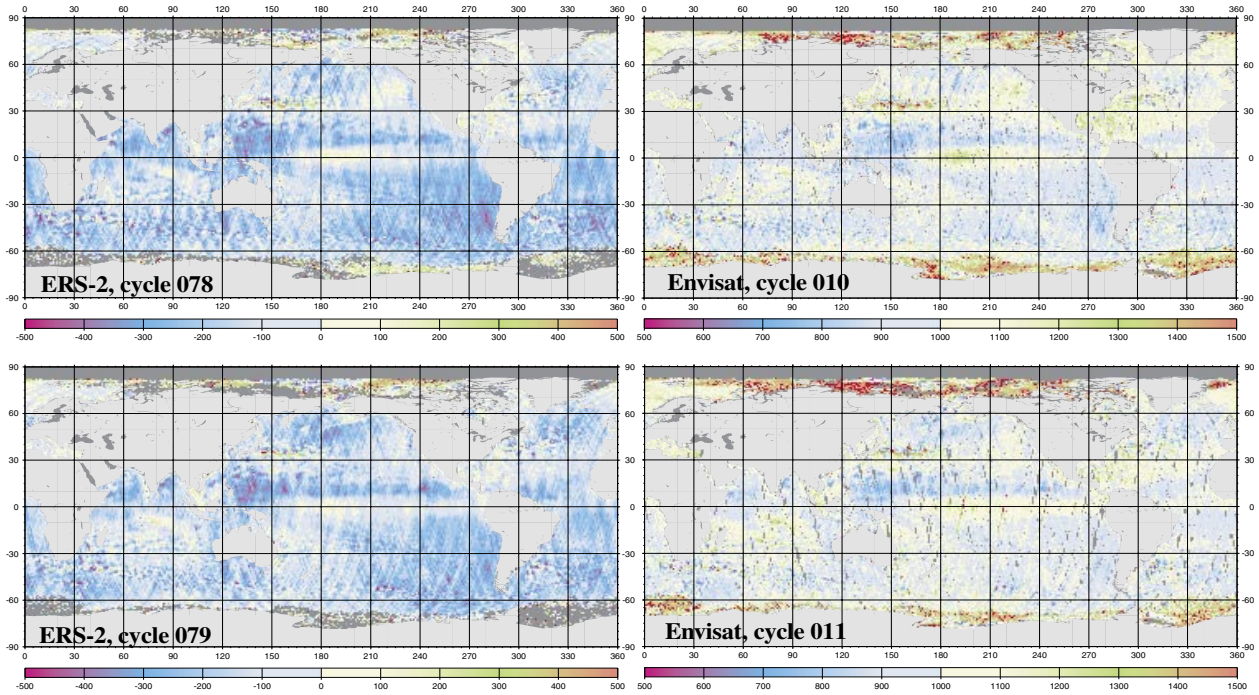

Fig. B3.1 Sea level anomalies for cycle 078 and 079 of ERS-2 (left) and cycle 010 and 011 of ENVISAT (right), computed relative to the CLS01 mean sea surface. Note, the means of the sea level anomalies differ through a 737 mm instrumental offset of ENVISAT which was not yet accounted for at the time of comparison.

level anomalies (SLA) were computed relative to CLS01, a mean sea surface model with 2'x2' resolution. Figure B3.1 shows the geographical distribution of these SLA.

Analysis of Sea Level Anomalies

In spite of the 737 mm instrumental offset both satellites show very similar pattern for the SLA. The sampling of ENVISAT has not yet the same quality (about 40% less valid data) as of ERS-2. On the other hand, the ERS-2 anomalies exhibit a more pronounced track pattern, indicated larger orbit errors than for ENVISAT. The SLAs at the polar areas are often degraded through ice coverage and other extreme weather conditions. Within ± 60° latitude (ice free area) the SLA were then fitted by least squares to the model

$$SLA = \Delta r + \Delta x \cos\phi \sin\lambda + \Delta y \cos\phi \cos\lambda + \Delta z \sin\phi$$

that accounts not only for a relative range bias Δr, but also for differences Δx, Δy, and Δz in the geocentric reference. Table B3.1 summarizes the results for the two pairs of cycles 078 (ERS-2) and 010 (ENVISAT), as well as 079 and 011. It should be emphasized that none of these estimated parameters can be taken in its absolute value. However, the differences and their standard deviations indicate a rather stable relationship between the range biases of ERS-2 and ENVISAT. From previous calibration campaigns it is known that the altimeter bias of ERS-2 is about 40 cm. There is only 7 mm difference between the two pairs of cycles. Also the differences to the geocentre have the same order of magnitude and the same sign for both pairs of cycles. This suggests that the orbits of both satellites do not consistently refer to the geocentre – a topic that requires further investigations.

Tab. B3.1 Summary of relative range biases and geocentre offsets between two pairs of cycles of ERS-2 and ENVISAT

	ERS-2	ENVISAT	Relative range-bias & geocentre offset
Latitude	<–60,+60>		
SLA edit	<–800,+800>	<+200,+1800>	
Cycle No	**078**	**010**	
Observations	1422138	868716	
Δr [mm]	–150.9 ± 0.1	249.8 ± 0.1	400.7 ± 0.1
Δx [mm]	–13.5 ± 0.2	5.7 ± 0.3	19.2 ± 0.4
Δy [mm]	14.1 ± 0.2	–7.1 ± 0.3	–21.2 ± 0.4
Δz [mm]	75.6 ± 0.3	42.9 ± 0.3	–32.7 ± 0.5
Cycle No.	**079**	**011**	
Observations	1369855	820388	
Δr [mm]	–141.4 ± 0.1	252.3 ± 0.1	393.7 ± 0.1
Δx [mm]	–6.9 ± 0.2	3.9 ± 0.3	10.8 ± 0.4
Δy [mm]	23.1 ± 0.2	–4.4 ± 0.3	–27.5 ± 0.4
Δz [mm]	34.1 ± 0.3	10.4 ± 0.3	–23.7 ± 0.5

Concept of Doubled Crossover Differences

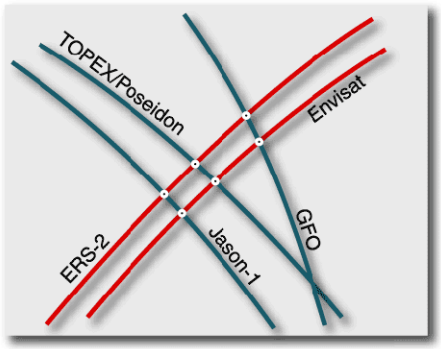

Fig. B3.2 Scenario to explain the concept of doubled crossover differences

A more precise application of the colinear analysis requires, however, a cross-track slope correction, because the cross-track distance may reach ± 1 km. This cross-track slope is usually interpolated from high resolution mean sea surfaces and therefore deviates from the actual cross-track slope. It was investigated if doubled crossover differences can be used to obtain the actual cross-track slope and to combine both, the colinear and the crossover analysis. The concept is illustrated in figure B3.2. Consider crossovers between the two tracks of the two missions in tandem configuration (e.g. ERS-2 and ENVISAT) and any third mission (e.g. TOPEX/Poseidon, JASON-1, GFO-1). For nearly simultaneous crossover events the actual along-track slope from the third satellite can be combined with doubled crossover differences (DXD) to set up observation equations for calibration parameters (e.g. bias).

For the period of one 35-day cycle of ERS-2 there are about 7618 nearly simultaneous crossover events with GFO-1, and about 6867 crossover events with TOPEX/Poseidon. Together with JASON-1 (shifted against TOPEX/Poseidon) about 15000 simultaneous crossovers within a single cycle of ERS-2 can be expected.

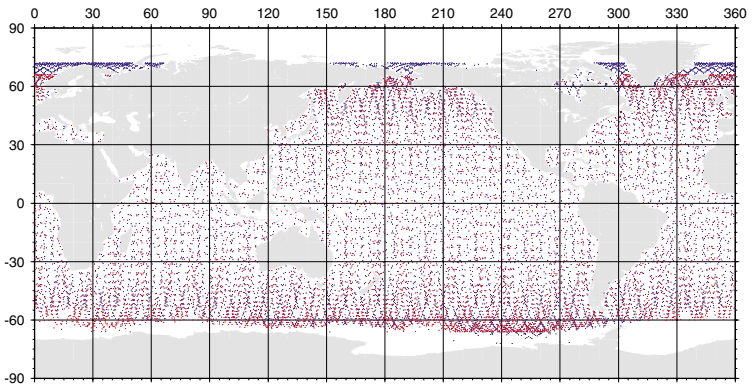

Fig. B3.3 Quasi simultaneous crossover events (time difference less than 24 hours) between ERS-2 and GFO (blue dots) and TOPEX/Poseidon (red dots).

B4 Investigations to Unify Height Systems

National height systems are traditionally defined through tide gauge registrations averaged over a certain period of time. This realisation of mean sea level is neither representative for other time periods nor does it coincide with a global height reference surface, the geoid. Therefore, it happens that there are contradictionary heights at the national boundaries and that the height systems on different continents are not related to the same height reference surface.

Sea Surface Topography

The difference between mean sea level and the geoid is called sea surface topography (SSTop). It depends on salinity, temperature, pressure, wind, etc. and reflects the water elevation affected by hydrodynamic processes. Because the SSTop is not considered in the definition of the conventional vertical datums, a systematic displacement of national height systems relative to the geoid is introduced. Thus, any knowledge about the SSTop helps to unify height systems.

The new gravity field models, in particular the GRACE solutions promise to provide an improved estimate of the long-wavelength structure of the SSTop. In principle, the SSTop can be derived from the differences between a mean sea surface and the GGM01S geoid. However, the spatial resolution is limited through the errors of the geoid. As indicated in project B1 the GMM01S has coefficients with a significant number of digits up to about degree 90 (see figure B1.1). It is also known that the CHAMP and GRACE gravity field models exhibit a pronounced meridional short-scale variation correlated with the ground track pattern. The differences between the mean sea level (CLS01) and the geoid (GGM01S) were therefore filtered to mean values or 2.5°x2.5° blocks. The result is shown in figure B4.1

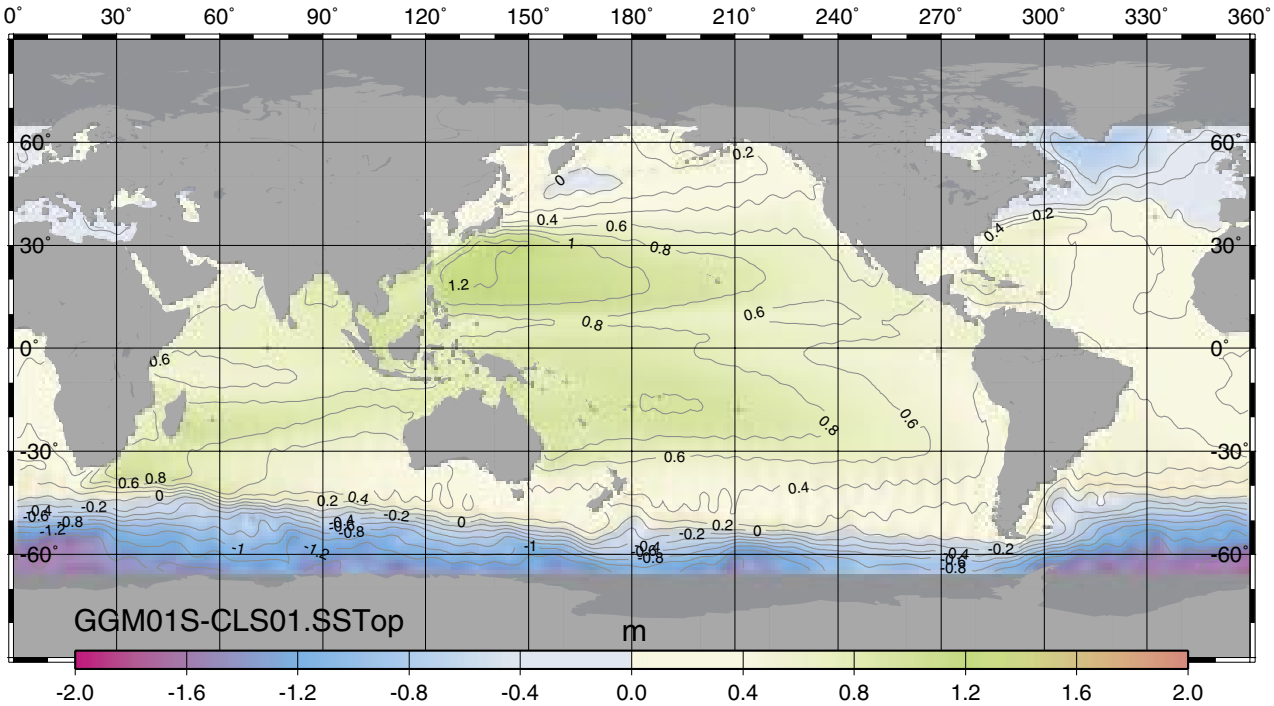

Fig. B4.1 New estimate of the large scale structure of the sea surface topography (SSTop). The differences between the CLS01 mean sea surface and the GGM01S geoid were smoothed by calculating mean values for 2.5°x2.5° blocks

Computation of High Resolution Geoids

In order to estimate the SSTop at the tide gauge location itself a high resolution geoid must be known. For the computation of a precise geoid at a coastal site several specific problems are to be considered:

1. A high resolution digital elevation model and detailed knowledge about the bathymetry are required to compute the residual terrain model correction for the remove-restore technique, generally applied in the geoid computations.
2. The terrestrial, the ship-born and the altimetry derived gravity data may be inconsistent and need to be evaluated for systematic offsets.

New Digital Terrain Models

Considerable progress has been achieved for the first point:

- NASA released the first subsets of the high resolution terrain model derived from the SRTM mission with SIR-C interferometry on the Shuttle. For North America a 1”x1” data set and for South America a 3”x3” data set (90 meter resolution) was already released. Data sets for other areas of the world will follow.

- GEBCO completed a new version of its global bathymetry data with depth defined on a 1’x1’ grid.

These data sets replaced GTOPO30 and the bathymetry of Sandwell&Smith used in previous computations. To assess the quality of SRTM, levelled heights and trigonometric heights were compared for the area of Venezuela. For 500 benchmarks with levelled heights and another 800 points with trigonometric heights the differences to the terrain model had r.m.s. of ±4 m and ±14 m respectively (for the same points GTOPO30 showed r.m.s. values of ±67 m and ±122m). The improved resolution of SRTM data versus GTOPO30 is shown in figure B4.2.

Fig. B4.2 A 1°x1° area of the Venezuelan Andes showing the GTOPO30 data (left) and the new SRTM elevation model (right). For a three-dimensional view use chromatic 3-D glasses attachted on inside backcover..

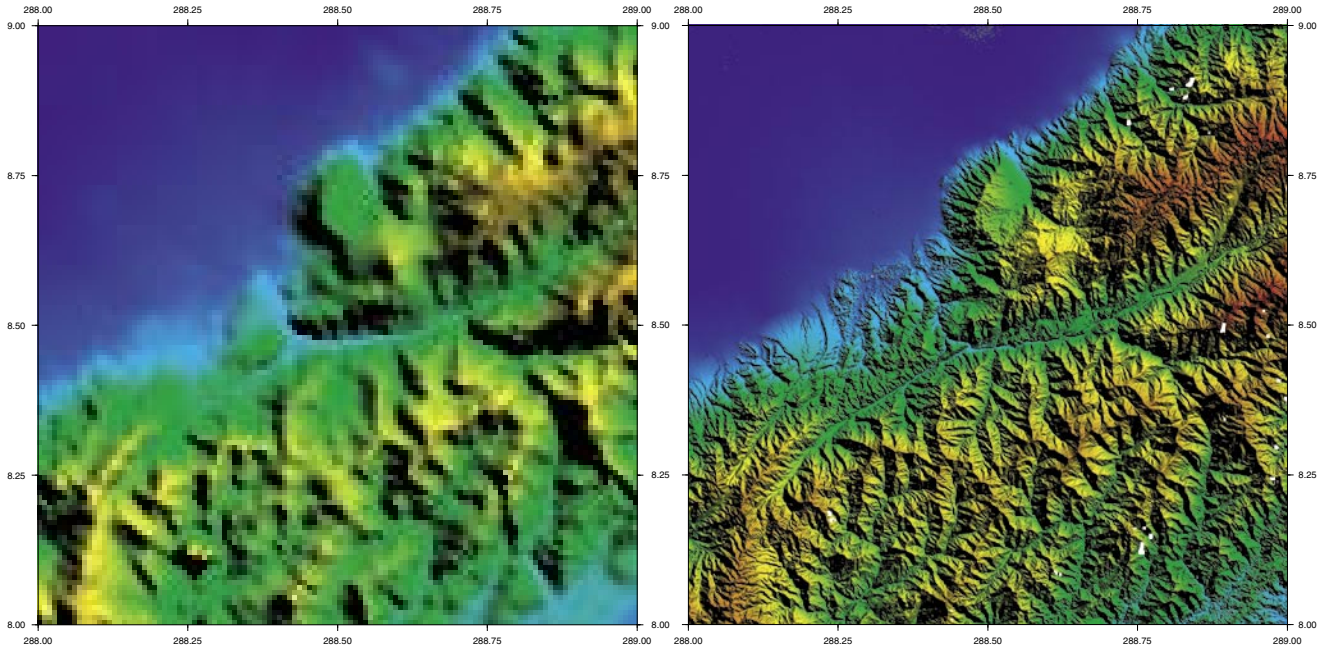

Consistent Surface Gravity Data

The second point concerning consistent surface gravity data is more demanding and difficult.

The *marine gravity data* was derived generating first a mean sea surface from multi-mission altimetry data (Seasat, Geosat, ERS-1, TOPEX/Poseidon, ERS-2 and GFO). All mission profiles were adjusted by crossover analysis and refered to the TOPEX/ Poseidon tracks. The mean sea surface was then corrected for the dynamic topography, using POCM-4B, a numerical model for the ocean circulation. The marine geoid surface obtained so far was then transformed to gravity anomalies by applying the inverse Stokes procedure.

The *ship-borne gravity data* often exhibit track dependent pattern caused by calibration errors in ports or instrumental drifts. A crossover adjustment with bias and tilt parameters was used to fix these tracks and to relate them to the marine gravity data.

The *land gravity data* was not changed. The new gravity field models do hardly allow to evaluate systematic errors of gravity data on a local scale. Moreover, necessary data and information to perform a correction or re-adjustment of the gravity network was not available.

Geoid Computation

The well-known remove-restore technique (realised with the GRAVSOFT software) was then applied to perform the geoid computations. The surface gravity was first reduced by the gravity effect of a reference gravity field (a hybrid TEG4/EGM96 model) and of the terrain model. The residual gravity anomalies were then transformed to height anomalies. The height effect of the reference gravity field and the terrain model was then restored to give the total height anomalies. In a final step these height anomalies were converted to geoid undulations.

The final geoid was then compared at 325 GPS sites where independent geoid heights could be performed by subtracting the heights obtained through levelling. Discrepancies were found up to + 1.55 m with a pronounced spatial distibution as shown in figure B4.3. The discrepancies indicate either significant errors in the land gravity data or short wavelength errors of the reference gravity field model. Therefore, the procedure to compute high resolution geoids requires further investigation.

Fig. B4.3 Spatial distributions of the smoothed differences between the gravimetric geoid and the geoid heights at 325 GPS/levelling sites.

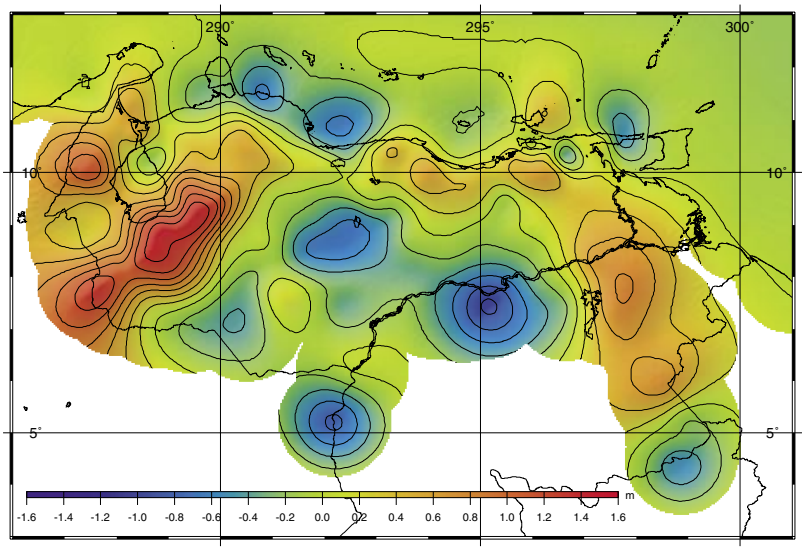

C Dynamic Processes

The consistent dynamic modelling of the physical processes in the Earth's interior and exterior is a prerequisite for the explanation of the variations of the Earth's geometrical shape, gravity field and rotation. These variations can be observed precisely by geodetic means on time scales from less than one day to decades and even longer. The understanding and numerical modelling of the dynamic processes are fundamental both for the geodetic reference systems and the combination of the space-geodetic techniques. At present, the respective research activities at DGFI are threefold: the modelling of the impact of mass redistributions on the rotation and the gravity field of the Earth, the development and adaption of analysis techniques for dynamic processes, and their application to (time) series of geodetic and geophysical parameters.

C1 Impact of Mass Redistribution on Surface, Rotation and Gravity Field of the Earth

Earth orientation parameters as observed by space-geodetic techniques show a broad spectrum of frequencies. In order to get insight into the rotational dynamics of the Earth and to study the interactions between the free and the forced polar motion, the non-linear gyroscopic Earth model DyMEG (Dynamic Model for Earth rotation and Gravity) has been developed at DGFI.

Dynamic Earth Model DyMEG

The model is based on a triaxial ellipsoid of inertia. It does not need any explicit information concerning amplitude, phase, and period of the Chandler oscillation. The characteristics of the Earth's free polar motion are reproduced by the model from rheological and geometrical parameters. Therefore, the traditional analytical solution is not applicable, and the Liouville equation is solved numerically as an initial value problem. The gyro is driven by consistent atmospheric and oceanic angular momenta which are deduced from two independent model combinations. First, atmospheric data based on the reanalyses of the National Centres of Environmental Prediction (NCEP) were applied in combination with the ocean model ECCO. The simulations cover a range of 23 years from 1980 until 2002. Second, the free atmospheric model ECHAM3-T21 GCM, which is driven by observed sea surface temperature (SST) fields, was used in combination with the ocean model OMCT for circulation and tides. The ECHAM3 + OMCT simulations cover a range of 22 years from 1973 until 1994.

The free wobble of the Earth is lengthened from the Euler period of 304 days (which would be the period if the Earth were a rigid body) to the observed Chandler period of about 434 days due to the influence of rotational deformations (pole tides). This back-coupling mechanism of rotational variations which are caused by mass redistributions induces perturbations of the second-degree spherical harmonic geopotential coefficients ΔC_{21} and ΔS_{21} which are directly linked to the Earth's tensor of inertia:

$$\Delta C_{21} = -\frac{\Omega^2 a^3}{3GM}(\Re(k_2)\cdot m_1 + \Im(k_2)\cdot m_2)$$

$$\Delta S_{21} = -\frac{\Omega^2 a^3}{3GM}(\Re(k_2)\cdot m_2 - \Im(k_2)\cdot m_1)$$

Here, a denotes the Earth's mean equatorial radius, M is the mass of the Earth and G is the gravitational constant. The effects on the

centrifugal potential due to the rheological characteristics of the model body are described by the complex pole tide Love number k_2.

In order to assess the dependence of the numerical results on rheological and geometrical input parameters as well as on the initial values and the starting date of the integration, a sensitivity analysis has been performed. In particular, the pole tide Love number k_2, the principal moments of inertia of the model body, the initial values, and the starting date of the integration were considered.

While the principal moments of inertia and the initial values were found to be uncritical parameters of DyMEG, the sensitivity analysis revealed that period and damping of the Chandler wobble as derived from the model strongly depend on the numerical value of k_2. As DyMEG accounts for the inelastic response of the Earth's mantle, which is accompanied by energy dissipation, the pole tide Love number k_2 is complex. The real part of k_2 influences the period of the Earth's free wobble, the complex part influences its damping due to the loss of energy.

In figure C1.1 the results for polar motion as derived from NCEP + ECCO forced model runs are shown for different values of the real part of k_2.

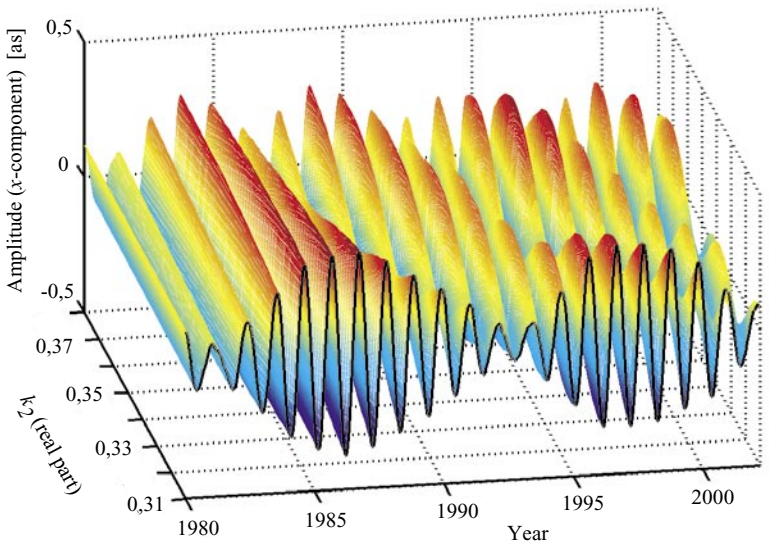

Fig. C1.1 Resulting time series of polar motion (x-component) for NCEP + ECCO forcing using different values of $\Re$ (k_2).

As clearly visible, the variation of the real part of k_2 causes a shift of the characteristic beat of free and forced oscillations. Maximum agreement with the observed Chandler period of 434 days is reached for $k_2 = 0.3520$. Here, the correlation between the model time series for polar motion and C04 reaches 0.97.

A similar analysis was performed for the imaginary part of k_2. While the value of the real part was set to 0.3520, the imaginary part was increased equidistantly from 0 (no damping) to 0.0060, which corresponds to a quality factor of Q = 48. Without forcing,

the results of DyMEG feature oscillations with a constant period of 434 days. However, they differ with respect to damping.

In order to assess the optimum damping for the NCEP + ECCO forced system, an annual oscillation with constant amplitude and a Chandler oscillation with a period of 434 days and a non-zero amplitude rate were fit to the model result by means of least-squares adjustment. The resulting Chandler amplitude rates from each model run were compared with the respective value derived from C04 for the time 1980 - 2002. From various model runs, the value $k_2 = 0.3520 + 0.0042i$ (Q = 69) was found to yield optimum agreement of the model result for polar motion with the C04 series of the IERS. When the experiments were repeated with ECHAM3 + OMCT forcing, the same value for k_2 was obtained.

The variation of the starting date of the integrations showed a different behaviour of the NCEP + ECCO and the ECHAM3 + OMCT forced results which has not been explained yet. Figure C1.2 displays r.m.s. values of the difference between the model result and C04 for polar motion (*x*-component) as well as the corresponding correlation coefficients against the varying starting date of the simulation.

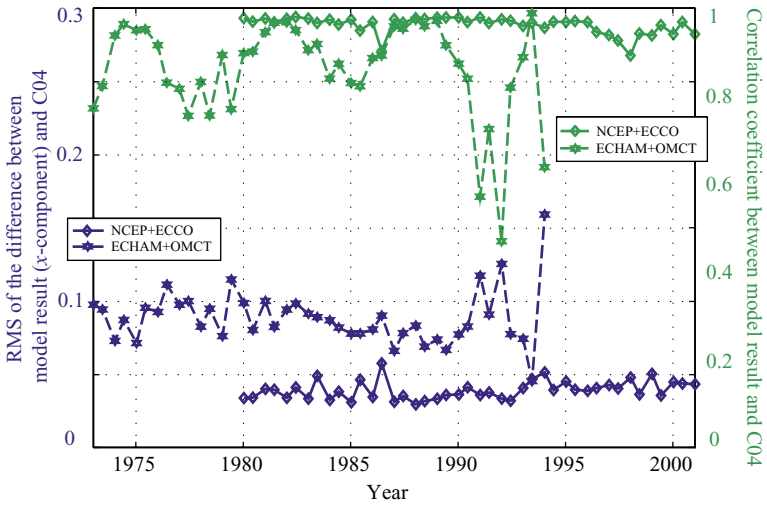

Fig. C1.2 r.m.s. values of the difference between model results and C04 (blue) and respective correlations (green) for different starting dates.

Results for Polar Motion

In general, the NCEP + ECCO results are in better agreement with C04 than those of ECHAM3 + OMCT. Obviously, certain starting dates lead to better results than other ones. For ECCO + NCEP, a start at 1.6.1986 is disadvantageous whereas the neighbouring starting dates lead to good results. For ECHAM3 + OMCT the correlations show an oscillation, which is not visible in the r.m.s. values. This oscillation does not show up in the case of NCEP + ECCO. Accordingly, the amplitudes of polar motion seem to be less affected than the phases and frequencies. During the last few years of the respective simulations, the correlations decrease because the considered polar motion series are rather short. Hence, this effect seems to be an artefact.

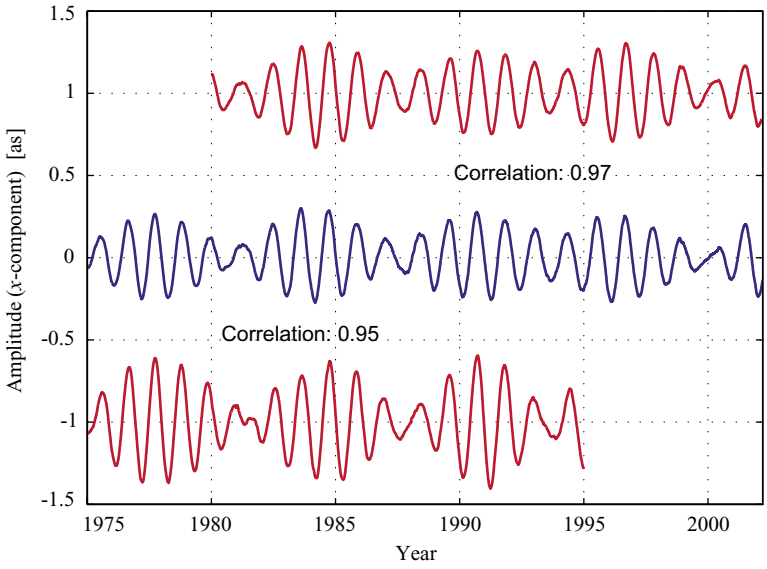

Fig. C1.3 Model results for DyMEG forced by NCEP + ECCO (top) and ECHAM3 + OMCT (bottom) in comparison with the geodetic observations C04 (middle). For better comparability, the model results are shifted by ± 1 as.

If the simulations are started at advantageous dates, the model results for polar motion are in good agreement with geodetic observations (figure C1.3). The correlations between the C04 values and the two displayed model runs NCEP + ECCO and ECHAM3 + OMCT are 0.97 and 0.95, respectively. The somewhat lower correlation for the ECHAM3 + OMCT forced result is due to an overestimated annual signal in the atmospheric excitations. Both resulting polar motion series show an undamped beat between free and forced polar motion. Hence, it can be concluded that the atmospheric and oceanic excitations are able to maintain the Chandler wobble.

An essential part of this project is funded by DFG grant DR 143/ 10.

C2 New Analysis Techniques for Observations of Dynamic Processes

During the reporting period the wavelet based analysis techniques, developed at DGFI in the last years, were applied not only to gravity data sets and Earth rotation time series but also to ionospheric models. Furthermore, fuzzy inference systems were used for short-term prediction of Earth rotation parameters.

Links Between Earth Rotation and Gravity Field Representation

In project B2 we explained how to achieve a multi-resolution representation of a signal in the spherical wavelet context. We want to mention that there generally exist two appropriate methods, namely (1) the wavelet-only approach and (2) the combined approach. The idea behind the wavelet concept is to break the signal under consideration into space and frequency dependent building blocks. Due to this localizing feature in both the spatial and the frequency domain, wavelets are an appropriate tool for detecting regional and local signal structures. In Earth rotation, however, gravity effects are monitored globally. In other words, since the Euler-Liouville differential equation includes the tensor of inertia, which is computed from the global mass distribution, regional and local gravity changes are hidden. In this context the question arises if wavelet analysis is able to provide information about these regional causes from Earth rotation data. According to Eq. (3) of project B2, the detail signal $g_i(\mathbf{t})$ of resolution level i is computed by

$$g_i(\mathbf{t}) = (\psi_i^R * \psi_i^R * x)(\mathbf{t}) = (\psi_i^R * X_i^R)(\mathbf{t}) \; . \tag{1}$$

Herein the space dependent wavelet coefficient

$$X_i^R(\mathbf{t}_p) = (\psi_i^R * x)(\mathbf{t}_p) = \int_{\Omega_R} \psi_i^R(\mathbf{t}_q, \mathbf{t}_p)\, x(\mathbf{t}_q)\, d\omega_R(\mathbf{t}_q) \tag{2}$$

gives the information about the signal structure in the vicinity of the computation point $P(\mathbf{t}_p)$ related to a certain frequency band defined by the level value i; furthermore in Eq. (2) $d\omega_R(\mathbf{t}_q)$ denotes the surface element on the sphere Ω_R. Rewriting Eq. (2) in the frequency domain yields

$$X_i^R(\mathbf{t}_p) = \sum_{n=0}^{\infty} \sum_{m=-n}^{n} \Psi_i(n)\, X_{n,m}^R\, Y_{n,m}^R(\mathbf{t}_p) \; ; \tag{3}$$

all the specific quantities of this equation are also defined in project B2. Note, that in spherical signal analysis the frequency is identified with the degree n with $n \in \mathrm{N}_0$. The five Stokes coefficients $X_{2,m}^R$ with $-2 \le m \le 2$ are functions of the six elements $I_{j,k}$ of the tensor of inertia, e.g.

$$X_{2,0}^R = -\frac{\sqrt{4\pi}\, G}{R^2} \left(I_{3,3} - \frac{I_{1,1} + I_{2,2}}{2} \right) = -\sqrt{4\pi}\, G M_e\, J_2 \tag{4}$$

Herein G, M_e and J_2 mean the gravitational constant, the total mass of the Earth and the dynamic form factor, respectively. Due to Eq. (4) and the corresponding expressions for the remaining Stokes coefficients of degree $n = 2$, Eq. (3) implicates the tensor of inertia with the wavelet coefficients. To be more specific, applying the orthogonality condition for spherical harmonics to Eq. (3) yields

$$X_{n,m}^R = \frac{1}{\Psi_i(n)} \int_{\Omega_R} X_i^R(\mathbf{t}_p) Y_{n,m}^R(\mathbf{t}_p) d\omega_R(\mathbf{t}_p) \tag{5}$$

with $\mathbf{t}_p \in \Omega_R$ and $\Psi_i(n) \neq 0$. By setting n=2, m=0 and equating the right hand sides of formulae (4) and (5) we obtain the expression

$$J_2(t) = -\frac{1}{\sqrt{4\pi}\, GM_e\, \Psi_i(2)} \int_{\Omega_R} X_i^R(\mathbf{t}_p, t) Y_{n,m}^R(\mathbf{t}_p) d\omega_R(\mathbf{t}_p) \tag{6}$$

which relates the dynamic form factor J_2 to the wavelet coefficients $X_i^R(\mathbf{t}_p)$. Similar results can be derived for all the elements of the tensor of inertia. The bottom line of these equations is that global quantities like J_2 are modeled by space dependent parameters. Hence, we are in the position to study the effect of regional variations on global parameters by means of forward modelling. Furthermore, in Eq. (6) a time dependency is considered, because the satellite gravity missions provide time series for the wavelet coefficients, namely $X_i^R(\mathbf{t}_p, t)$.

Total Electron Content of the Ionosphere

A second focal point of project C2 concerns the modelling of the total electron content (TEC) of the ionosphere. It is well-known that satellite measurements are affected by the electron distribution in the ionosphere. The basic observation equation, the so-called tomographic equation, given as

$$P_{j,4}^k(t) + e_{j,4}^k(t) \approx C_{j,p}^k + k_4\, TEC(t) \tag{7}$$

relates the total electron content

$$TEC(t) := \int_{R_j}^{S^k} N_e(\mathbf{t}, t)\, ds \tag{8}$$

to the inter-frequency measurement $P_{j,4}^k(t) := P_{j,2}^k(t) - P_{j,1}^k(t)$, which is computed from the two pseudo range measurements $P_{j,1}^k(t)$ and $P_{j,2}^k(t)$ to a GPS satellite on the frequencies f_1 and f_2. The indices j and k indicate receiver position $R(\mathbf{t}_j) = R_j$ at receiving time t_j and satellite position $S(\mathbf{t}_k) = S^k$ at transmitting time t_k, respectively. Furthermore, we assume that all the time independent quantities are merged to the constant $C_{j,p}^k$; the constant k_4 is defined via the relation

$$k_4 := 40.28 \frac{f_2^2 - f_1^2}{f_1^2\, f_2^2}, \tag{9}$$

$e_{j,4}^k(t)$ means the observation error. A similar equation can be derived for the inter-frequency phase difference measurement. In Eq. (8) $N_e(\mathbf{t},t)$ means the space and time dependent electron density along the signal path between S^k and R_j. Usually, the TEC value is transformed into the vertical total electron content (VTEC) by means of a zenith dependent mapping function.

Wavelet Modelling of Electron Density

Ionospheric models like the International Reference Ionosphere (IRI) or CODE's Global Ionospheric Map (CODE-GIM) describe the distribution of the electron density based on spherical shells. Frequently it is assumed that the electron content is concentrated in an infinitesimal thin shell. In this way VTEC is modeled by

means of a low-degree spherical harmonics approach. We intend, however, to describe the four-dimensional electron density by a four-dimensional wavelet approach based on so-called tensor product wavelets. There are two main reasons for applying wavelets to model the electron density of the ionosphere, namely:

- The spatial distribution of the measurements is not equal, i.e. data gaps exist in certain regions. Hence, the qualifications for applying a spherical harmonics model to VTEC data sets are not fulfiled.

- The study of regional features like the equatorial anomaly is of great interest. There are, for instance, theories that electric and magnetic disturbances are linked to earthquakes. Thus, TEC variations could serve as short-term forerunners.

In order to gather some experience with wavelet modelling of TEC data, we decomposed the twelve VTEC data sets from CODE-GIM for August 17, 2002. Figure C2.1 shows the time evolution of the detail signal of resolution level i=2 during the day. According to Eq. (1) Figure C2.1 shows the detail signal $g_2(\mathbf{t},t)$ varying with time, i.e. discrete values of the signal $g_2(\lambda, \beta, h$=450km, $t)$ with longitude λ, latitude β, height h above

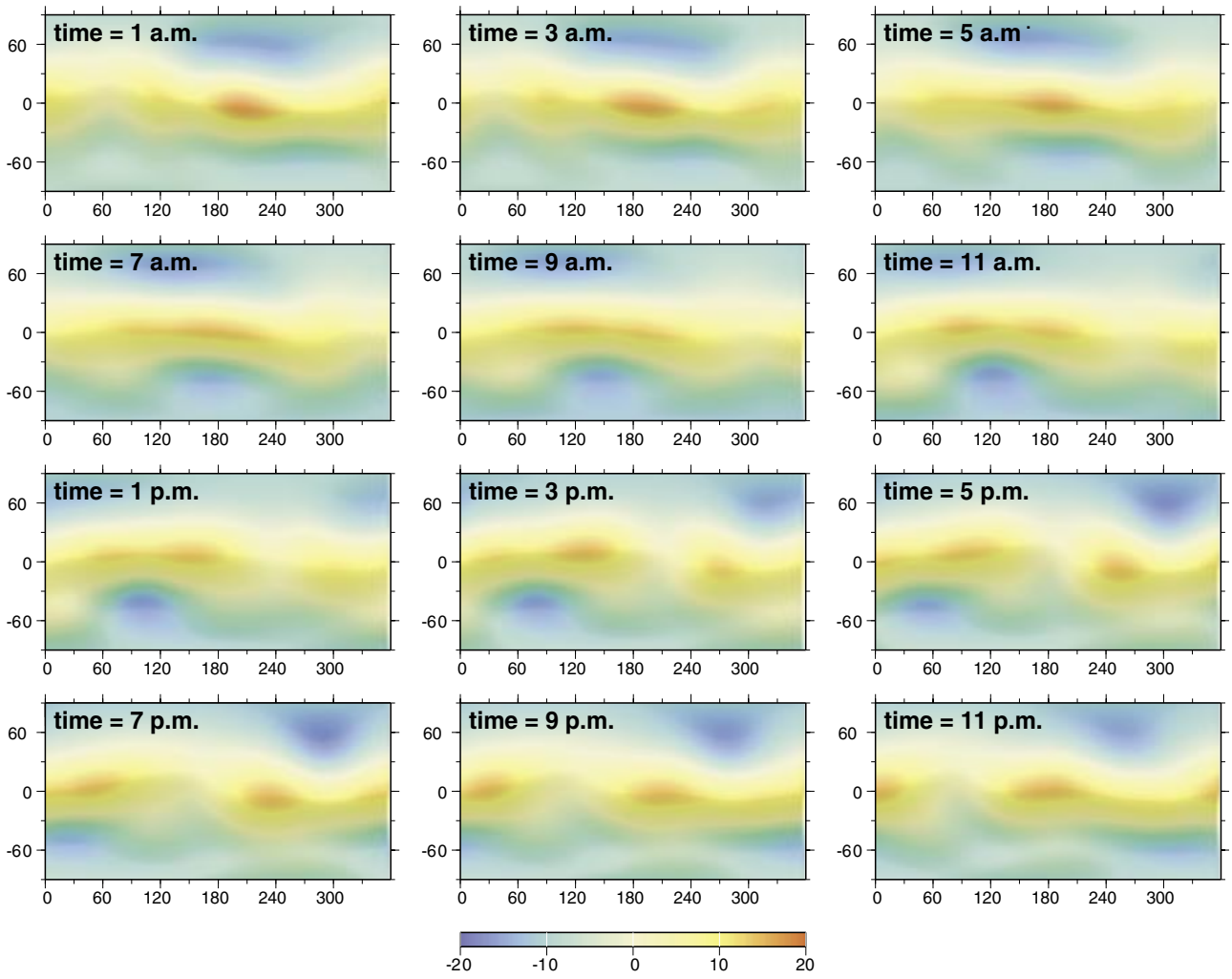

Fig. C2.1. Spatial variation of the detail signal of level i = 2 of the CODE-GIM VTEC data set during one particular day. The coordinate system is Earth-fixed.

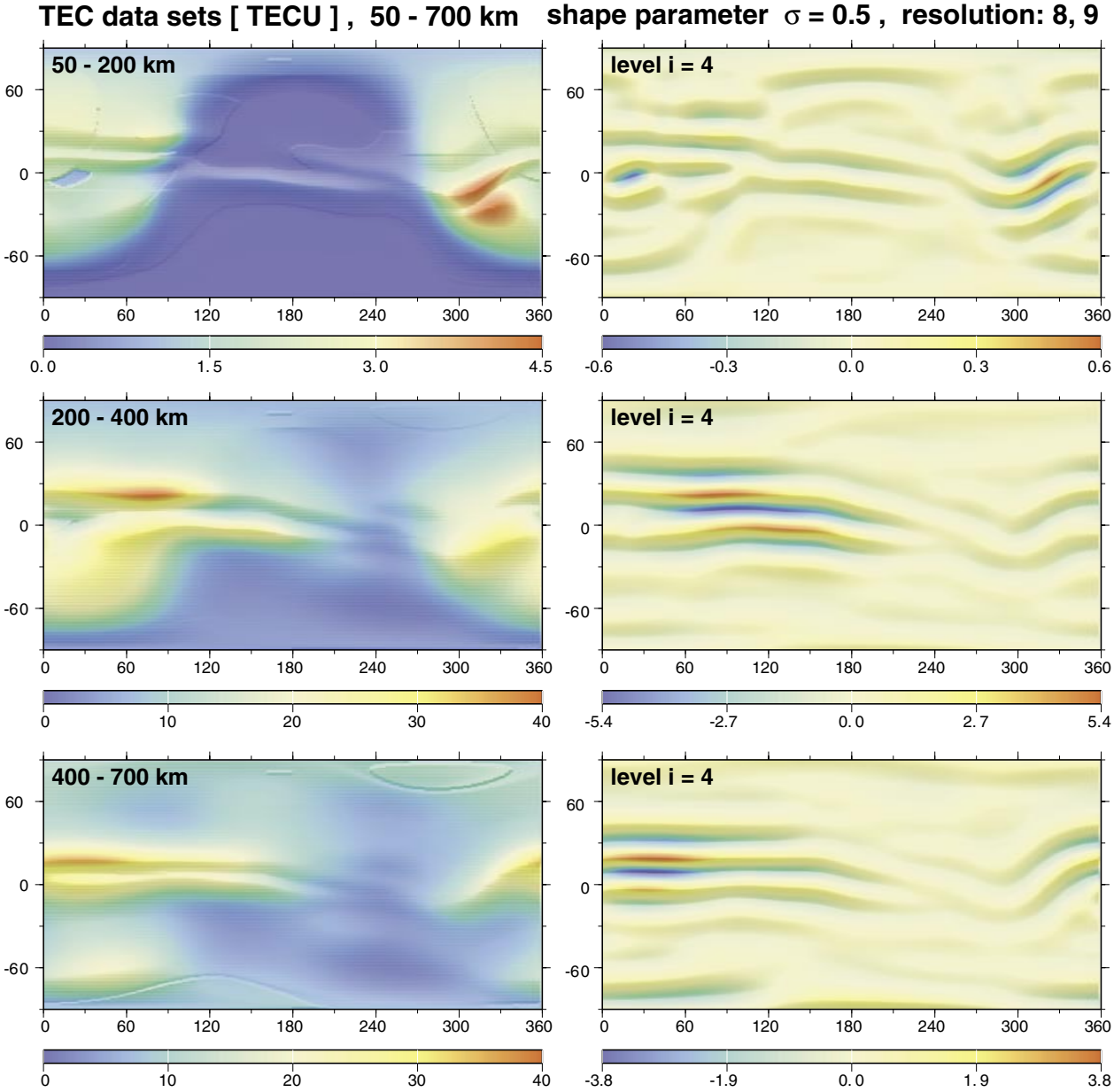

Fig. C2.2. Height variations of the detail signal of level i = 4 (right hand side) related to the corresponding VTEC data sets (left hand side) of different shells.

a spherical Earth and time *t*. On the other hand, Figure C2.2 displays the height dependency of VTEC. The three panels on the left hand side show the radial variation of the total electron content. The signals are computed from IRI 2001 and related to three different shells, namely from 50 to 200 km, from 200 to 400 km and from 400 to 700 km. The corresponding panels on the right hand side show the detail signals of resolution level *i*=4, i.e., $g_2(\lambda, \beta, h, t{=}31.7.2001{,}12h)$.

Short-term Prediction of Earth Rotation Parameters by ANFIS

Adaptive network based fuzzy inference systems (ANFIS) use fuzzy logic and fuzzy control. They consist of a classical fuzzy inference system (FIS) with a fuzzification unit (definition of linguistic variables), a rule base (logical combination of input quantities, implication rules) and a defuzzification unit (derivation of a precise output). Here, a Takagi-Sugeno-type FIS was considered. The FIS is enclosed by an algorithmic unit which allows to tune and to optimize the variables and rules (adaptive network). The ANFIS technology was applied to the

prediction of Earth rotation parameters (ERP), i.e. the Length of Day (LOD) and polar motion. The ERP C04 time series of the International Earth Rotation Service (IERS) was used as input for the prediction. Well-known tidal effects in the ERP series were removed a priori from the C04 series. The residual series were used for training (i.e. optimization of parameters) as well as for validation (i.e. comparison of predicted data with independent observed data) of the network.

Different network architectures were discussed and compared in order to find the most adequate rules for the ANFIS. The following formula represents the prediction rule for LOD for the first day in future which was found as optimum in a best-fit sense.

$$\{x(t-4), x(t-3), x(t-2), x(t-1), x(t)\} \rightarrow x(t+1)$$

Hence, just the data of the last five days were introduced to the prediction. There was no gain in precision when using days which were further in the past. The results of the prediction were analysed and compared with those of other methods. It could be shown that short-term ERP values predicted by ANFIS yielded r.m.s. errors which were equal or even lower than those from other methods which applied, e.g., stochastic processes or Artificial Neural Networks. Figure C2.3 shows ANFIS results for the prediction of LOD. The study revealed that the prediction by ANFIS is rather easy to establish.

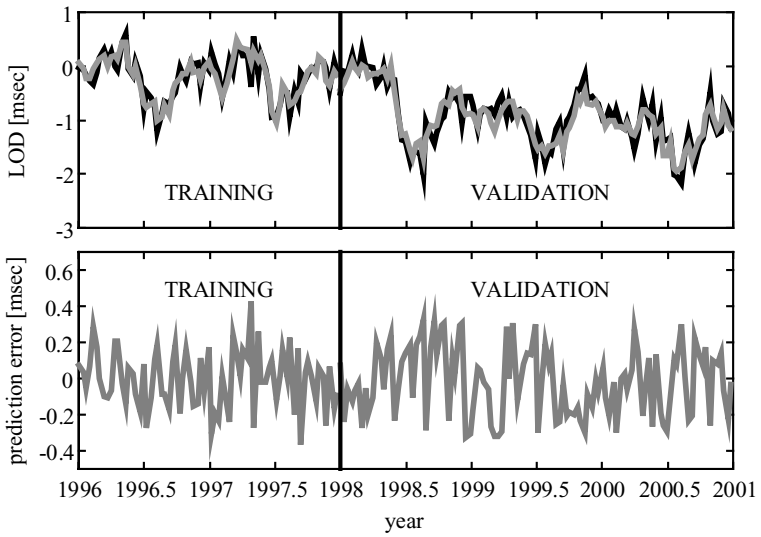

Figure C2.3 Prediction of LOD values (10th day in future) using ANFIS. The upper graph shows the observed (gray) and predicted (black) data for a part of the training period (1980...1997) and for the validation period (1998...2000). The lower graph shows the corresponding prediction errors.

C3 Analysis of Time Series of Geophysical Processes

The work on the analysis of time series of geophysical processes has been continued. One topic was concerned with the relationship between Earth orientation parameters (EOP) and the Stokes coefficients of degree 2 of the gravity field. A second part of the work was dedicated to the empirical analysis of time series in order to identify characteristic asymmetric signal structures.

Variation of ΔC_{20}

As there is a functional relationship between the variations ΔI of the tensor of inertia and those of the Stokes coefficients of degree 2 (C_{2i}, S_{2i}) of the Earth's gravity field, the gyroscopic model DyMEG (see project C1) was extended in order to additionally derive time series of the variations of these coefficients. In case of ΔC_{20} the respective equation reads as

$$\Delta C_{20} = \frac{1}{2\sqrt{5}Ma^2}\left(\Delta I_{11} + \Delta I_{22} - \Delta I_{33}\right)$$

where M denotes the total mass and a the semi-major axis of the Earth. Hence, the computed time series of gravity field coefficients are consistent with the series of Earth orientation parameters (EOP) which are commonly produced by DyMEG. The forcing mechanisms of the variations of the gravity field coefficients and the EOP differ with respect to the motion terms (due to atmospheric and oceanic circulation) which only in uence the latter. But as the corresponding matter terms in uence both parameter groups, the time series of the Stokes coefficients should be capable for an independent validation of DyMEG with data from Satellite Laser Ranging (SLR) or from the gravity field missions (CHAMP, GRACE).

At present, only SLR data provides the temporal variation of the Stokes coefficients of degree 2, mainly of ΔC_{20}. For this reason first studies on ΔC_{20} were carried out. The model series with daily values was derived by means of DyMEG. Here, the model combination NCEP+ECCO (see project C1) was considered for atmospheric and oceanic forcing. The data series which has weekly values was supplied by DGFI's SLR group (see project A2). It is based on LAGEOS-2 observations. Both time series are compiled in Figure C3.1.

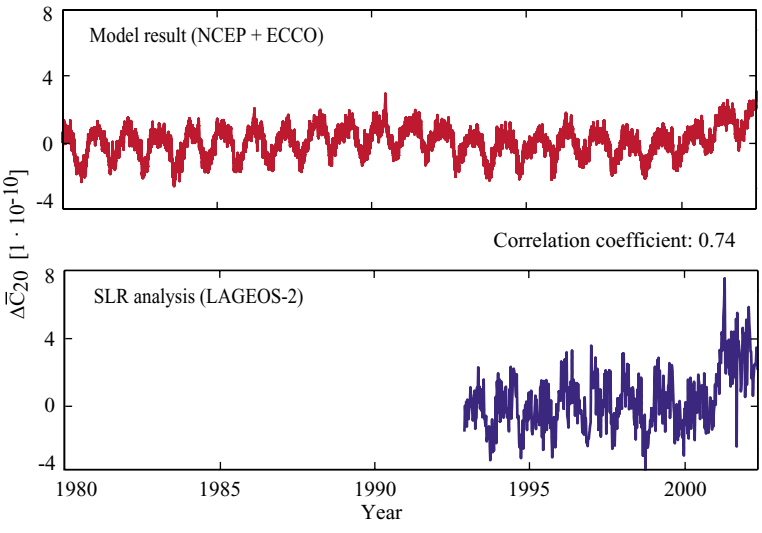

Fig. C3.1 Time series of the variation of Stokes cofficient ΔC_{20}. The upper plot shows the model results from DyMEG, the lower plot represents SLR observations.

The annual signal can clearly be seen in both series. However, the SLR series shows an additional semi-annual signal which is not visible in the model series. This effect could not be explained yet. Hence, further studies are needed both on the model side and on the observation side.

Asymmmetric Signal Components in LOD

Typical analysis strategies such as the Fourier analysis or the Morlet Wavelet analysis imply symmetry (or better: sine form) of the periodic signal components. The deviation from the sine form would cause, e.g., overtones to the fundamental oscillation. If ones studies only a special period band such as, e.g., the annual one, the interpretation could be incomplete. Several analysis approaches have been applied to the C04 Length-of-Day (LOD) time series of the IERS in order to assess possible deviations from the sine form. The main focus was put on the derivation of a realistic annual signal. In this case both the longterm signal component and the well-known tidal effects on LOD were reduced in advance. First results are given below.

A first analysis approach was based on moving average operators in order to distinguish between a short-term signal component (monthly and shorter periods), an annual (or mean-term) component and a long-term component. The different components are shown in Figure C3.2. The mean-term component was then used for the calculation of a mean annual signal. This very smooth signal is shown in Figure C3.3 (‘moving average‘).

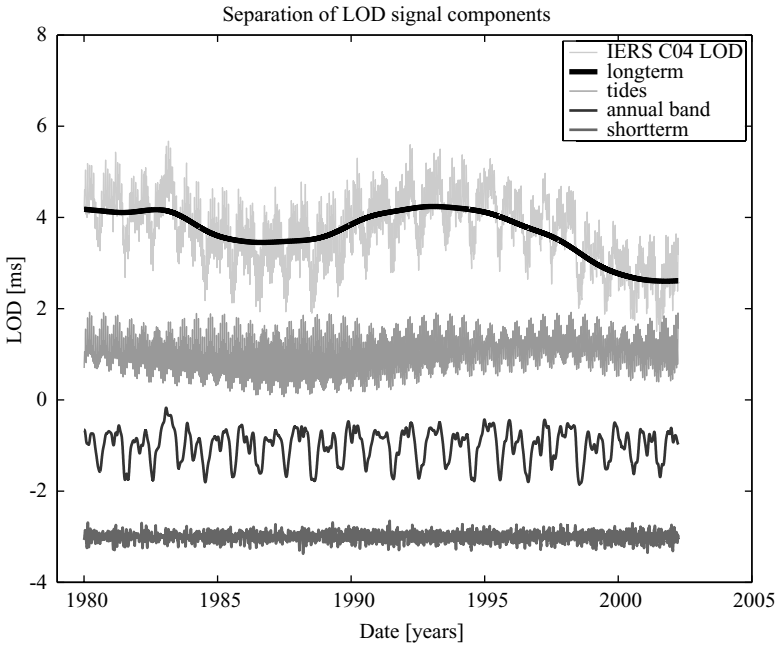

Fig. C3.2 Separation of IERS C04 LOD into different period regions (long-term, annual, short-term) and the variations induced by tides.

A second approach is based on the least-squares estimation and robust estimation, respectively, of amplitude and phase of the annual sine signal and of a certain number of overtones. Depending on the level of significance, statistical tests showed relevant overtones of the annual period down to periods of 30 to 72 days. Figure C3.2 shows the annual signal which was reconstructed from the fundamental annual period and four (light gray) and ten (medium gray) overtones, respectively.

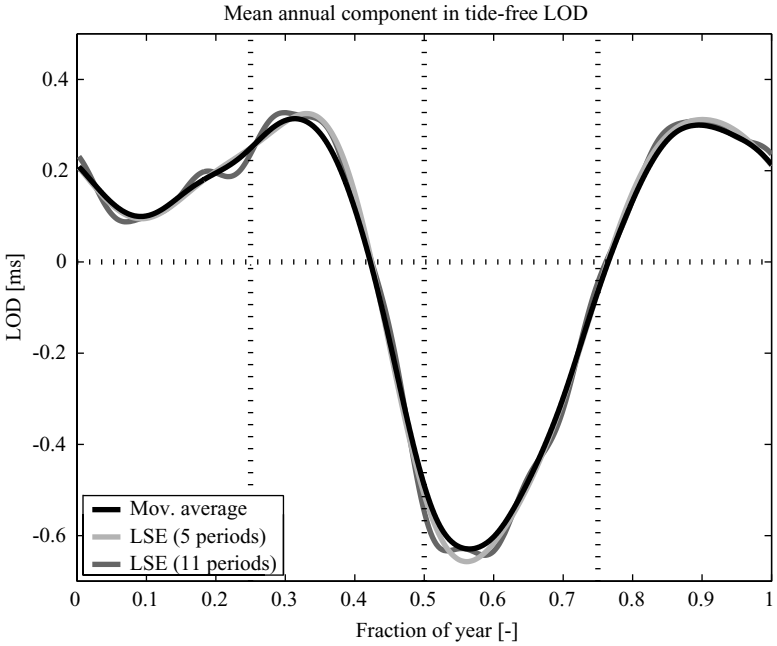

Fig. C3.3 Comparison of mean annual signals in LOD derived on the one hand by a moving average operator and on the other hand by least-squares estimation of the annual signal and a certain number of overtones (5 periods, 11 periods).

Obviously, both analysis approaches yield in general quite similar results. However, there are differences in the details such as the additional oscillation in case of the function consisting of 11 periods. Further work is needed in order to assign these results to signal components in the atmospheric and oceanic excitation.

D International Services

DGFI participates intensively in several scientific services of the International Association of Geodesy (IAG). By this means it contributes significantly to the international scientific cooperation and provides its research results directly to the scientific community. On the other hand it gets direct access to the original data and results of other institutions and research groups for its own investigations. In the International Earth Rotation and Reference Systems Service (IERS) DGFI acts as a Combination Centre for the International Terrestrial Reference Frame (ITRF) and as a Combination Research Centre (CRC). In the International GPS Service (IGS) DGFI operates the Regional Network Associate Analysis Centre for South America (RNAAC-SIRGAS). For the International Laser Ranging Service (ILRS) DGFI holds one of the two global data centres, the EUROLAS Data Centre (EDC), and works as an Associate Analysis Centre (AAC). DGFI is a Special Analysis Centre of the International VLBI Service for Geodesy and Astrometry (IVS). Furthermore, DGFI investigates the possibilities and requirements for the establishment of an International Altimeter Service (IAS) and participates in the installation of the newly created IAG Project on an Integrated Global Geodetic Observing System (IGGOS). In the frame of international cooperation DGFI drives several permanent GPS stations for the realisation of reference frames and monitoring crustal deformations, in particular at tide gauges.

D1 ITRS Combination Centre / IERS Combination Research Centre

DGFI contributes to the International Earth Rotation and Reference System Service (IERS) as an ITRS Combination Centre. Within the Research Group on Satellite Geodesy (Forschungsgruppe Satellitengeodäsie, FGS), DGFI, FESG (Forschungseinrichtung Satellitengeodäsie, TU München) and GIUB (Geodätisches Institut, Universität Bonn) established a joint IERS Combination Research Centre. The work within D1 is partly funded by the "Bundesministerium für Bildung und Forschung (BMBF), Forschungsvorhaben: IERS(F0336C)".

ITRS Combination Centre

The ITRS Combination Centre is responsible for the generation of highly accurate and reliable ITRS products from the combination of data (solutions) of different space geodetic techniques (VLBI, SLR/LLR, GPS, and DORIS) which are provided by the specific services (IVS, ILRS, IGS and IDS) and/or by individual analysis centres.

The work related to further developments of the ITRS Combination Centre, which is described in A4, includes software enhancement, refinements of the combination methodology, and improvement of tools and software for the analysis and quality control of input data and combination results. An overview of the combination procedure, the processing flow and the relevant software packages is shown in Figure A4.4.

Combined TRF Solution 2002

A major activity was the computation of a combined TRF solution from multi-year solutions with station positions and velocities. Table D1.1 gives an overview of the input data (solutions) that were used for the TRF computation.

Combination Methodology

The combination methodology is based on following major steps:

– Validation and analysis of individual solutions: The available solutions were checked concerning various aspects such as format and the suitability for combination.

Table D1.1 Summary of solutions used for TRF computation. Stations with an observation time span less than one year were excluded. The numbers in paranthesis identicate: (1) unconstrained normal equation; (2) loosely constrained solution; (3) minimally constrained solution.

Technique	AC/Solution	Data Span	# Stations orig./used	Source	
DORIS	(GRGS)00D01	1993--1998	70/69	ITRF2000	(3)
DORIS	(IGN)02D04	1993--2002	111/109	IGN/CDDIS	(2)
GPS	(IGS)03P01	1996--2002	216/207	NRCan	(3)
SLR	(CRL)00L02	1990--2000	62/62	ITRF2000	(2)
SLR	(CSR)00L04	1976--2000	141/106	ITRF2000	(2)
SLR	(DGFI)01L01	1981--2001	113/96	DGFI	(1)
SLR	(JCET)00L05	1993--2000	63/55	ITRF2000	(2)
VLBI	(DGFI)02R02	1984--2002	49/49	DGFI	(1)
VLBI	(GIUB)00R01	1984--1999	53/53	ITRF2000	(2)
VLBI	(GSFC)00R01	1979--1999	138/88	ITRF2000	(2)
VLBI	(SHA)00R01	1979--1999	129/88	ITRF2000	(2)

– Reconstruction of unconstrained normal equations: According to our combination strategy on the level of free normal equations we have to remove the datum constraints which are applied to the solutions.

– Preprocessing of individual solutions: For some of the input solutions it was necessary to perform preprocessing, e.g. epoch transformation for station positions, renaming and reducing of parameters.

– Intra-technique combination: The combination of data (solutions) of the same observation technique should be done by the corresponding technique centres (IGS, ILRS, IVS, IDS) in near future. At present, combined multi-year solutions with station positions and velocities are provided by the IGS only. The intra-technique combination for VLBI, SLR and DORIS was done at DGFI.

– Inter-technique combination: Input are the combined intra-technique normal equations resulting from the previous processing step. Important tasks include the comparison of solutions of the different techniques (especially at co-location sites), the estimation of weight factors (e.g. variance component estimation), handling of local ties, setting velocities at co-location sites identical, and the datum definition.

– Final combined solution: To generate the final combined solution we realised the geodetic datum by applying no net rotation conditions w.r.t. ITRF2000 station positions and velocities. The origin (translations and their rates) is realised by SLR, the scale and its rate by SLR and VLBI.

Results As an example for the intra-technique combination the results of a Helmert transformation between the individual and the combined SLR solutions are shown in Table D1.2. They demonstrate the high stability of the origin and scale. The four VLBI solutions prove the capability of this technique to estimate precise station positions and velocities and to realise the TRF scale. The r.m.s. residuals of the individual VLBI solutions w.r.t. the combined intra-technique solution are 2-3 mm for positions and about 0.5 mm/yr for velocities. The scale agrees within 0.3 parts per billion

Tab. D1.2 Results of a Helmert transformation of individual SLR solutions w.r.t. combined intra-technique solution.

H.-T. Results	CRL	CSR	DGFI	JCET
Tx [mm]	-0.1	1.4	0.9	2.4
Ty [mm]	1.5	-0.6	-1.3	-5.0
Tz [mm]	0.3	1.0	0.2	0.8
Scale [ppb]	0.03	0.09	-0.26	-0.10
Tx rate [mm/yr]	0.8	0.1	-0.2	-0.4
Ty rate [mm/yr]	-1.4	-0.1	0.1	1.1
Tz rate [mm/yr]	-1.6	-0.3	1.1	-0.1
Scale rate [ppb/yr]	-0.09	0.04	-0.08	0.18
Pos r.m.s. [mm]	4.1	4.9	2.3	3.7
Vel r.m.s. [mm/yr]	1.6	1.4	0.7	1.2

(ppb) and 0.08 ppb/yr for the rate. Both DORIS solutions agree within about 7-8 mm and 2 mm/yr for station positions and velocities, respectively.

In the inter-technique combination co-location sites and intra-site vectors (local ties) play a dominant role. Major questions are: Are the local ties sufficiently well determined to introduce them as a constraint, and are different velocity estimations at the same site identical? To find a correct answer, it is essential to validate the local ties and the velocity estimations at co-location sites, before combining different techniques. Table D1.3 gives an overview of the corresponding results. For six co-locations (3 GPS-VLBI, 3 GPS-SLR) there is an excellent agreement between the local tie measurements and the space geodetic solutions (the absolute differences are below 5 mm). But on the other hand, there are many other co-locations (especially with DORIS), where the differences exceed 2 cm. The station velocity estimations of different techniques agree very well for eight co-locations (the absolute velocity differences are below 1 mm/yr), whereas in many other cases these differences exceed 5 mm/yr. A correct interpretation of these discrepancies is difficult and requires further research, since various factors need to be considered (e.g. systematic biases between space geodetic solutions, non-linear site motions, local site-dependent effects, errors in local tie measurements, small inconsistencies related to datum definition). Based on various criteria we selected suitable local ties and identified sites for equating velocities to generate the final combined TRF solution.

Tab. D1.3 Comparison of space techniques at co-location sites. Shown are differences between local ties and computed station coordinates (upper part) and velocity differences between various techniques (lower part).

	GPS-VLBI	GPS-SLR	GPS-DORIS	SLR-VLBI
co-locations	35	24	21	12
missing ties	5	4	1	2
local tie differences				
< 5 mm	3	3	-	-
5 - 10 mm	6	5	-	2
10 - 20 mm	10	6	3	3
> 20 mm	11	6	17	5
velocity differences				
< 1 mm/yr	5	2	-	1
1 - 2.5 mm/yr	12	9	3	5
2.5 - 5 mm/yr	9	8	9	3
> 5 mm/yr	7	5	9	3

Comparison with ITRF2000

As an example the station velocities of the DGFI solution compared to ITRF2000 are shown in Figure D1.1. There is in general a good agreement between both TRF realisations, but for a few sites larger (and significant) differences exist, which need to be further investigated. The combined TRF solution of DGFI contains less sites compared to ITRF2000, since we excluded a number of stations with short data time spans (e.g. < 1 yr), which do not allow accurate and reliable velocity estimations.

IERS Combination Research Centre

The tasks of the IERS Combination Research Centre (CRC) are closely related with most of the projects in A. The activities and results concerning modelling of the different space techniques (A1: GNSS, A2: SLR, A3: VLBI) contribute to the development

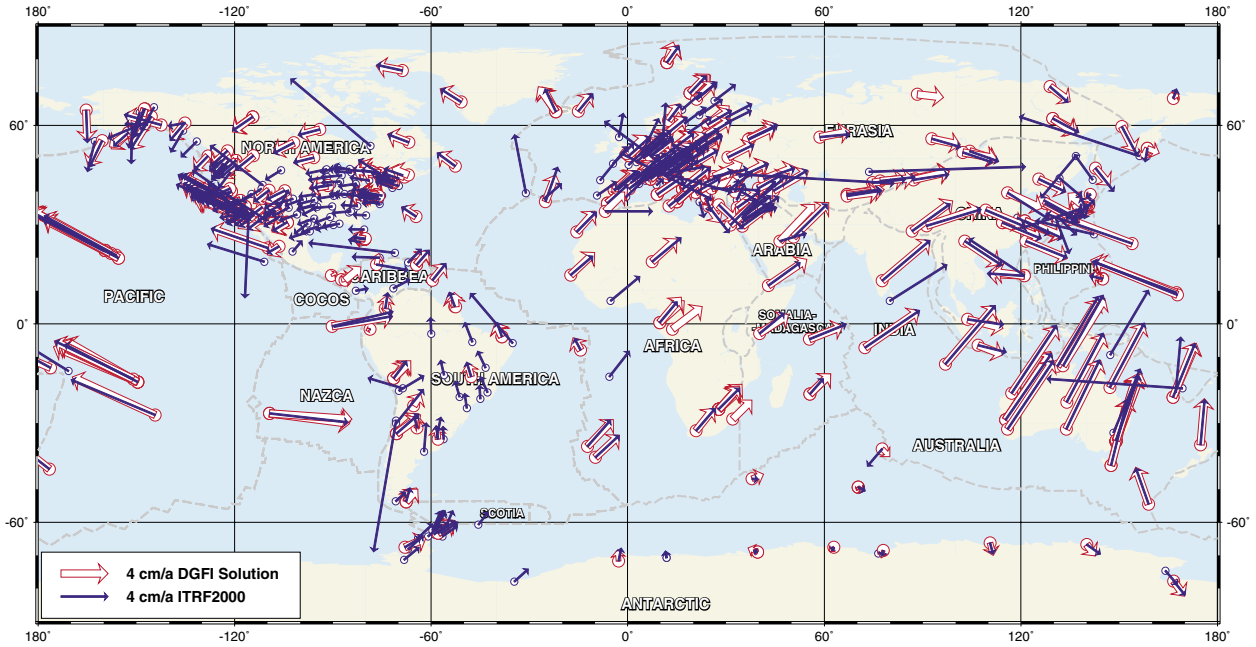

Fig. D1.1 Station velocities of DGFI solution compared to ITRF2000

of rigorous combination methods. The results of project A6 are essential to realise the kinematic datum for the TRF computations. Theoretical research related to the combination of space geodetic data, the development of refined combination methods and the software enhancement are major tasks within A4, which are closely related to the research activities of the CRC. The CRC work can be divided into three major topics:

- Special investigations related to ITRF relevant issues;
- Contributions for the IERS SINEX Combination Campaign;
- Rigorous combination of VLBI and GPS data (CONT02).

ITRF Related Investigations

Various investigations related to TRF relevant issues were performed, including:

- Analysis of solutions regarding various aspects (e.g. constraints, rank deficiencies, datum definition). Additionally systematic differences between different solutions were analysed to understand their origin (e.g. software-related aspects, model differences, parametrisation, datum definition, processing strategies, etc.);

- Studies on the combination methodology including weighting for the intra- and inter-technique combination (e.g. variance component estimation), handling of local ties, equating velocities at co-location sites, datum definition issues;

- The time series analysis of station position and datum parameters (origin and scale), obtained from VLBI, SLR, GPS and DORIS solutions, showed that the observed non-linear effects in the position time series are in conflict with the assumption of constant velocities, which may degrade the accuracy and consistency of the ITRF. Hence, a better monitoring of the terrestrial reference frame may require a non-linear representation of site positions and datum parameters.

IERS SINEX Combination Campaign

The IERS SINEX Combination Campaign was initiated by the IERS Analysis Coordinator to analyse solutions of the different techniques concerning various aspects (e.g. SINEX format, parameter definition, rank defects, suitability for combination), to combine station coordinates and EOPs and to develop and investigate strategies for a rigorous combination of these parameters (see http://alpha.fesg.tu-muenchen.de/iers/sinex).

In the framework of this IERS project DGFI has provided SLR, VLBI and GPS solutions and/or free normal equations and combined weekly solutions of the different techniques containing station positions and EOPs. Important tasks were the selection of suitable local ties to connect the different techniques, the weighting of solutions and the datum definition of the individual and the weekly combined solutions.

A major focus was on the definition of the geodetic datum for the weekly solutions. Especially in case of VLBI the realisation of a consistent datum is a critical issue, as typically only 4-6 telescopes observe simultaneously within one daily session, and the station configuration often changes from one to the other session. To investigate the impact of the VLBI datum definition on the estimated parameters we accumulated (e.g. monthly) VLBI 24 h session solutions by stacking the station positions of the daily normal equations and we compared the results with daily solutions. Examples are shown for the VLBI scale (see figure D1.2)

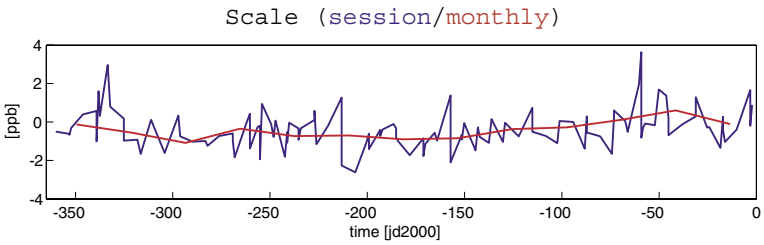

Fig. D1.2 VLBI scale variations obtained from daily session and accumulated monthly solutions derived by a 7 parameter Helmert transformation on ITRF2000.

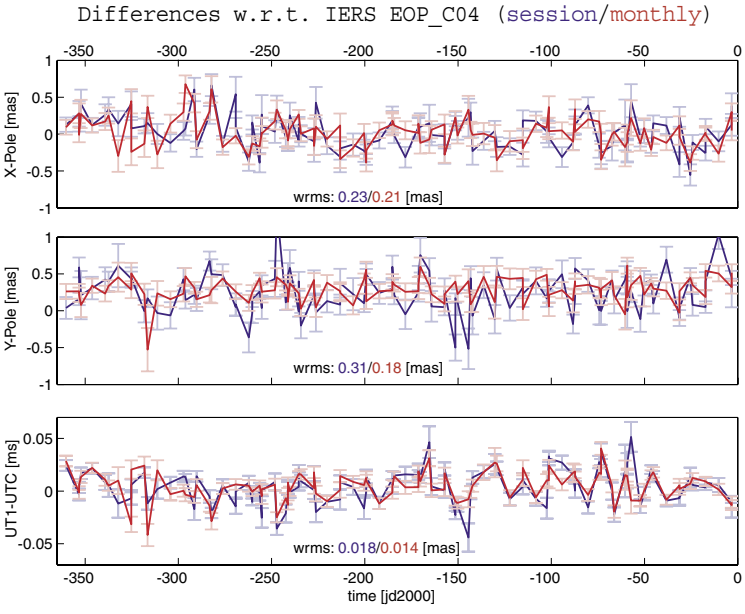

Fig. D1.3 EOP estimations w.r.t. IERS EOP C04. The wrms differences on the basis of the monthly datum definition are smaller by 10 to 40% compared to the daily solutions.

and for EOP estimations (see Figure D1.3). The results proof the stabilisation of the VLBI reference frame due to the accumulation.

CONT02 Combination

The IVS has initiated an intensive 15-days VLBI campaign (October 16-31, 2002) with eight participating stations, named CONT02. A joint project of Forschungseinrichtung Satellitengeodäsie (FESG) and DGFI aims towards a rigorous combination using the CONT02 VLBI data and global GPS data of the same time span. The computations of the GPS normal equations were done at the FESG with the Bernese GPS Software. The VLBI normal equations were generated at DGFI using the VLBI software OCCAM (see A3). The free normal equations were generated taking much care to adopt common models and parametrisations for the analysis of the GPS and VLBI data.

In a first step single solutions for each technique were computed, and the results for common parameters (e.g. daily station coordinates, 2 h EOPs, 2 h tropospheric zenith delays per station and day, tropospheric gradients, daily nutation parameters) were compared. The repeatability of station coordinates shows slightly higher variations for VLBI (north=3.6 mm, east=2.2 mm, up=8.4 mm) compared to GPS (north=2.2 mm, east=2.5 mm, up=5.9 mm). The time series of the sub-daily EOPs are in good agreement, except for an offset of 0.4 mas for the y-pole components between both techniques. This bias most likely results from a reference frame inconsistency between GPS and VLBI. The separately estimated sub-daily tropospheric zenith delays and the gradients show a very similar behaviour, except for an offset between both techniques, which needs to be further studied.

In a second step, the normal equations of both techniques were combined. As expected, the results are very sensitive to the selection of local ties. Several criteria were applied to identify suitable local ties for the combination. As an example first combination results are shown for the x- and y-pole (see Figure D1.4). The final goal is a rigorous combination of all parameters that are common to VLBI and GPS.

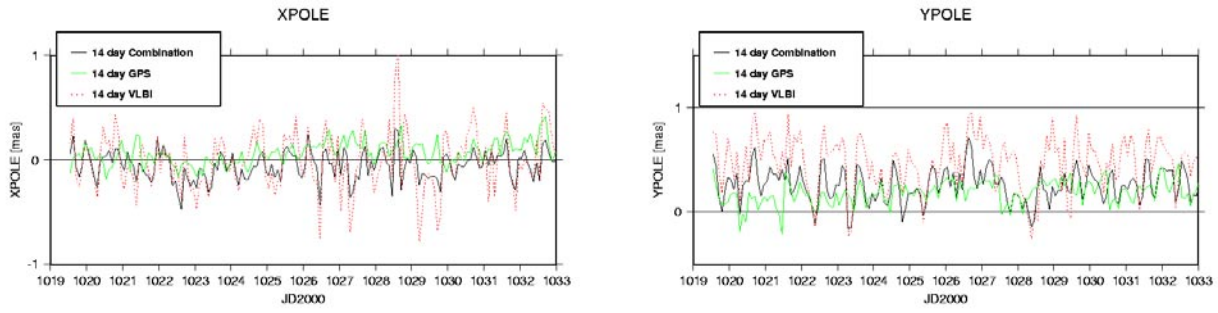

Fig. D1.4 Combined solution for the x- and y-pole compared to the individual VLBI and GPS solutions.

D2 Regional Network Associate Analysis Centre

The International GPS Service (IGS) started in June 1996 the densification of the IERS Terrestrial Reference Frame (ITRF) through regional GPS networks. DGFI is acting from the beginning as the IGS Regional Network Associate Analysis Centre for South America (SIRGAS) and surrounding areas (IGS RNAAC SIR). The number of processed global and regional GPS stations is continuously increasing.

The western part of this network covers a seismically very active region along the boundaries of the Cocos, Nazca, Caribbean, North and South American tectonic plates. In the DGFI Annual Report 2002 we presented the impact of two earthquakes in San Salvador and Arequipa on GPS station positions. This year we detected displacements of the GPS station Manzanillo/Mexico caused by another earthquake.

RNAAC SIR Network

End of September 2003 the RNAAC SIRGAS network consisted of 48 global IGS and 21 regional stations (see figure D2.1). Not all stations deliver their data in time to be included in the regular processing according to the tight time schedule of IGS, and some stations stopped observations in 2003. E.g., station Limon observed only until GPS week 0950 (March 1998), Barbados

Fig. D2.1 Station network processed by IGS RNAAC SIR indicating also the earthquake locations with impact on station positions from June 1996 to September 2003

until week 1101 (February 2001), Riobamba until week 1147 (January 2002), Aguascalientes until week 1158 (March 2002), and Galapagos until week 1192 (November 2002). Station Cachoeira (CHPI) provided one RINEX file of May 12, 2002, in time to be included in the processing, and since GPS week 1223 data is delivered regularly. Data of Cartagena/Colombia is not available since mid of 2003. The average number of stations contributing to the weekly solutions is 50. Table D2.1 shows the data sources, where IGS RNAAC SIR retrieves the RINEX files.

Tab. D2.1 Data sources for RINEX files

global		regional	
retrieved from	**for stations**	**retrieved from**	**for stations**
CDDIS / NASA, USA	aoml, areq, asc1, barb, bogt, brmu, cfag, chpi, cic1, conz, cord, coyq, cro1, eis1, esti, fort, free, gala, goug, guat, ineg, jama, kour, lpgs, mana, manz, moin, ohig, ohi2, palm parc, riog, riop, sant, scub, slor, ssia, tegu, teg1, tgcv, unsa, valp, ves1,	Instituto Geografico Agustin Codazzi (IGAC), Bogotá, Colombia	cart, boga
		La Universidad del Zulia (LUZ), Maracaibo, Venezuela	mara
		Instituto Brasileiro de Geografia e Estatistica (IBGE), Rio de Janeiro, Brasil	bomj, crat, cuib, impz, manu, para, poal, refc, riod, salv, smar, uepp, vico
NGS / NOAA, USA	pur3	Universidad de La Plata, La Plata, Argentina	mpla, pdes, rwsn, vbca
University of Hawaii, School of Ocean & Earth Science & Technology (SOEST), Hawaii	antc, autf, bhma, copo, iqqe, manz, parc, tgcv, tucu, valp	Instituto Geográfico Militar (IGM), Buenos Aires, Argentina	igm0

IGS RNAAC SIR Processing/ Strategy

For the routine processing of the RNAAC SIR network the automated Bernese GPS software (Bernese Processing Engine), version 4.2, is used. The main features of the processing are:

- sampling rate of 30 sec. for daily and weekly solutions,
- slevation angle cutoff 10 degrees,
- final IGS orbits/EOP,
- station coordinates in a free network adjustment,
- zenith delays estimated once per 2 hours for each station,
- ocean loading effects (modelled since March 2002).

The more dense network and an improved processing strategy has strengthened the daily solutions so that the repeatability from day to day processing is below one centimetre for the North and east components, and about one centimetre for the height component.

Monitoring of Earthquakes in South America and Surrounding Areas

It becomes more and more evident that we have to consider seriously the proper modelling of episodic events like earthquakes in the GPS station coordinates and velocities. Figures D2.2 and D2.3 show the effect of earthquakes near Manzanillo/Mexico in November 2002 and January/February 2003. These co-seismic and post-seimic displacements were detected by analyzing the time series of weekly solutions, and correlating it with earthquakes in the RNAAC SIR region listed in the catalogue (United States Geological Service, USGS, National Earthquake Information Centre, see also figure D2.1). They have to be taken into account when generating the station coordinates and

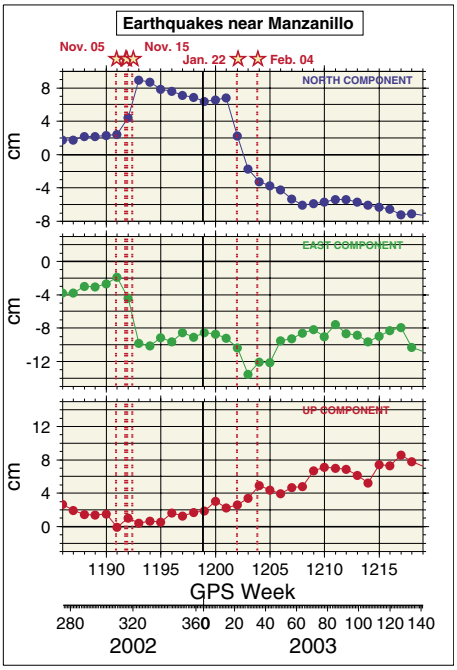

Fig. D2.2 Detection of displacements by analyzing time series of weekly solutions after earthquakes near Manzanillo

velocities solutions, because nonlinear displacements falsify the linear velocities. Figure D2.3 shows the displacement of 9.6 cm after the first earthquake (co-seismic), then the creeping of 4.7 cm between the two earthquakes with the largest effect (post-seismic), and again the coseismic displacement of 5.3 cm after the second earthquake. It is remarkable that the strongest and/or nearest earthquakes do not generate the largest effect on the station positions. The depth of the epicentre seems to be more important, and/or the fact whether the epicentre is located in the ocean or on land (see figure D2.3).

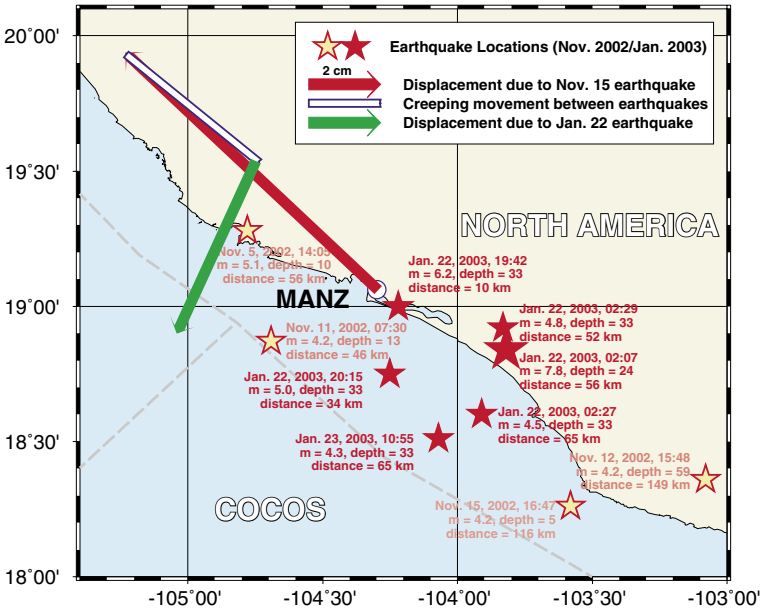

Fig. D2.3 Earthquakes near Manzanillo (MANZ) and the corresponding displacements due to these earthquakes

D3 Permanent GPS Stations

At present DGFI operates seven permanent GPS stations in cooperation with national institutions. As the local host facilities cannot always provide a continuous supervision and maintenance, the operation of the stations is controlled by DGFI and automated as far as possible. The data transfer is done via Internet. Table D3.1 lists the stations, their locations, installation dates and the installed receiver and antenna systems.

During the period covered by this report loss of observations occurred due to the following reasons :

- Failure of the computer at TORS from early October 2002 to early January 2003;
- A total breakdown of the connection to CART probably due to a failure of the local computer system since end of march 2003.

Tab. D3.1 Permanent GPS stations operated by DGFI

ID	Location,Country	Inst.Date	Receiver	Antenna
VBCA	Bahia Blanca,Argentina	Dec.98	LEICA SR9500	LEIAT303
BOGA	Bogota,Colombia	Feb.00	LEICA CRS1000	LEIAT504 LEIS
CART	Cartagena,Colombia	Jan.00	LEICA CRS1000	LEIAT504 LEIS
MARA	Maracaibo,Venezuela	Feb.98	LEICA SR9500	LEIAT303
MPLA	Mar del Plata,Argentina	Sep.02	LEICA MC1000	LEIAT504
RWSN	Rawson,Argentina	Nov.99	Ashtech UZ-12	ASH700936D_M
TORS	Torshavn,Faroe Island	Feb.01	LEICA CRS1000	LEIAT504 LEIS

The four-character identifications are those used by the International GPS Service (IGS). All stations except TORS are included in the regional IGS network for South America which is operationally processed by DGFI (see project D2).

In response to an IGS call for participation to a **TI**de **GA**uge benchmark monitoring project (TIGA), DGFI has submitted a proposal to process a network covering the North and South Atlantic oceans. The permanent stations TORS, CART, MPLA, VBCA and RWSN are included in this network.

Figure D3.1 displays the entire network processed by DGFI for the TIGA project. So far, 36 one-week data sets evenly distributed between December 1999 and November 2002 were analysed. The characteristics of the data processing with the Bernese GPS software can be summarized as follows:

- Accounting for the data completeness and quality in the network processing design;
- Using IGS orbits, satellite clock and earth rotation parameters;
- Exploiting the full data rate of 30 seconds, setting the elevation mark to 10° and estimating zenith tropospheric

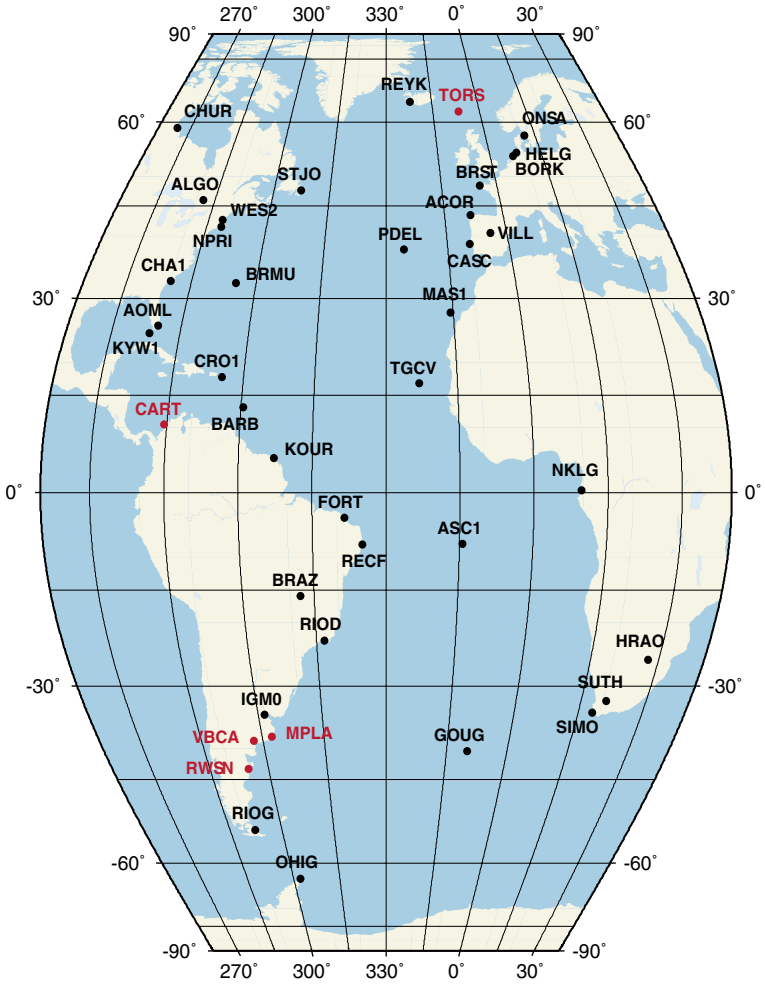

Fig. D3.1 GPS network processed by DGFI in the frame of the TIGA project.

delays for each two hours interval, weighting as function of the zenit angle with $\cos^2 z + 0{,}3 \sin^2 z$;

– Performing consistency checks between daily and weekly combined adjustments before submitting weekly SINEX-files to the TIGA data centres.

The installation of further permanent GPS stations at the South American Atlantic coast in particular for tasks as addressed by the TIGA project are planned.

D4 ILRS Associate Analysis Centre

The activities within this project concentrate on the processing of satellite laser ranging data of the global SLR tracking network to Lageos-1/2 with the DGFI software DOGS-OC (see A2). The estimated parameters include station positions and velocities, Earth orientation parameters, lower gravity field coefficients, orbit parameters, etc. The project contributes to the activities of the ILRS Analysis Working Group (ILRS AWG). The work can be divided into three major topics:

- Contributions to the software benchmarking pilot project of the ILRS AWG;
- Operational processing and combination of SLR data within the ILRS AWG project "Positioning & Earth Orientation";
- Continuous processing of SLR data for various scientific investigations.

ILRS AWG Software Benchmarking Pilot Project

The intention of the pilot project on software benchmarking is the harmonization and control of the software packages used for processing of the offical ILRS products. Results from this project are the basis to detect inconsistencies between the individual orbit generation programmes and help to detect software problems.

Each analysis centre had to deliver a processed orbit, the residuals and a station coordinate and EOP solution from SLR tracking data to Lageos-1 in the period from October 10 to November 6, 1999. The analysis centres provided a series of solutions since a number of software problems were identified in this process. To participate in the ILRS as an analysis centre it is necessary to pass certain criteria, like a maximum 2.5 sigma deviation from the reference solution. Since the discrepancies between individual analysis centre solutions are still too large further investigations and processing are required. As an example the orbit differences between the DGFI and ASI solution are shown (see figure D4.1). These two orbits agree to 3.5 cm radial, 7.9 cm along-track and 8.3 cm cross-track after similarity transformation.

ILRS AWG Operational Processing (Test Phase)

The ILRS is responsible for the generation of quality-controlled operational and scientific products, for inclusion in various official IERS products. The ILRS AWG is in the process of developing such a unique and quality controlled official ILRS product (for various parameters). The ILRS has released a call

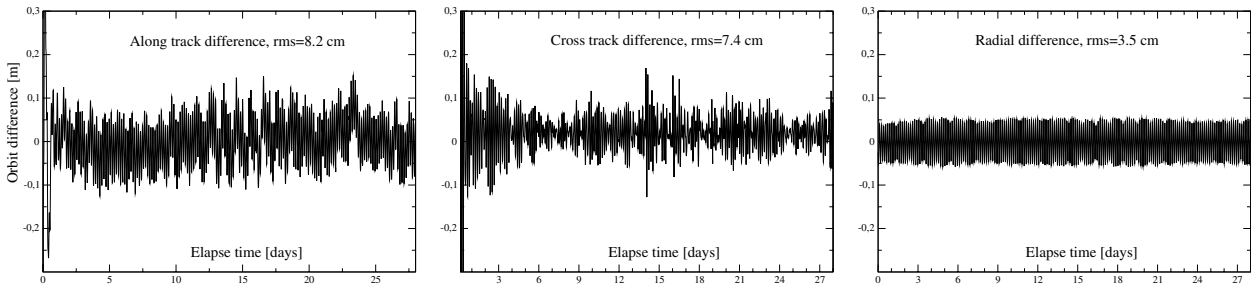

Fig. D4.1 Orbit comparison between solutions D of DGFI and ASI generated for the ILRS AWG Benchmarking Pilot Project

for participation "Positioning & Earth Orientation" for two types of contributions:

- providing individual SLR solutions and/or
- the quality control and combination of such individual solutions to an official ILRS product.

DGFI participates as analysis and combination centre, the test phase started in June 2003. The products (station positions and daily earth orientation parameters) are generated weekly based on shifted 28-day data arcs.

ILRS AWG Analysis Centre (Positioning and Earth Orientation)

DGFI participates as analysis centre since July 2003. After some difficulties with modelling and formats the regular processing of LAGEOS-1/2 solutions works without problems. As an example the Helmert transformation parameters and the mean 3D weighted r.m.s. of station positions to ITRF2000 are shown for four individual solutions provided by DGFI, Agenzia Spatiale Italiana (ASI), GeoForschungsZentrum Potsdam (GFZ) and Natural Environment Research Council, Space Geodesy Facility of Great Britain (NERC), see Table D4.1. The translation parameters of the four solutions agree within a few millimeters, but the z-component of the SLR solutions differs by 1-2 cm from ITRF2000. The three solutions provided by ASI, DGFI and GFZ show a similar accuracy for station positions, whereas the NERC solution shows larger discrepancies w.r.t. ITRF2000.

Tab. D4.1 Transformation parameters between four individual SLR solutions and ITRF2000 (solutions: October 13, 2003). Note, that the rotation parameters are not displayed, since SLR does not contain information to estimate these parameters.

Solution	Tx [mm]	Ty [mm]	Tz [mm]	Scale [ppm]	3D-Wr.m.s. [mm]
ASI	0.9	3.7	-11.7	-0.92	8.2
DGFI	1.1	0.5	-12.6	0.75	8.5
GFZ	-0.4	4.5	-11.0	-0.3	8.8
NERC	-2.4	4.6	-18.9	-0.23	13.7

ILRS AWG Combination Centre (Positioning and Earth Orientation)

The objective of the combination centre is to compute a combined solution in an automated process using individual SLR solutions. The DGFI concept of this processing is outlined in A4. Here, some numerical results are presented.

Quality criteria after the combination (see figure A4.3) are the r.m.s. parameter differences between the input solutions and the combined solution. Some results are presented in table D4.2, including r.m.s. differences for station positions, pole coordinates and length of day (LOD). The test phase is not yet finished so that these results have to be considered as preliminary.

Tab. D4.2 r.m.s. differences between individual and combined SLR solutions (four-week solutions for October 13, 2003). The solution provided by NERC could not be used, because the EOP parameters were not complete.

AC	X [mm]	Y [mm]	Z [mm]	PX [mas]	PY [mas]	LOD [ms]
ASI	4.7	3.0	4.4	0.20	0.12	0.08
DGFI	5.2	4.4	5.3	0.20	0.22	0.11
GFZ	4.3	3.6	4.4	0.19	0.20	0.12

Continuous Processing of SLR Data

The SLR tracking data are being processed continuously on a weekly basis. The arcs will be reprocessed if new tracking data become available. We use the results to check data quality and distribution: Some of the problems with wrong tracking data or biases could be solved after consultation with data centres and tracking sites.

The quality of SLR observations to LAGEOS-1/2 has improved in the last years but there is still a discrepancy in data quality and amount between the various sites of the SLR network (see table D4.3). The number of rejected normal points is very low for most stations. Most of the tracking sites have an accuracy of better than 1 cm to both LAGEOS satellites, only some suffer from calibration or performance problems. The tracking performance to any satellite depends on the priority lists and especially in regions with a dense tracking network LAGEOS-1/2 has low priority on some stations. It is obvious from table D4.3 that the southern hemisphere has a deficit on tracking sites even if these stations have a good tracking performance.

Tab. D4.3 Overview of SLR tracking in 2003 (until Oct. 21), ordered by the LAGEOS-1 r.m.s. orbital fit. The columns show for LAGEOS-1 resp. LAGEOS-2 the number of passes, normal points used for processing, rejected normal points and the r.m.s. orbital fit for all good observations in the weekly arcs.

Station Name	CDP Number	LAGEOS-1				LAGEOS-2			
		Normalpoints		Passes	r.m.s. [mm]	Normalpoints		Passes	r.m.s. [mm]
		used	bad			used	bad		
Potsdam	7841	812	22	53	6.3	560	10	35	6.2
Arequipa	7403	579	5	68	6.6	459	0	47	4.5
Washington	7105	4067	13	416	7.5	1562	5	175	8.2
Graz	7839	5486	31	454	8.1	4400	16	330	7.6
Concepcion	7405	655	0	93	8.4	485	23	64	12.8
Fort Davis	7080	1949	5	245	8.7	2415	20	276	8.8
Hartebesthog	7501	4555	18	431	8.9	4368	24	367	8.8
Riyad	7832	3472	34	373	9.0	4576	33	443	8.7
Yarragadee	7090	7283	41	707	9.0	7153	36	560	8.3
Zimmerwald	7810	6819	24	517	9.3	5130	17	379	9.0
Wettzell	8834	3272	34	380	9.4	2903	13	283	9.9
Monument Peak	7110	4067	13	416	9.4	4401	24	392	9.5
Haleakala	7210	2530	13	279	9.5	3161	22	308	9.0
Borowiec	7811	613	27	64	10.1	663	2	56	10.2
Shanghai	7837	480	22	61	11.8	449	7	48	11.2
Simosato	7838	600	16	66	13.1	745	14	67	11.9
Maidanak	1864	414	21	53	16.4	822	36	94	15.4
Urumqi	7355	413	15	34	36.1	1079	60	92	26.4
Simeiz	1873	67	17	17	71.5	383	73	77	49.6
	Sums and mean values								
Southern Hemis.	6	13414	72	1351	9.3	12692	96	1074	8.9
Northern Hemis.	35	47629	706	4622	11.6	45020	766	4138	12.9

DGFI has reprocessed all laser tracking data to LAGEOS-1 (since January 1980) and LAGEOS-2 (since October 1992) on weekly arc basis with the latest version of the DGFI software DOGS-OC (see A2). Time series of the weekly station coordinates are the basis for data editing and quality control. These weekly solutions will be used to process a new multi-year SLR solution and low degree potential coefficients including time derivatives. Additionally we will solve for annual and semi annual periods of selected low degree harmonics. The SLR results (especially the time series of weekly estimated parameters) were analysed w.r.t. non-linear effects, seasonal variations, etc., and will help to validate and refine existing models (see A2). Furthermore they are used for the combination with other space techniques and for TRF computations (see D1). First comparisons of SLR-derived C_{20} variations show a promising agreement with results obtained from the non-linear gyroscopic model developed at DGFI (see C1).

D5 ILRS Global Data Centre / EUROLAS Data Centre

Since the foundation of the International Laser Ranging Service (ILRS) in November 1998 DGFI runs the ILRS Global Data Centre besides the EUROLAS Data Centre (EDC), which was installed in August 1991. The second Global Data Centre is at CDDIS/NASA. This report gives information about the transition of the prediction exploders from CDDIS/NASA to EDC and other changes and activities in 2003.

ILRS

The DGFI Annual Report 2000/2001 presented the backup procedures installed at EDC. After an agreement between CDDIS, Honeywell (HTSI) and EDC/DGFI it was decided that EDC becomes the primary prediction distributor for all IRVs of the various prediction providers (see table D5.1). The transition of this tasks happened on August 15, 2003. Since that date the daily and subdaily predictions of all satellites as well as manoeuvre predictions are successfully distributed by EDC without any problem.

Tab. D5.1 Prediction providers and their products (HTSI - Honeywell Technology Solutions, Inc., CDDIS - Crustal Dynamics Data Information System, NERC - Natural Environment Research Council, GFZ - GeoForschungsZentrum, ESOC - European Space Operations Centre, MCC - Mission Control Centre, NASDA - National Space Development Agency, JAXA - Japan Aerospace Exploration Agency)

Prediction Provider	Weekly/daily/subdaily Predicts for Satellites
HTSI / CDDIS, USA	daily predictions and manoeuvre prediction for AJISAI, BEACON-C, CHAMP, ENVISAT, ERS-2, ETALON-1/2, GPS-35/36, GLONASS-84/87/89, GFO-1, JASON-1, LAGEOS-1/2, METEOR-3M, STARLETTE, STELLA, TOPEX
NERC, UK	daily and subdaily predictions for GPS-35/36, GLONASS-84/87/89 daily predictions for all other satellites
GFZ-Potsdam, D	weekly and manoeuvre predictions for ERS-2 subdaily predictions and drag functions for CHAMP, GRACE-A and -B
ESOC, Darmstadt, D	daily and manoeuvre predictions for ENVISAT
MCC, Moscow, RUS	daily predictions for METEOR-3M
NASDA (now JAXA), JP	daily predictions for AJISAI and LAGEOS-1/2

Still EDC is responsible for the SLRmail and SLReport exploders. Since the implementation of these both exploders in November 1995 1134 SLRmails and 3174 SLReports were received and distributed to interested users. Besides these exploders EDC is now also responsible for the URGENT Mail exploder. This mail exploder started on August 15, 2003.

ILRS started a pilot project for the generation of ILRS products like positions, earth rotation parameters (EOPs), positions and EOPs, and summary files. EDC installed a mirror for these ILRS products at CDDIS/NASA since the beginning of this pilot project.

At the ILRS Laser Ranging Workshop in October 2002 in Washington D.C., USA, the necessary arrangements for delivery and archiving of SLR full-rate data were discussed. The re-archiving of the product full-rate data started in April of this year. Still some problems exist in the automatic handling of this

data type due to wrong file naming conventions and compression procedures done by some SLR stations.

The SLR station Zimmerwald started in 2002 sending two colour laser ranging data. One more station joined in sending on-site normal points with two wavelengths. It's the SLR station in Concepcion with the laser ranging system of the German **T**ransportable **I**ntegrated **G**eodetic **O**bservatory (TIGO). The current whole SLR network with its three sub-networks is shown in figure D5.1.

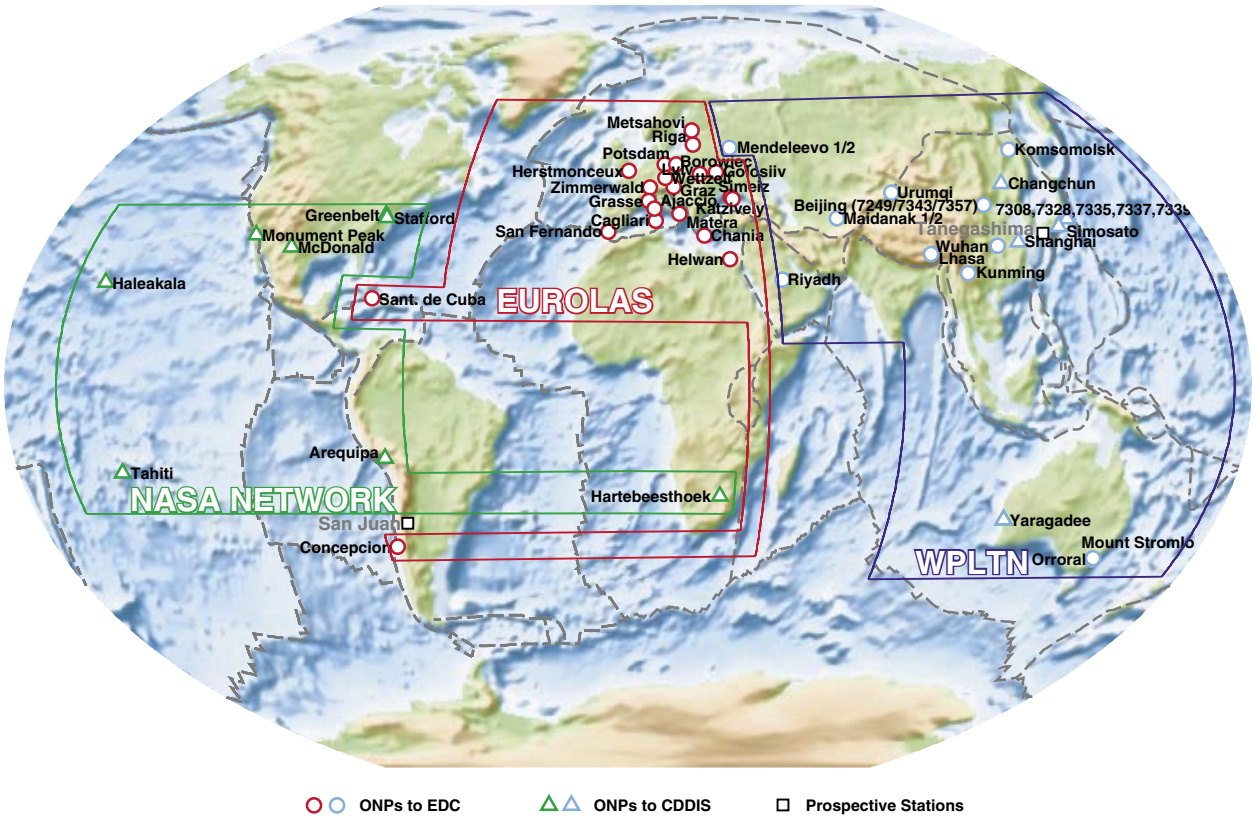

Fig. D5.1 Current SLR network with its three sub-networks supporting ILRS

In the last meeting of the ILRS Data Formats and Procedures Working Group of April 2003 in Nice, France, the rule for archiving all data releases of on-site normal points was revised. Only the latest data release has to be archived, and the former one should be deleted.

Observation Campaigns

Again the ILRS Governing Board under participation of the author has decided about finishing, continuing or agreement of new SLR campaigns. The REFLECTOR campaign has finished, and the new ADEOS-2 campaign ended this year. The JASON-1 - TOPEX Tandem, ETALON-1/2, and ENVISAT campaigns will continue. New satellites for SLR observations are LASSO, ADEOS-2, and ICESAT.

In the time period from September 2002 to September 2003 43 SLR stations observed 30 satellites (including the four moon

Tab. D5.2 Content of ILRS/EDC data base on September 30, 2003 for the product normal points in number of passes (including Lunar Laser Ranging (LLR) observations to four moon reflectors)

	number of passes			number of passes			number of passes	
Satellite	increase 03	total 2003	Satellite	increase 03	total 2003	Satellite	increase 03	total 2003
ADEOS		671	GLONASS-71		2617	METEOR-3		409
ADEOS-2	182	182	GLONASS-72		3260	METEOR-3M	667	942
AJISAI	11840	72611	GLONASS-74		39	MOND-1	23	281
BEACON-C	7319	26089	GLONASS-75		300	MOND-2		188
CHAMP	1999	5083	GLONASS-76		301	MOND-3	16	1678
DIADEME-1C		1393	GLONASS-77		343	MOND-4	272	570
DIADEME-1D		1585	GLONASS-78		2712	MSTI-2		35
ENVISAT	6006	8217	GLONASS-79		3237	REFLECTOR	1562	3722
ERS-1		10524	GLONASS-80		4466	RESURS-01-3		2011
ERS-2	6306	38147	GLONASS-81		275	STARLETTE	9196	54109
ETALON-1	1679	7888	GLONASS-82		244	STARSHINE-3	8	48
ETALON-2	1562	8129	GLONASS-84	1752	3986	STELLA	5446	35847
FIZAU		4243	GLONASS-86	779	1291	SUNSAT		1864
GEOS-3		2237	GLONASS-87	1339	2118	TIPS		1849
GFO-1	5169	19317	GLONASS-88		9	TOPEX/POS.	11139	66408
GFZ-1		5606	GLONASS-89	1135	1135	WESTPAC-1		5620
GLONASS-62		963	GPS-35	634	4550	ZEIA		146
GLONASS-63		1952	GPS-36	629	3894			
GLONASS-64		81	GRACE-A	2149	2827			
GLONASS-65		397	GRACE-B	1932	2372			
GLONASS-66		1544	ICESAT	41	41			
GLONASS-67		4299	JASON-1	8341	12334			
GLONASS-68		875	LAGEOS-1	8692	53146			
GLONASS-69,		945	LAGEOS-2	8316	46970			
GLONASS-70		1430	LRE/H2		5	Sum of all	106030	552677

reflectors). Table D5.2 shows the EDC data base content with the number of passes on September 30, 2003. This content is compared with the content of the CDDIS data base, and has to be updated at EDC and/or CDDIS if data is missing.

D6 IVS Special Analysis Centre

DGFI contributes to the International VLBI Service (IVS) of the IAG as a Special Analysis Centre. Its objectives are to improve the space-geodetic observation technique Very Long Baseline Interferometry (VLBI) and the analysis of its observations, respectively, by participating in pilot projects and by research projects which are mainly concerned with the modelling of VLBI observations. As there were no pilot projects during the reported period, the work of DGFI was focussed on the following activities.

IVS OCCAM Working Group

The software OCCAM which is used at DGFI to analyse VLBI observations is continuously improved by a group of scientists from Geoscience Australia (Canberra, Australia), the Vienna University of Technology (Vienna, Austria), the St. Petersburg University, the Institute of Applied Astronomy (both St. Petersburg, Russia) and DGFI. As the groups concentrate on different research fields, it is important to keep an official version of the source code which reflects the common interest. This version is updated if needed. The forthcoming version will be 6.0. The group met twice on the occasion of international scientific meetings (4th IVS Analysis meeting in Paris, France; Les Journées 2003, St. Petersburg, Russia) in order to define and to partially elaborate the source code changes. DGFI's most important contributions to the new version of OCCAM are an advanced outlier rejection routine and a first version of a refined stochastic model for VLBI observations (for details see A3). There is also a new interface for the conversion of OCCAM internal normal equations into a DOGS-CS readable format.

Scheduling of VLBI Sessions for Subdiurnal Resolution of EOP

The studies on the subdiurnal resolution of Earth orientation parameters (EOP) have been continued during the last year. Here, the adequate scheduling of VLBI sessions is a very important quality issue. Eleven parallel VLBI sessions from the CORE-A and the NEOS-A programs were analysed regarding the significant benefit of a higher temporal parameter resolution which was checked by means of an F-test. As the results should be identical for simultaneous sessions, the different degrees of significance reflect influences of the respective scheduling. Figure D6.1 shows the statistical significance of the possible gain of information by doubling the temporal resolution step by step from 24 h to 0.75 h. The test statistics values of CORE-A which are greater than the corresponding NEOS-A values are caused by the not-shown standard deviations of the estimated parameters. They occur in the denominator of the test statistics and are always smaller for CORE-A than for NEOS-A. If instead the values of NEOS-A are greater, this is very likely due to uncompensated effects of the weaker network geometry.

The CONT02 VLBI observation campaign which is under the auspices of the IVS was run from October 16 to October 31, 2003. This campaign comprises a homogeneous network of eight globally distributed VLBI sites which observed continuously for 15 days. It is therefore especially suitable for research on VLBI-determined subdaily EOP. The IVS Special Analysis

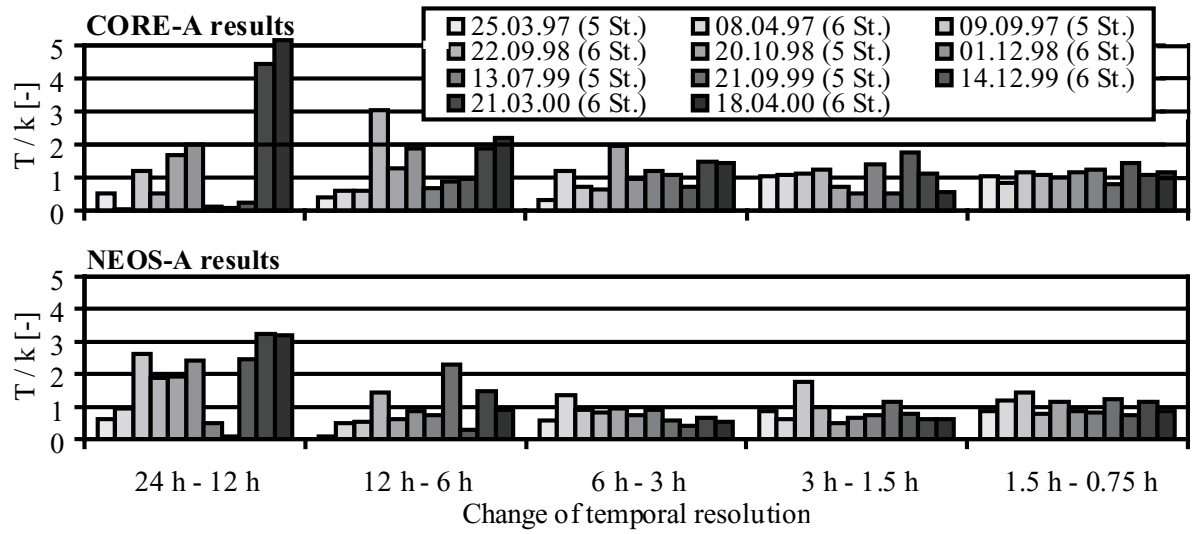

Fig. D6.1 Significance of an increased temporal resolution of the EOP: The values of the test statistics T divided by the 0.99 fractile value k of the respective F-distribution are plotted; values greater than 1 are significant. The test statistics are free from diurnal and semi-diurnal tidal signals according to the Ray model (IERS Conventions 1996).

Centre at DGFI assisted in preparing the scheduling strategy using its extensive experiences with subdaily EOP from VLBI.

The activities of the IVS Special Analysis Centre at DGFI are strongly connected with the scientific work of project A3 (Modelling for VLBI). There are also links to the projects A4 and D1 which deal with the combination of different space-geodetic techniques. Some work within D6 is funded by the German research association 'Deutsche Forschungsgemeinschaft (DFG)' under the contract DR 143/11-1.

D7 Developments for an International Altimeter Service

The need for an as long as possible time series of precise altimeter observations with up-to-date geophysical corrections and consolidated geocentric reference is a generally accepted requirement. For this it is mandatory to harmonize and cross-calibrate all contemporary and follow-on altimeter missions. But also missions with new technologies like laser altimetry (GLAS on ICESAT), interferometric altimetry (CRYOSAT, to be launched in 2004), or the wide-swath altimetry (proposed for JASON-2) are to be cross-calibrated with the classical pulse-limited altimeter systems. This task is

- international,
- interdisciplinary,
- mission-overlapping, and
- agency-independent.

It suggests itself to fulfil these requirements by the establishment of an International Altimeter Service, IAS.

The rational for an IAS was discussed within the CSTG subcommission on "Multi-mission satellite altimetry" and the feasibility and scope of such a service is now further studied by a working group, created within the IAG intercommission project "ICP1.1 Satellite Altimetry".

Major drawbacks of the existing altimeter mission data are the inhomogeneous formats and out-of-date record parameters. OpenADB, an altimeter data base with a generic data format, the capability of fast parameter updates, and the potential to generate data base extracts with user defined content and format was further developed.

Following tasks have been performed:

- Interfaces to all mission data that have become available have been developed. The status of the transformation into the OpenADB format is shown in table D7.1.
- A new data base server with sufficient disc space and a DVD recorder has been installed. The volume of the original mission data (in particular for Envisat) is extremely large. Therefore a new concept for back up storage and background archiving has been realised.
- Unrecognised leap seconds in the UTC time scale may cause inconsistencies in cross-over analysis. Therefore, OpenADB uses a continuous time scale, synchronous to the TAI. The

Tab. D7.1 The status of altimeter mission data transformed to the OpenADB system.

Mission (phases)	Repeat [days]	Mission data				Transformation to OpenADB			
		Source	Access	Media CD/DVD/ ftp	Volume [GByte]	Cycles	Volume/ cycle [MByte]	Total volume [GByte]	Interface/ Activity
GEOSAT (GM)	-	NOAA	free	10/-/-	~6.5	~25	~55	?	ready/evaluation
GEOSAT (ERM)	17		free			68			ready/evaluation
ERS-1 (A,C)	3	CERSAT	PI only						
ERS-1 (B,D)	35								
ERS-1 (E/F)	168								
TOPEX/Pos.	10	CNES	free	120/-/-	78.0	364	~66	23	ready/completed
ERS-2	35	CERSAT	A0416	80/-/-	52.0	77	~121	~11	ready/evaluation
GFO	17	NOAA	free	-/3/FTP	6.0 ++	78	~74	5.5	ready/ongoing
ENVISAT	35	ESA	A0416	-/1/FTP	6.5 ++	3	~153	0.62	developm/ongoing
JASON-1	10	CNES	free	-/2/FTP	18 ++	61	~45	2.8	developm/ongoing

transformation between UTC and TAI time scale was verified.

- The CLS01 mean sea surface height model has been interpolated to all tracks of the OpenADB data base.
- The GOT99.2 ocean tide model was interpolated to all tracks of the OpenADB data base.

Binread

Up to now, altimeter mission data is always provided in binary coded form with any parameter coded as scaled integers with one, two or three Byte in length. However, every new altimeter mission created another data format with a different compilation of record parameters. Binread is a C-program, designed to read any of these formats and is provided as a service to altimeter user which are enabled to extract altimeter mission data without the need to programme always new mission-specific interfaces. Binread has been extended, and was modified in order to be applicable also to the Envisat data, characterized by a extremely large record size with a very large number of parameters. Binread provides many options (see figure D7.1) and can extract the data even for individual bits set to indicate measurement quality. The program code is available at the ftp-server under the URL

ftp://ftp.dgfi.badw.de/pub/altimetry/binread/

The program is complemented by a documentation and example record maps, ASCII files that define the record formats for most of the altimeter missions.

Fig. D7.1 Screenshot of the short hand description, printed if the binread command is given without argument. The options allow to extract data even for individual bits set in so called quality flags.

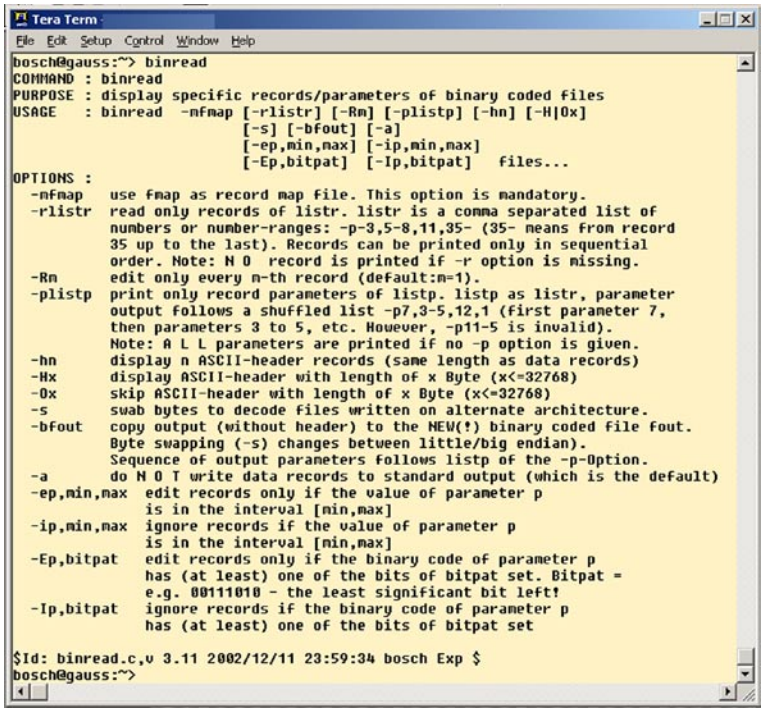

D8 Contributions to IGGOS

The Integrated Global Geodetic Observing System (IGGOS) was installed by the International Association of Geodesy (IAG) as its first project during the General Assembly of the International Union of Geodesy and Geophysics (IUGG) in Sapporo (Japan), July 2003. The aim of IGGOS is to integrate the different geodetic techniques, models and approaches in order to achieve a better consistency, long-term reliability and understanding of geodetic, geodynamic and global change processes. It is geodesy's contribution in terms of products and discoveries to Earth sciences and the bridge to the other disciplines.

The mission of IGGOS is to ensure the robustness of the three fundamental fields of geodesy: geometry and kinematics, Earth orientation and rotation, gravity field and its variability. The principal objectives are to maintain the stability of existing time series of geometric and gravimetric reference frames and to ensure the consistency of geometric and gravimetric products. IGGOS is geodesy's central interface to the scientific community and to society in general. It is based on the close cooperation with IAG's Commissions and Services.

In the initial phase of IGGOS the general structure shall be defined and a science plan shall be developed. For this purpose a Project Board, Steering Committee and Science Council as well as several Working Groups are set up.The Working Groups include topics like the synergies of services, strategy and funding, integration into IUGG entities, copyright and data access policy, data and product standards, user integration (science, industry, authorities).

DGFI is involved in the initial phase of IGGOS and participates in the realisation of the IGGOS objectives by analysing geodetic results and working on the consistency of products from geometric and gravimetric modelling. The experiences in scientific research and product generation in the different services is used to provide significant input to IGGOS.

E Information Services and Scientific Transfer

In order to make research and the results of it known for the scientific community as well as to the public, adequate procedures have to be developed and applied. Besides the publications in scientific journals and series, the DGFI maintains an information system in the internet. Moreover the DGFI has an intensive data exchange with various scientific groups. Adequate structures for regulating this exchange on internal as well as external basis are to be installed. This exchange especially refers to the contribution and collaboration to large international projects and services which can only be accomplished by the cooperation of many institutions.
Members of the staff of the DGFI participated in numerous congresses and other meetings, they gave lectures and submitted reports. Further on, the DGFI is represented by its co-workers in numerous national and international bodies. The information exchange is extended by working visits at other institutes as well as scientific guests working from time to time in the DGFI.

E1 Geodesy Information System GeodIS

GeodIS is an information system for geodesy. Since some years it is maintained by DGFI with the objective to compile information about the most important areas of physical geodesy, namely geometry and reference systems, Earth rotation and orientation and the gravity field. This information is prepared for the Internet and is made available under the location

http://www.dgfi.badw.de/~geodis/ .

It is not the intention of GeodIS to teach readers about geodesy or to substitute a text book on geodesy but to help people in finding information and data they are interested in. As an example, GeodIS provides a summary about the relevant scientifc organisations and the international services with direct links to the corresponding homepages. Such a comprehensive summary is other wise not available.

E2 DGFI Home Page

The home page of DGFI intends to inform about the research performed at the institute and the results that were achieved. It is available under the location

http://www.dgfi.badw.de/ .

The home page represents structure and content of the research program, the national and international projects, the DGFI is involved in and the contributions of DGFI to international services. The homepage also provides a list of papers and reports published by the employees and compiles all their posters and presentations. An increasing number of publications and posters is made available in electronic form, mostly with the portable document format (pdf), a de-facto standard for the exchange of electronic documents.

There is an increasing number of pages that are to be developed and maintained. The uniform layout requires intensive knowledge of HTML and CSS (Cascading Style Sheets). Moreover, there are growing demands to include interactive and dynamic content, for example results of a data base query which implies

expertise with data base systems like MySQL. Script languages like PHP are required in addition to perform data base functions and to display results within an internet page. Long time all this was realised by a coordinator and a few scientific helpers who generated the content of the pages according to the request of the DGFI scientists who got rid of the detailed coding with HTML, CSS, MySQL and PHP. Due to the growing number of pages this mode of working was no longer practical.

Content Management System (CMS)

It was decided to implement and apply a "Content Management System" (CMS). These systems administrate the pages of an Internet site by a data base system, ensure a common layout by predefined templates and provide simple interfaces to the authors who can use any browser to create, modify or delete pages – without experiences in HTML, CSS and additional languages.

The CMS to be selected should allow to

- imitate the existing layout of the DGFI homepage
- realise a dual language capability in order to serve german as well as english speaking users
- administrate so-called backend users, DGFI scientists that can act as authors for those pages they are responsible of.
- Commercial systems were excluded due to high cost for procurement and maintenance

Typo3

After a careful evaluation of different systems and some test installations the decision was made for 'Typo3', an Open Source project that is based on MySQL and PHP, two languages already used at DGFI. At the time of decision, Typo3 was already applied by a number of commercial sites and appeared as one of the most actively developed management systems suggesting reliability, further extensions and regular updates. Typo3 provides comfortable functions to handle graphics – a welcome feature supporting

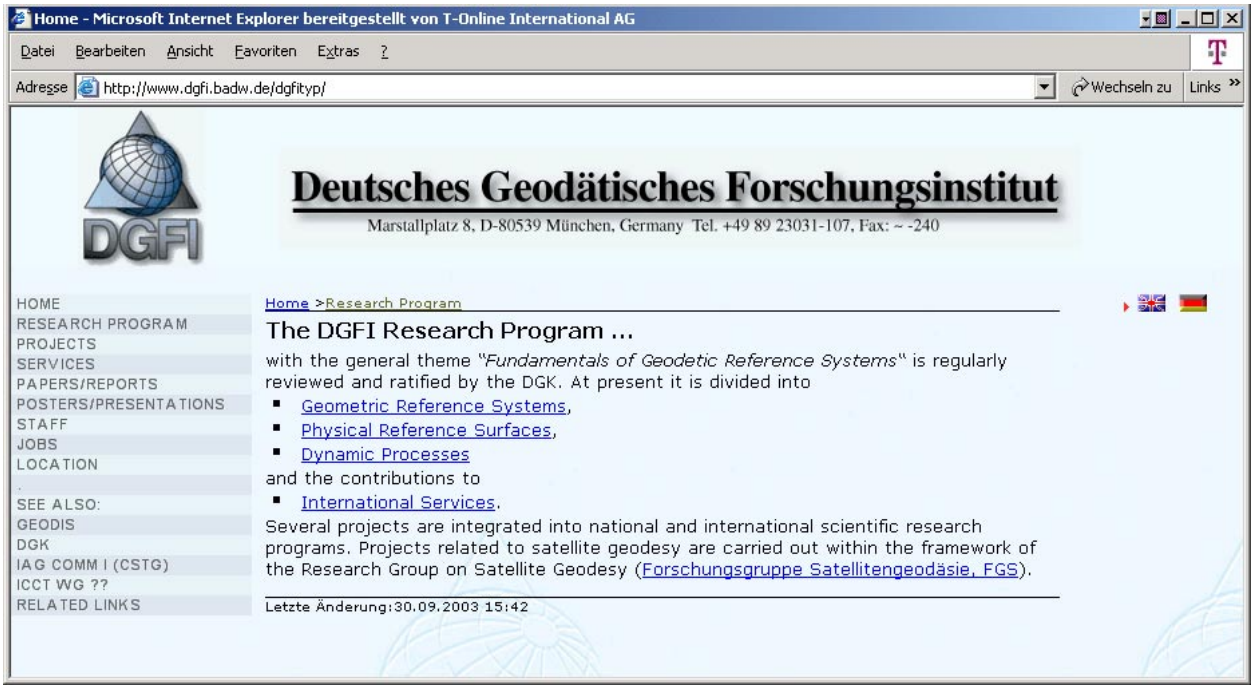

Fig. E2.1 Bilingual design of the new DGFI home page realised with the Open Source Typo3 Content Management System

the presentation of scientific results. The system is very powerful and flexible, but also pretentious to administrate.

The Typo3 system was installed and first used for the Intranet pages in order to become familiar with the definition of layouts and the administration of backend users. It was then applied to the DGFI home page. The conversion of the existing pages to the Typo3-system and the training of the DGFI scientists is an ongoing activity, but is completed in 2003. The layout, imitating rather closely the previous home page is shown in figure E2.1.

New Internet Site for IAG, Commission 1

With the restructuring of IAG at the IUGG General Assembly in Sapporo DGFI scientists took over leading roles within the new organisation (President of Commission 1, Chair of Inter-Commission Projects and of Study Groups, etc.). This led to the requirement of another Internet representation for IAG, Commission 1. With the experiences of the Content Management Systems, it suggested itself to realise this new site also with Typo3. Within two weeks it was possible to create a new home page for IAG, Commision 1 (see figure E2.2), including

- a design similar to that of the new IAG home page;
- numerous sub-pages for subcommissions, inter-commission projects, and study groups;
- the capability to let the sub-pages be maintained by those external scientists responsible for the sub-entities within IAG, Commission1.

The IAG, Commission 1 home page is available at the location

http://iag.dgfi.badw.de/

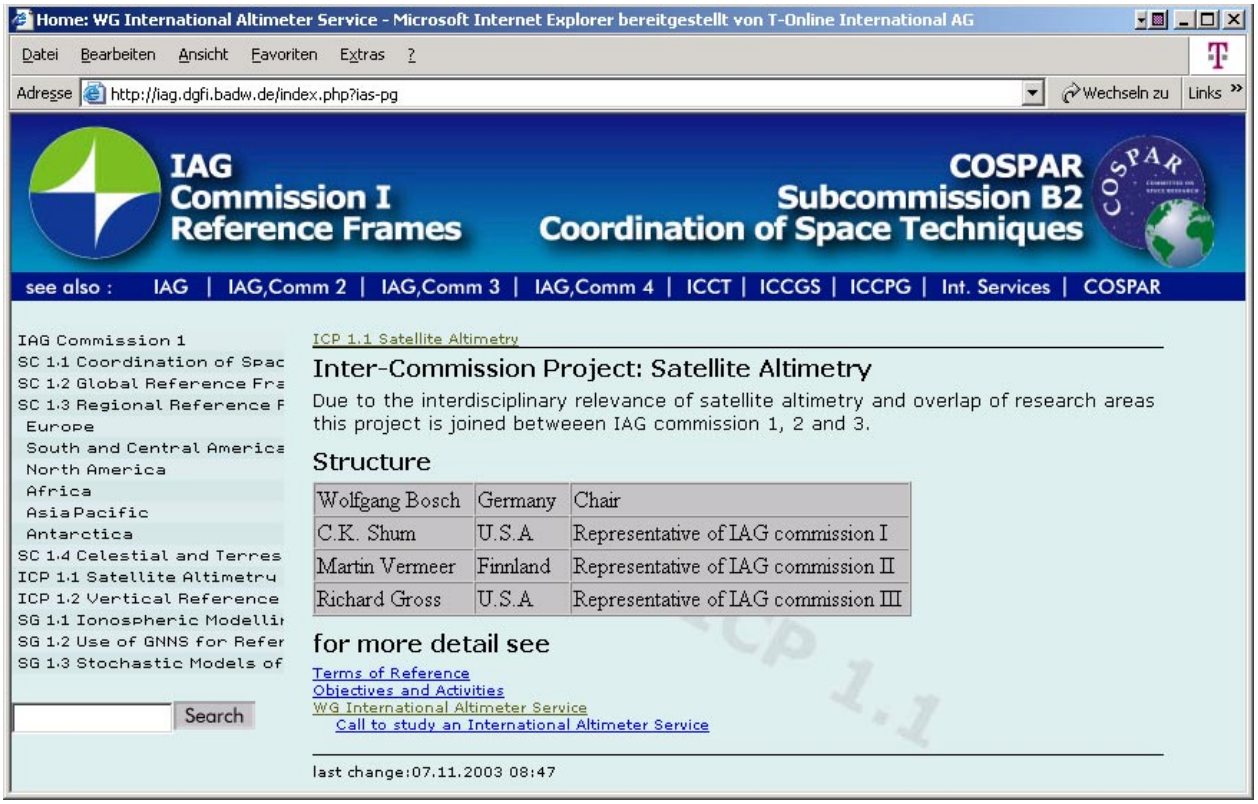

Fig. B2.2 Design of the new Internet site for IAG, Commission 1, realised with the Typo3 Content Management System

E3 Intranet

The DGFI Intranet is subject of permanent change. First there is new hardware to be integrated into the system, second there is a constant handling of backups, security and SPAM-Mail.

Hardware

During the year all servers have been replaced by new Linux-PCs with fast Pentium 4 processors, up to 2GByte RAM and as well as 360 GBytes diskspace. Additionally a PC with DVD-writer was purchased. All Linux PCs have SuSE Linux from version 8.1 to 9.0 as operating system, for the Windows PCs we use Windows98, Windows 2000 and Windows XP. Figure E.3.1 gives an overview on the DGFI hardware configuration.

Data Security

A considerable permanent problem relating to the amount of data stored at the DGFI data bases is the data security. There is no possibility for a complete backup of all disks, even on the archiving system in our computing centre „Leibniz Rechenzentrum“ we do not have the necessary capacity. Our data storage concept, already installed on the new servers, looks as follows

- no backup of the base operating system
- home-directories on a software raid-1 system (mirroring on local disks)
- Backup on demand on long term storage in the computing centre.
- additional system software: backup on server
- data directories: copy on backup PC

Fig. E3.1 DGFI Hardware Configuration

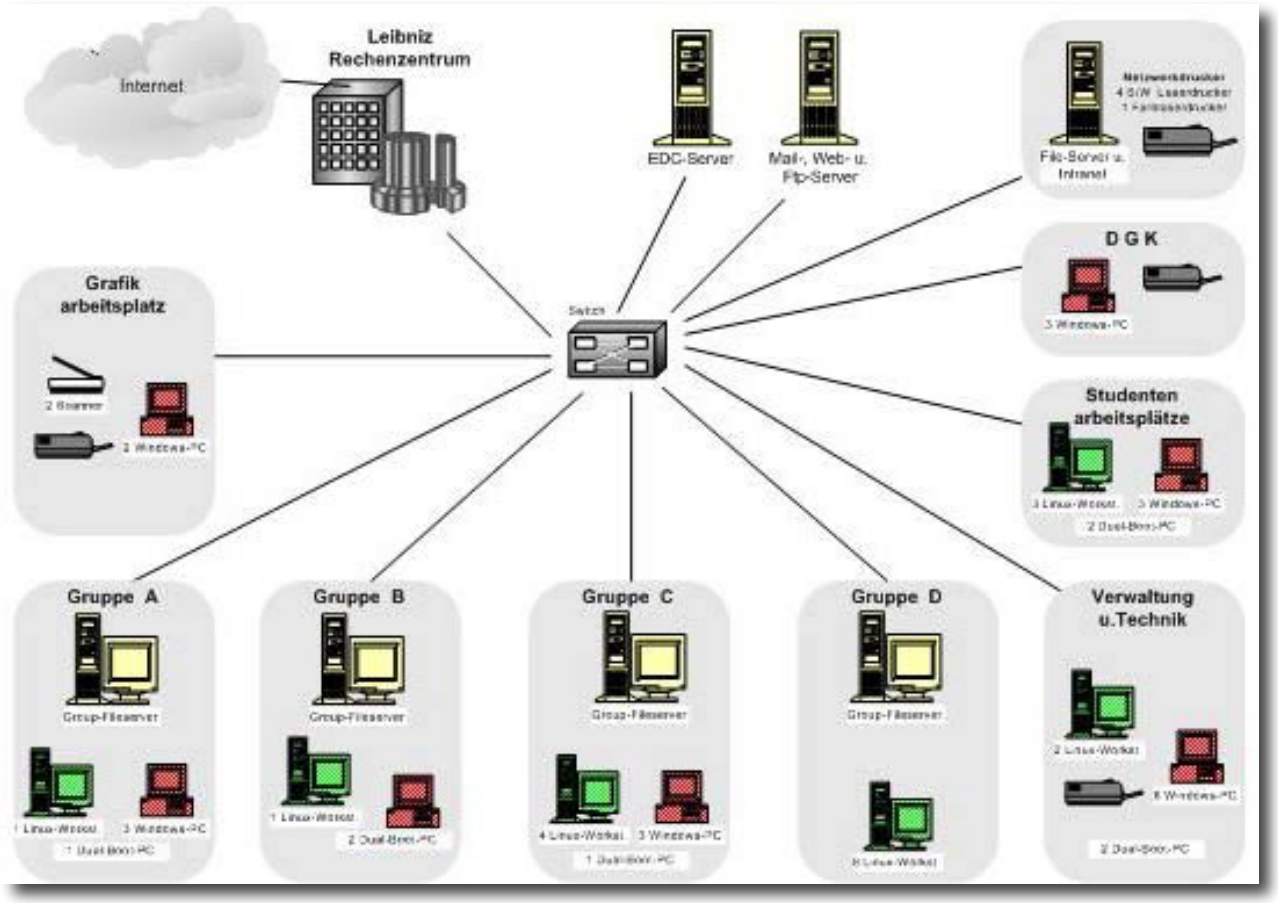

That means we use only half of the available diskspace for the data base and synchronize this diskspace with a mirror on a regular basis, depending on the relevance of the data between 5 min. and 24 hour intervals, using the rsync and unison software packages.

Our Intranet is separated from the Internet on the IP level, which means that no traffic from the net can affect our PCs. Net traffic is only possible from our Intranet to the Internet, only outgoing connections can receive data from the net.

Our critical servers, outside of our firewall, to which everyone can get access to from the Internet (EDC, http, ftp and mail server) are mirrored to an internal computer. In case of data damage or other problems, we can easily restore the previous data structure on these servers

SPAM Mail

In the last years, mainly in the last 2-3 months, a prevalence of unwelcome mail (SPAM mail) can generally be observed. It is nuisance to remove these mails from the mail box. Therefore we looked for a remedy for this problem. However, on the server side no operational software exists. So we suggest to use the SPAM filter capability of the Netscape email client, which works satisfying. A SPAM filter on the mail gateway in our computing centre is planned to be installed in the near future.

E4 Publications

Albertz, J., H.-P. Bähr, H. Hornik, R. Rummel (Eds.): Am Puls von Raum und Zeit - 50 Jahre Deutsche Geodätische Kommission - Festschrift. DGK, Reihe E, Heft 26, 306 S., München 2002.

Angermann, D., M. Krügel, B. Meisel, H. Müller, V. Tesmer: Time series of station positions and datum parameters. In: GEOTECHNOLOGIEN Science Report No. 3, 17-21, Koordinierungsbüro Geotechnologien, Potsdam, 2003.

Angermann, D., H. Drewes: Status and future of ITRF combination. In: GEOTECHNOLOGIEN Science Report No. 3, 12-16, Koordinierungsbüro Geotechnologien, Potsdam, 2003.

Angermann, D., H. Drewes, M. Gerstl, R. Kelm, M. Krügel, B. Meisel: IERS Combination Research Centre at DGFI. In: IERS Annual Report 2002, 94-95, BKG, Frankfurt a.M., 2003.

Angermann, D., H. Drewes, M. Gerstl, R. Kelm, M. Krügel, B. Meisel, H. Müller, W. Seemüller: ITRS Combination Centre at DGFI. In: IERS Annual Report 2002, 82-86, BKG, Frankfurt a.M., 2003.

Böhm, J., H. Schuh, V. Tesmer, H. Schmitz-Hübsch: Determination of tropospheric parameters by VLBI as a contribution to climatological studies. Österreichische Zeitschrift für Vermessung und Geoinformation, 91(1), 21-28, 2003.

Bosch, W.: Satellitenmissionen - Chancen und Herausforderungen für die Physikalische Geodäsie. In: Albertz, J., H.-P. Bähr, H. Hornik, R. Rummel (Eds.): Am Puls von Raum und Zeit - 50 Jahre Deutsche Geodätische Kommission - Festschrift. DGK, Reihe E, Heft 26, 74-83, München 2002.

Bosch, W.: Satellite altimetry. In: National Report of the Federal Republic of Germany on the Geodetic Activities in the Years 1999-2003. Deutsche Geodätische Kommission, Reihe B, Heft 312, 63-67, München, 2003.

Drewes, H.: The ILRS within the new structure of IAG and the Integrated Global Geodetic Observing System. ILRS 2001 Annual Report, NASA/TP-2002-211610, IX-X, Goddard Space Flight Center, Greenbelt, MD, 2002.

Drewes, H.: Das Deutsche Geodätische Forschungsinstitut - ehemals Abteilung I: Theoretische Geodäsie. In: Albertz, J., H.-P. Bähr, H. Hornik, R. Rummel (Eds.): Am Puls von Raum und Zeit - 50 Jahre Deutsche Geodätische Kommission - Festschrift. DGK, Reihe E, Heft 26, 159-177, München 2002.

Drewes, H.: Die Entwicklung der geodätischen Referenzsysteme in der Geodäsie. In: Albertz, J., H.-P. Bähr, H. Hornik, R. Rummel (Eds.): Am Puls von Raum und Zeit - 50 Jahre Deutsche Geodätische Kommission - Festschrift. DGK, Reihe E, Heft 26, 47-53, München 2002.

Drewes, H., B. Meisel: An actual plate motion and deformation model as a kinematic terrestrial reference system. In: GEOTECHNOLOGIEN Science Report No. 3, 40-43, Koordinierungsbüro Geotechnologien, Potsdam, 2003.

Drewes, H.: Report 1999-2003 of IAG Commission VIII „International Coordination of Space Techniques for Geodesy and Geodynamics". In: Travaux International Association of Geodesy, Vol. 32, 5 pp, 2003.

Drewes, H.: Report 1999-2003 on the Geocentric Reference System for the Americas (SIRGAS). In: Travaux International Association of Geodesy, Vol. 32, 2 pp, 2003.

Drewes, H.: Geodynamics - overview and highlights. In: National Report of the Federal Republic of Germany on the Geodetic Activities in the years 1999-2003, DGK, Reihe B, No. 312, 121-122, München 2003.

Drewes, H., B. Richter, M. Soffel: Earth rotation. In: National Report of the Federal Republic of Germany on the Geodetic Activities in the years 1999-2003, DGK, Reihe B, No. 312, 137-142, München 2003.

Fabert, O., M. Schmidt: Wavelet filtering with high time-frequency resolution and effective numerical implementation applied on polar motion. Artificial Satellites, Vol. 38, No. 1, 3-13, 2003.

Heck, B., H. Hornik, R. Rummel (Eds.): National Report of the Federal Republic of Germany on the Geodetic Activities in the Years 1999-2003. XXIII General Assembly of the International Union for Geodesy and Geophysics (IUGG) 2003 in Sapporo/Japan. DGK, Reihe B, No. 312, 143 S., München, 2003.

Heidbach, O., H. Drewes: 3-D finite element model of major tectonic processes in the Eastern Mediterranean. In: Nieuwland, D. (Ed.): New insigths in structural interpretation and modelling, Geol. Soc. Spec. Publs. (212) 261-274, London, 2003.

Hornik, H., G. Kirschmer, K. Schnädelbach, R. Sigl: 50 Jahre Deutsche Geodätische Kommission. In: Albertz, J., H.-P. Bähr, H. Hornik, R. Rummel (Eds.): Am Puls von Raum und Zeit - 50 Jahre Deutsche Geodätische Kommission - Festschrift. DGK, Reihe E, Heft 26, 99-110, München 2002.

Hornik, H., H. Tremel: Punktbestimmung im Rahmen der photogrammetrischen Neuaufnahme des Gletschergebietes Tujuksu, Tienschan. AVN 110(1), 10-15, 2003.

Ihde, J., H. Habrich, H. Hornik, K. H. Pahler, W. Schlüter: Precise positioning on global and regional scales. In: Heck, B., H. Hornik, R. Rummel (Eds.): National Report of the Federal Republic of Germany on the Geodetic Activities in the Years 1999-2003. XXIII General Assembly of the International Union for Geodesy and Geophysics (IUGG) 2003 in Sapporo/Japan. DGK, Reihe B, No. 312, 11-19, München, 2003.

Kaniuth, K., C. Völksen: Comparison of the BERNESE and GIPSY/OASIS II software systems using EUREF data. Mitt. des Bundesamtes für Kartographie und Geodäsie 29, 314-319, 2003.

Kaniuth, K., S. Huber: Nachweis von Höhenänderungen aufgrund atmosphärischer Druckvariationen aus GPS-Messungen. ZfV 128(4), 278-283, 2003.

Kaniuth, K., S. Huber: An assessment of radome effects on height estimates in the EUREF network. Mitt. des Bundesamtes für Kartographie und Geodäsie 29, 97-102, 2003.

Kelm, R.: Automated combination of SLR solutions within ILRS. In: GEOTECHNOLOGIEN Science Report No. 3, 89-91, Koordinierungsbüro Geotechnologien, Potsdam, 2003.

Krügel, M., B. Meisel: DGFI results of the IERS SINEX combination campaign. In: GEOTECHNOLOGIEN Science Report No. 3, 96-100, Koordinierungsbüro Geotechnologien, Potsdam, 2003.

Kutterer, H.: Joint treatment of random variability and imprecision in GPS data analysis. Journal of Global Positioning Systems, Vol. 1, No. 2, 96-105, 2002.

Kutterer, H., M. Schmidt: Non-stochastic methods of data evaluation. In: National Report of the Federal Republic of Germany on the Geodetic Activities in the Years 1999-2003, DGK, Reihe B, No. 312, 114-117, München 2003.

Meisel, B., M. Krügel, D. Angermann, M. Gerstl, R. Kelm: Intra- and inter-technique combination for the ITRF. In: GEOTECHNOLOGIEN Science Report No. 3, 108-111, Koordinierungsbüro Geotechnologien, Potsdam, 2003.

Müller, H., D. Angermann, R. Kelm: DGFI Associate Analysis Center. In: ILRS 2001 Annual Report, NASA/TP-2002-211610, 7/17-18.

Nothnagel, A, D. Angermann, J. Campbell, D. Fischer, M. Gerstl, R. Kelm, M. Krügel, B. Meisel, M. Rothacher, Ch. Steinforth, D. Thaller, M. Vennebusch: Combination of Earth monitoring products by IERS combination research centers. In: GEOTECHNOLOGIEN Science Report No. 3, 120-125, Koordinierungsbüro Geotechnologien, Potsdam, 2003.

Popinski,W., W. Kosek, H. Schuh, M. Schmidt: Comparison of two Wavelet Transform Coherence and Cross-covariance Functions Applied on Polar Motion and Atmospheric Excitation. Stud. Geophys. Geod. 46, 455-465, 2002.

Rothacher, M., J. Campbell, A. Nothnagel, H. Drewes, D. Angermann, D. Grünreich, B. Richter, Ch. Reigber, S. Y. Zhu: Integration of space geodetic techniques and establishment of a user center in the framework of the International Earth Rotation and Reference Systems Service (IERS). In: GEOTECHNOLOGIEN Science Report No. 3, 137-141, Koordinierungsbüro Geotechnologien, Potsdam, 2003.

Tesmer, V., H. Kutterer, H. Drewes: DGFI Analysis Center Annual Report 2002. In: Vandenberg, N. und K. Baver (Eds.): International VLBI Service for Geodesy and Astrometry, Annual Report 2002, 238-240, 2003.

E5 Posters and Oral Presentations

Acuña, G., W. Bosch: VGM02, a new high-resolution geoid for Venezuela and eastern Caribbean Sea. EGS-AGU-EUG 2003 Joint Assembly, Nice, France, 07.04.2003 (Poster).

Acuña, G., W. Bosch: Combining terrestrial, marine, and satellite gravity for geoid modeling in Venezuela. IUGG XXIII General Assembly, IAG Symposium G03, Determination of the gravity field, Sapporo, Japan, 07.07.2003 (Poster).

Akyilmaz, O., H. Kutterer: Fuzzy inference systems for the prediction of Earth rotation parameters. IUGG XXIII General Assembly, IAG Symposium G05, Geodynamics, Sapporo, Japan, 04.07.2003 (Poster).

Angermann, D.: ITRF-Kombination - aber wie? Geodätische Woche 2002, Frankfurt a.M., 17.10.2002.

Angermann, D.: Issues of a rigorous combination, part 3: IERS/SINEX Combination Campaign. IERS Workshop on Combination Research and Global Geophysical Fluids, München, 19.11.2002.

Angermann, D.: Status and future of ITRF Combination. Statusseminar Geotechnologien “Erfassung des Systems Erde aus dem Weltraum”, München, 12.06.2003.

Angermann, D.: ITRF Combination - Status and recommendations for the future. IUGG XXIII General Assembly, IAG Symposium G01, Positioning, Sapporo, Japan, 03.07.2003.

Angermann, D., M. Krügel, B. Meisel, H. Müller, V. Tesmer: Time evolution of the terrestrial reference frame.IUGG XXIII General Assembly, IAG Symposium G01, Positioning, Sapporo, Japan, 30.06.-11.07.2003 (Poster).

Angermann, D., B. Meisel, M. Krügel, H. Müller, V. Tesmer: Analysis of VLBI, SLR, GPS and DORIS site position time series. IERS Workshop on Combination Research and Global Geophysical Fluids, München, 18.-21.11.2002 (Poster).

Angermann, D., M. Krügel, B. Meisel, H. Müller, V. Tesmer: Time series of station positions and datum parameters. Statusseminar Geotechnologien “Erfassung des Systems Erde aus dem Weltraum”, München, 12.-13.06.2003 (Poster).

Bosch, W.: Satellitenmissionen - Chancen und Herausforderungen für die Physikalische Geodäsie. Festveranstaltung 50 Jahre DGK, Bayerische Akademie der Wissenschaften, München, 25.10.2002.

Bosch, W.: OpenADB - an open altimeter data base. EGS-AGU-EUG 2003 Joint Assembly, Nice, France, 09.04.2003 (Poster).

Bosch, W.: Combined crossover- and repeat-pass-analysis for cross-calibration of altimeter missions. EGS-AGU-EUG 2003 Joint Assembly, Nice, France, 09.04.2003 (Poster).

Bosch, W.: On the combination of altimetry and satellite derived gravity field models. IUGG XXIII General Assembly, Joint Symposium ISG02, Interdisciplinary Earth Science from Improved Gravity Field Modeling, Sapporo, Japan, 09.07.2003 (Poster).

Bosch, W.: Altimetry as a new service in IGGOS. IUGG XXIII General Assembly, IAG Symposium G07, Global Geodetic Observing System, Sapporo, Japan, 10.07.2003.

Bosch, W.: Dekodieren und Extrahieren von Altimeterdaten mit binread. Geodätische Woche 2003, Hamburg, 16.-19.09.2003 (Poster).

Bosch, W., R. Savcenko: Geodätische Anwendungen der Satellitenaltimetrie. Geodätische Woche 2003, Hamburg, 17.-19.09.2003 (Poster).

Dill, R., F. Seitz: The influence of load deformations on Earth rotation. IUGG XXIII General Assembly, IAG Symposium G06, Insight into Earth System Science: Variations in the Earth’s Rotation and its Gravity Field, Sapporo, Japan, 04.07.2003 (Poster).

Drewes, H.: Sistemas de referencia en geodesia. Fortbildungskursus, IGM Buenos Aires, Argentina, 15.10.-18.10.2002.

Drewes, H.: The Actual Plate KInematic and crustal deformation Model (APKIM) derived from space geodetic observations. IAG Symposium “Crustal Deformations in South America and Surrounding Regions”, Santiago, Chile, 21.-25.10.2002 (Poster).

Drewes, H.: Use of SIRGAS final results. SIRGAS Workshop, Santiago, Chile, 21.10.2002.

Drewes, H.: Determination of SIRGAS station velocities. SIRGAS Workshop, Santiago, Chile, 21.10.2002.

Drewes, H.: The realisation of the height reference surface - W_0 considerations. SIRGAS Workshop, Santiago, Chile, 22.10.2002.

Drewes, H.: The urgent need of modern vertical reference systems. SIRGAS Workshop, Santiago, Chile, 22.10.2002.

Drewes, H.: Possible IGGOS Structure(s). Second Meeting of the IGGOS Planning Group, Munich, 22.11.2002.

Drewes, H.: Die Entwicklung der geometrischen Referenzsysteme in der Geodäsie. Festveranstaltung 50 Jahre DGK, München, 25.11.2002.

Drewes, H.: Die Arbeiten des DGFI im Jahr 2001/2002. Jahresvollsitzung der DGK, Kloster Seeon, 26.11.2002.

Drewes, H.: Forschungsplan 2003/2004 für das DGFI. Jahresvollsitzung der DGK, Kloster Seeon, 26.11.2002.

Drewes, H.: Deformation models of the South American crust. 18. Geowiss. Lateinamerika Kolloquium, Freiberg/Sachsen, 03.04.2003.

Drewes, H.: Das Internationale Terrestrische Referenzsystem (ITRS) und seine Realisierung durch die Dienste der IAG. Geodätisches Kolloquium der Fachhochschule Anhalt, Dessau, 04.04.2003.

Drewes, H.: Curso Sistemas de Referencia en Geodesia. Curitiba, Brazil, 05.-06.05.2003.

Drewes, H.: Activities and products of the services of the International Association of Geodesy (IAG). III Colóquio Brasileiro de Ciências Geodésicas, Curitiba, Brazil, 07.05.2003.

Drewes, H.: Report of Commission VIII „International Coordination of Space Techniques for Geodesy and Geodynamics (CSTG). XXIII IUGG Gen. Ass., Symposium G02, Sapporo, Japan, 04.07.2003.

Drewes, H.: Deformation of the South American crust from finite element and collocation methods. XXIII IUGG Gen. Ass., Symposium G05, Sapporo, Japan, 04.07.2003.

Drewes, H.: Sistemas de referencia en el mundo. XXI Congresso Brasileiro de Cartografia. Belo Horizonte, Brazil, 01.10.2003.

Drewes, H.: Avances en la realización de los sistemas de referencia terrestres. Instituto Geográfico Agustin Codazzi, Bogotá, Colombia, 10.10.2003.

Drewes, H.: Remarks on some problems in the combination of station coordinate and velocity solutions. IERS Workshop, München, 18.11.2002.

Drewes, H., B. Meisel: An actual plate motion and deformation model as a kinematic terrestrial reference system. Statusseminar Geotechnologien “Erfassung des Systems Erde aus dem Weltraum”, München, 12.-13.06.2003 (Poster).

Drewes, H., K. Kaniuth, C. Völksen, S.M. Costa, L.P. Fortes: Results of the SIRGAS campaign 2000 and coordinate variations with respect to the 1995 South American geocentric reference frame. XXIII IUGG Gen. Ass., Symposium G01, Sapporo, Japan, 03.07.2003 (Poster).

Drewes, H.: A finite element crustal deformation model for South America. IAG Symposium “Crustal Deformations in South America and Surrounding Regions”, Santiago, Chile, 22.10.2002.

Fabert, O.: Regional equipotential surfaces from satellite and regional terrestrial data using multiresolution analysis. EGS-AGU-EUG 2003 Joint Assembly, Nice, France, 07.04.2003.

Fabert, O., M. Schmidt: A wavelet filterbank for high resolution signal decomposition - Extraction of the Chandler Wobble. Weikko A. Heiskanen Symposium, Columbus/Ohio, U.S.A., 1.-4.10., 2002 (Poster).

Huber, S., K. Kaniuth: On the weighting of GPS phase observations in the EUREF network processing. EUREF Symposium, Toledo, Spain, 04.-07.06.2003 (Poster).

Kaniuth, K.: Results of the SIRGAS 2000 GPS campaign. IAG Symposium "Recent crustal deformations in South America and surrounding area", Santiago, Chile, 22.10.2002.

Kaniuth, K.: Continuous and episodic deformations along the Caribbean-South American plate boundary derived from repeated GPS observations in the CASA project. IAG Symposium "Recent crustal deformations in South America and surrounding area", Santiago, Chile, 22.10.2002.

Kaniuth, K.: Modelling vertical site displacements due to atmospheric pressure loading with the Bernese GPS software - A demonstration using EUREF data. EUREF Symposium, Toledo, Spain, 05.06.2003.

Kelm, R.: Automated combination of SLR solutions within ILRS. Statusseminar Geotechnologien "Erfassung des Systems Erde aus dem Weltraum", München, 12.-13.06.2003 (Poster).

Kelm, R.: Rank defect analysis and variance component estimation for inter-technique combination. IERS Workshop on Combination Research and Global Geophysical Fluids, München, 19.11.2002.

Krügel, M.: DGFI results of the IERS SINEX combination campaign. EGS-AGU-EUG 2003 Joint Assembly, Nice, France, 10.04.2003.

Krügel, M., B. Meisel: DGFI results of the IERS SINEX combination campaign. Statusseminar Geotechnologien "Erfassung des Systems Erde aus dem Weltraum", Bayerisches Landesvermessungsamt, München, 12.-13.06.2003 (Poster).

Kutterer, H.: Parameterschätzung und Hypothesentests für impräzise Daten. Geodätische Woche, Frankfurt a.M., 15.10.2002.

Kutterer, H.: Arbeitsgruppe "Rotation der Erde" - Stand des Konzeptpapiers. DFG-Treffen "Erdrotationsvektor", TU Dresden, 22.10.2002.

Kutterer, H.: Die Messung in der Geodäsie - Standpunkt und Zielrichtung. Antrittsvorlesung, Fakultät für Bauingenieur- und Vermessungswesen, Universität Karlsruhe, 08.11.2002.

Kutterer, H.: Robust parameter estimation in VLBI data analysis. OCCAM Workshop, Paris Observatory, Paris, France, 02.04.2003.

Kutterer, H.: The role of parameter constraints in VLBI data analysis. IVS Analysis Workshop, Paris Observatory, Paris, France, 03.04.2003.

Kutterer, H.: Konzeptpapier Erdrotation - System Erde und seine Komponenten. DFG-Rundgespräch "Erdrotation und globale dynamische Prozesse", Höllenstein, 28.04.2003.

Kutterer, H.: Konzeptpapier Erdrotation - Analyse zeitlich und räumlich verteilter Daten. DFG-Rundgespräch "Erdrotation und globale dynamische Prozesse", Höllenstein, 28.04.2003.

Kutterer, H.: Konzeptpapier Erdrotation - Auswertung der Daten und Analyse der Ergebnisse. DFG-Rundgespräch "Erdrotation und globale dynamische Prozesse", Höllenstein, 29.04.2003.

Kutterer, H.: Statistische Aspekte der subtäglichen Auflösung von Erdrotationsparametern mit VLBI. DFG-Rundgespräch "Erdrotation und globale dynamische Prozesse", Höllenstein, 29.04.2003.

Kutterer, H.: The role of parameter constraints in VLBI data analysis. 16th Working Meeting on European VLBI, Leipzig, 09.05.-10.05.2003.

Kutterer, H.: Realistic uncertainty measures for GPS observations. IUGG XXIII General Assembly, IAG Symposium G01, Positioning, Sapporo, Japan, 02.07.2003.

Kutterer, H.: Alternatives for the modeling of uncertainty in geodetic positioning. IUGG XXIII General Assembly, IAG Symposium G01, Positioning, Sapporo, Japan, 02.07.2003.

Kutterer, H.: Joint treatment of random variability and imprecision in GPS data analysis. IUGG XXIII General Assembly, IAG Symposium G01, Positioning, Sapporo, Japan, 03.07.2003 (Poster).

Kutterer, H.: IAG SSG 4.190 final report. IUGG XXIII General Assembly, IAG Symposium G04, General Theory and Methodology, Sapporo, Japan, 07.07.2003.

Kutterer, H., R. Heinkelmann, V. Tesmer: Robust outlier detection in VLBI data analysis. 16th Working Meeting on European VLBI, Leipzig, 09.05.-10.05.2003 (Poster).

Kutterer, H., V. Tesmer: VLBI activities at DGFI. IUGG XXIII General Assembly, IAG Symposium G05, Geodynamics, Sapporo, Japan, 04.07.2003 (Poster).

Meisel, B.: IDS - ein IAG Service im Aufbau. Geodätische Woche 2002, Frankfurt a.M., 16.10.2002.

Meisel, B.: ITRF Combination Center at DGFI - combined solution 2002, Geodätische Woche 2003, Hamburg, 17.09.2003.

Meisel, B.: Intra-technique combination at DGFI: some aspects related to DORIS. IDS-Analysis Workshop, Marne la Vallée, France, 21.02.2003.

Meisel, B., D. Angermann, R. Kelm, M. Krügel: Datum definition for the combination of station positions and Earth orientation parameters. EGS-AGU-EUG 2003 Joint Assembly, Nice, France, 06.-11.04.2003 (Poster).

Meisel, B., M. Krügel, D. Angermann, M. Gerstl, R. Kelm: Intra- and inter-technique combination for the ITRF. Statusseminar Geotechnologien "Erfassung des Systems Erde aus dem Weltraum", München, 12.-13.06.2003 (Poster).

Miller, R., D. Angermann, M. Krügel, B. Meisel: Analyse von Stationskoordinaten globaler Wochenlösungen verschiedener Raumverfahren, Geodätische Woche 2003, Hamburg, 16.-19.09.2003 (Poster).

Müller, H.: DGFI results, pilot project on benchmarking. 8th ILRS/AWG Workshop, Nice, France, 03.04.2003.

Popinski,W., W. Kosek, H. Schuh, M. Schmidt: Is there any frequency dependent time lag between polar motion and its atmospheric excitation? XXVII EGS Gen. Ass. EGS, Nice, France, 21.-26.04.2002 (Poster).

Richter, B.: Das neue zälestische und terrestrische Äquatorsystem. Geodätische Woche 2002, Frankfurt a.M., 16.10.2002.

Sánchez, L., H. Drewes: Realisation of the South American vertical reference system. IAG Symposium "Crustal Deformations in South America and Surrounding Regions", Santiago de Chile, 21.-25.10. 2002 (Poster).

Savcenko, R.: Über die Berechnung von Schwereanomalien aus Altimeterdaten. Geodätische Woche 2003, Hamburg, 19.09.2003.

Schmidt, M.: Towards the estimation of a multi-resolution representation of the gravity field based on spherical wavelets. IUGG XXIII General Assembly, IAG Symposium G03, Determination of the gravity field, Sapporo, Japan, 05.07.2003.

Schmidt, M.:Towards the estimation of a multi-resolution gravity field representation based on spherical harmonics and wavelets. 2nd CHAMP Science Meeting, Potsdam, 03.09.2003.

Schmidt, M.: Applications of spherical wavelets in meteorological and space weather studies. Radio Occultation Science Workshop, Boulder/Colorado, U.S.A., 22.08. 2002.

Schmidt, M.: Multi-resolution representation of the gravity field using spherical wavelets. Weikko A. Heiskanen Symposium, Columbus/Ohio, U.S.A., 03.10. 2002.

Schmidt, M., O. Fabert, C.K. Shum: Multi-resolution representation and estimation of the gravity field using spherical wavelets. AGU 2002 Fall Meeting, San Francisco/California, U.S.A., 06.-10.12. 2002 (Poster).

Schmidt, M., O. Fabert, C.K. Shum: On the estimation of a multi-resolution representation of the gravity field based on spherical harmonics and wavelets. EGS-AGU-EUG 2003 Joint Assembly, Nice, France, 06.-11.04.2003 (Poster).

Schön, S.: Imprecision in geodetic observations - Case study GPS monitoring network. 11th International Symposium on Deformation Measurements, Santorini, Greece, 27.05.2003.

Schön, S.: Ansätze zu einer realistischeren Unsicherheitsbetrachtung für GPS-Trägerphasenbeobachtungen. Geodätische Woche 2003, Hamburg, 16.09.2003.

Schön, S.: Zonotope als Impräzisionsmaße. Geodätische Woche 2003, Hamburg, 18.09.2003.

Seemüller, W.: ILRS data formats & procedures working group report, 13th International Workshop on Laser Ranging, Washington D.C., USA, 08.10.2002.

Seemüller, W.: ILRS Data Centers report, 13th International Workshop on Laser Ranging, Washington D.C., USA, 11.10.2002.

Seemüller, W.: Kinematics of the IGS regional reference network for South America, IAG Symposium "Crustal Deformation", Santiago, Chile, 22.10.2002.

Seemüller, W., K. Kaniuth: Impact of earthquakes on the IGS regional reference network for South America, IAG Symposium "Crustal Deformation", Santiago, Chile, 21.-25.10.2002 (Poster).

Seitz, F.: Untersuchungen zur Rotationsdynamik der Erde mit einem freien Kreiselmodell. Geodätische Woche 2002, Frankfurt a.M., 17.10.2002.

Seitz, F.: Studies on Chandler wobble excitation using a non-linear gyroscopic Earth model. Geodätisches Oberseminar am Geodätischen Institut, Universität Stuttgart, 18.02.2003.

Seitz, F.: Ein nichtlineares Systemmodell zur konsistenten Untersuchung von Rotation, Oberflächengestalt und Schwerefeld der Erde. DFG-Rundgespräch "Erdrotation und globale dynamische Prozesse", Höllenstein, 28.04.2003.

Seitz, F.: Sensitivity analysis of the non-linear Liouville equation. IUGG XXIII General Assembly, IAG Symposium G06, Insight into Earth System Science: Variations in the Earth's Rotation and its Gravity Field, Sapporo, Japan, 03.07.2003.

Seitz, F.: DyMEG: Ein konsistentes Erdsystemmodell zur Untersuchung von Erdrotations- und Schwerefeldvariationen. Geodätische Woche 2003, Hamburg, 17.09.2003.

Seitz, F., J. Stuck, M. Thomas: Consistent atmosphereic and oceanic excitation of a Free Gyroscopic Earth model. AGU 2002 Fall Meeting, San Francisco, USA, 09.12.2002 (Poster).

Seitz, F., J. Stuck, M. Thomas: High frequency Chandler wobble excitation. EGS-AGU-EUG Joint Assembly, Nice, France, 07.04.2003 (Poster).

Seitz, F., D. Angermann, H. Müller, H. Kutterer: Consistent model DyMEG for Earth rotation and gravitation. IUGG XXIII General Assembly, IAG Symposium G06, Insight into Earth System Science: Variations in the Earth's Rotation and its Gravity Field, Sapporo, Japan, 04.07.2003 (Poster).

Tesmer, V.: Refinement of the stochastic model for VLBI data analysis. 4th IVS Analysis Workshop, Paris, France, 04.04.2003.

Tesmer, V.: Refinement of the stochastic model for VLBI data analysis. 16th Working Meeting on European VLBI, Leipzig, 10.05.2003.

E6 Membership in Scientific Bodies

International Council for Science (ICSU)
- International Lithosphere Program (ILP) (Bureau Member: H. Drewes)
- Committee on Space Research (COSPAR): Subcommission B2 International Coordination of Space Techniques for Geodesy and Geodynamics (President: H. Drewes)

International Union of Geodesy and Geophysics (IUGG)
- IUGG Representative to Panamerican Institute for Geography and History, PAIGH (H. Drewes)
- IUGG Representative to United Nations Cartographic Office (H. Drewes)

International Association of Geodesy (IAG)
- Commission 1: Reference Frames (President: H. Drewes)
- Inter-commission Project 1.1: Satellite Altimetry (Chairman: W. Bosch)
- Subcommission 1.3a: EUREF (Secretary: H. Hornik)
- Subcommission 1.3a: EUREF Technical Working Group (H. Hornik)
- Working Group 1.2.3 and ICCT WG3: Integrated theory for crustal deformation (B. Meisel)
- IAG-Representative to Sistema de Referencia Geocéntrico para las Américas, SIRGAS (H. Drewes)
- Study Group 1.1: Ionosphere Modelling (M. Schmidt)
- Study Group 1.3 and ICCT Working Group: Quality measures, quality control, and quality improvement (Chairman: H. Kutterer, members: M. Krügel, S. Schön)
- Study Group 2.3: Satellite Altimetry: data quality improvement and coastal applications (W. Bosch)
- Project Integrated Global Geodetic Observing System, IGGOS (Secretary: H. Drewes)
- International Laser Ranging Service (ILRS): Governing Board (H. Drewes, W. Seemüller)
- International Laser Ranging Service (ILRS): Analysis Working Group (D. Angermann, R. Kelm, H. Müller)
- International Laser Ranging Service (ILRS): Data Formats and Procedures Working Group (Chairman: W. Seemüller)
- International VLBI Service for Geodesy and Astrometry (IVS) – Special Analysis Center (H. Drewes, H. Kutterer, V. Tesmer)

European Space Agency (ESA)
- Radar Altimeter 2 Science Advisory Group, RA2SAG (W. Bosch)

Consortium of European Laser Stations EUROLAS
- Member in the EUROLAS Board of Representatives (W. Seemüller)
- EUROLAS Secretary (W. Seemüller)

Deutsche Geodätische Kommission (DGK)
- 'Ständiger Gast' (H. Drewes)
- Working Group "Rezente Krustenbewegungen", "Theoretische Geodäsie" (several collaborators)

Deutsche Forschungsgemeinschaft (DFG)
- Deutscher Landesausschuß für das Internationale Lithosphärenprogramm (H. Drewes)

Deutscher Verein für Vermessungswesen (DVW), Gesellschaft für Geodäsie, Geoinformation und Landmanagement
- Working Group 10 „Experimentelle, angewandte und theoretische Geodäsie" (H. Drewes)

Forschungsgruppe Satellitengeodäsie (FGS)
- Members of the managing board (W. Bosch, H. Drewes)

E7 Participation in Meetings, Symposia, Conferences

NIMA NURI 2002 Symposium USGS, Reston/Virginia, USA, 16.-17.7.2002 (Schmidt)

13th International Workshop on Laser Ranging, "Towards Millimeter Accuracy", Washington D.C., USA, 07.-11.10.2002 (Seemüller)

Geodätische Woche, Frankfurt a.M., 15.-17.10.2002 (Angermann, Kutterer, Meisel, Richter, Seitz)

IAG Symposium „Recent Crustal Deformations in South America and Surrounding Regions", Santiago, Chile, 21.-22.10.2002 (Drewes, Kaniuth, Seemüller)

DFG-Treffen "Erdrotationsvektor", Institut für Planetare Geodäsie, TU Dresden, 21.-22.10.2002 (Kutterer, Seitz)

Jahresvollsitzung der DGK, München und Kloster Seeon, 24.10. und 26.10.2002 (Drewes, Hornik)

Festveranstaltung 50 Jahre DGK, Bayerische Akademie der Wissenschaften, München, 25.10.2002 (several collaborators of DGFI)

EUREF TWG Meeting, Delft, 07.-08.11.2002 (Hornik)

IERS Workshop on Combination Research and Global Geophysical Fluids, Bayerische Akademie der Wissenschaften, München, 18.11.-21.11.2002 (several collaborators of DGFI)

AGU 2002 Fall Meeting, San Francisco, USA, 06.-10.12.2002 (Schmidt, Seitz)

Geotechnologien-Projekt IERS/ITRF, Frankfurt/Main, 24.-25.02.2003 (Angermann, Drewes, Kelm, Krügel, Meisel)

Meeting of the EUREF Technical Working Group, Paris, France, 06-07.03.2003 (Hornik)

FGS Vorstands- und Stationsleiter-Sitzung, Wettzell, 17.-18.03.2003 (Bosch, Drewes)

Weikko A. Heiskanen Symposium, Columbus/Ohio, U.S.A., 01.-04.10.2002 (Schmidt)

Radio Occultation Science Workshop, Boulder/Colorado, U.S.A., 21.-23.08.2002 (Schmidt)

Workshop zum 6. Forschungsrahmenprogramm der EU, Bonn, 11.11.2002 (Bosch)

ENVISAT RA2 Cross-Calibration and Validation Team (CCVT) Meeting, Frascati, Italy, 03.-04.12.2002 (Bosch)

Koordinatorentreffen DFG-Schwerpunkt "Mass Transports and Mass Distribution in the Earth System", Hannover, 24.01.2003 (Bosch)

DGK, Sitzung des Wissenschaftl. Beirats, Bayerische Akademie der Wissenschaften, München, 20.02.2003 (Angermann, Bosch, Drewes, Hornik, Kutterer)

IDS-Analysis Workshop, Marne la Vallée, France, 20.-21.02.2003 (Meisel)

Koordinatorentreffen DFG-Schwerpunkt "Mass Transports and Mass Distribution in the Earth System", Frankfurt, 14.03.2003 (Bosch)

OCCAM Workshop, Paris Observatory, Paris, France, 02.04.03 (Kutterer, Tesmer)

IVS Analysis Workshop, Paris Observatory, Paris, France, 03.04.03 (Kutterer, Tesmer)

18. Geowissenschaftliches Lateinamerika-Kolloquium, Freiberg, Sachsen, 02.-05.04.2003 (Drewes)

8th ILRS/AWG Workshop, Nice, France, 03.-04.04.2003 (Kelm, Müller)

EGS/AGU-EUG 2003 Joint Assembly, Nice, France, 07.-11.04.2003 (Bosch, Drewes, Fabert, Krügel, Meisel, Schmidt, Seemüller)

ILRS Data Formats & Procedures Work Group Meeting, Nice, France, 08.04.2003 (Seemüller)

CSTG Executive Committee Meeting, Nice, France, 09.04.2003 (Bosch, Drewes)

ILRS Governing Board Meeting, Nice, France, 09.04.2003 (Seemüller, Drewes)

ILRS General Assembly, Nice, France, 10.04.2003 (Seemüller)

IAG Executive Committee Meeting, Nice, France, 10.-11.04.2003 (Drewes)

DFG-Rundgespräch „Erdrotation und globale dynamische Prozesse", Höllenstein, 28.-29.04.2003 (Kutterer, Schmidt, Seitz)

16th Working Meeting on European VLBI, Leipzig, 09./10.05.2003 (Kutterer, Tesmer)

III. Colóquio Brasileiro de Ciências Geodésicas, Curitiba, Brazil, 06.-09.05.2003 (Drewes)

FIG 11th International Symposium on Deformation Measurements, Santorini, Greece, 25.-28.05.2003 (Schön)

EUREF Symposium, Toledo, Spain, 04.-07.06.2003 (Hornik, Huber, Kaniuth)

Statusseminar Geotechnologien "Erfassung des Systems Erde aus dem Weltraum", Bayerisches Landesvermessungsamt, München, 12.-13.06.2003 (Angermann, Drewes, Kelm, Krügel, Meisel, Müller)

IUGG 2003, XXIII General Assembly of the International Union of Geodesy and Geophysics, Sapporo, Japan, 30.06.-11.07.2003 (Angermann, Bosch, Drewes, Kutterer, Seitz)

IGGOS Planning Group Meeting, Sapporo, Japan, 02.07.2003 (Drewes)

CSTG Executive Committee Meeting, Sapporo, Japan, 04.07.2003 (Drewes)

IAG Executive Committee Meeting, Sapporo, Japan, 05.07. and 07.07.2003 (Drewes)

IAG Commission 1 Steering Committee Meeting, Sapporo, Japan, 07.07.2003 (Bosch, Drewes)

ILP Bureau Meeting, Sapporo, Japan, 09.07.2003 (Drewes)

2nd CHAMP Science Meeting, GeoForschungsZentrum, Potsdam, 01.-04.09.2003 (Bosch)

DFG CHAMP-Bündeltreffen, GeoForschungsZentrum, Potsdam, 04.09.2003 (Bosch)

Koordinatorentreffen DFG-Schwerpunkt "Mass Transport and Mass Distribution in the Earth System", GeoForschungsZentrum, Potsdam, 05.09.2003 (Bosch)

Geodätische Woche 2003, Hamburg, 16.-19.09.2003 (Meisel, Miller, Savcenko, Schön, Seitz)

Journées 2003: Astrometry, Geodynamics and Solar System Dynamics: from Milliarcseconds to Microarcseconds, St. Petersburg, Russia, 22.-23.09.2003 (Tesmer)

OCCAM User Group Arbeitstreffen, St. Petersburg, Russia, 24.-25.09.2003 (Tesmer)

XXI Congresso Brasileiro de Cartografia, Belo Horizonte, Brazil, 29.09.-03.10.2003 (Drewes)

E8 Guests

06.-30.11.2002:	Monica Fiore, Servicio de Hidrografía y Oceanografía, Buenos Aires, Argentina.
12.11.-10.12.2002:	Paula Natali de Moirano, Univ. Nac. de La Plata, Argentina.
02.-03.12.2002:	Dr. Oliver Heidbach, Heidelberger Akademie der Wissenschaften.
06.12.2002:	Delegation of the Observatory Shanghai, Chinese Academy of Sciences.
13.03.2003:	Dr.-Ing. Th. Gruber, IAPG, Technische Universität München
17.04.-13.07.2003:	Orhan Akyilmaz, Technical University Istanbul
30.04.2003:	Prof. Dr. H. Igel, Universität München
05.07.2003:	Prof. Dr. J. Kusche, DEOS, Delft Technical University
12.08.2003:	Lic. Francisco Azpilicueta, Universidad Nacional de La Plata, Argentina
08.09.2003:	Dr. Herbert Wilmes, Bundesamt für Kartographie und Geodäsie, Frankfurt
10.-12.09.2003:	Dr. Oliver Heidbach, Geophysikalisches Institut, Universität Karlsruhe
14.09.2003:	Ing. Eduardo Lauría, IGM Argentina, Buenos Aires, Argentina

Prof. Msc. Gustavo Acuña, Universidad del Zulia, Maracaibo, Venezuela, works at DGFI in the frame of his PhD study at Technische Universität München.

Prof. Dr. Claudio Brunini, Universidad Nacional de La Plata, Argentina, worked at DGFI from 01.06. to 30.11.2003 in the frame of a grant of the Alexander von Humboldt Foundation.

Ing. Laura Sánchez, Instituto Geográfico Agustin Codazzi, Bogotá, Colombia, performed the investigations for the Diploma Thesis at Technische Universität Dresden at DGFI in summer 2003.

F Personnel

F1 Number of Personnel

The total staff of DGFI during the 2002/2003 period was (incl. DGK Office):

- from regular budget:

11 scientists
12 technical and administrative employees
2 workers
8 student helpers with an average of 294 hours/year
4 students in practical courses
3 minor time employees

- from project funds:

5 scientific employees

F2 Lectures at Universities

The following university courses were given by DGFI scientists;

Hon.-Prof. Dr. H. Drewes: “Geodetic Geodynamics”, Technische Universität München

Dr. B. Richter: “Kinematics and Dynamics of Geodetic Reference Systems”, Universität Stuttgart

F3 Graduations

The following doctoral graduation was completed:

17.07.2003: Dipl.-Ing. Steffen Schön: Analyse und Optimierung geodätischer Messanordnungen unter besonderer Berücksichtigung des Intervallansatzes. Fakultät für Bauingenieur-, Geo- und Umweltwissenschaften, Universität Fridericiana, Karlsruhe.